

Mitochondrial Transcription Factor A (TFAM) as a Novel Intercellular Signaling Molecule of
the Brain: Its Role in Glial Cell Activation and Neuroinflammation

by

Stephanie Maricel Schindler

B.Sc., The University of British Columbia, 2011

A THESIS SUBMITTED IN PARTIAL FULFILLMENT OF
THE REQUIREMENTS FOR THE DEGREE OF

MASTER OF SCIENCE

in

THE COLLEGE OF GRADUATE STUDIES

(Biology)

THE UNIVERSITY OF BRITISH COLUMBIA
(Okanagan)

April 2015

© Stephanie Maricel Schindler 2015

Abstract

Microglia, a subtype of non-neuronal glial cells, represent the innate immune system of the brain. In Alzheimer's disease, chronic neuroinflammation caused by dysregulated activation of microglia (termed microgliosis) contributes to neuronal cell death. Endogenous molecules including damage-associated molecular patterns (DAMPs) have been implicated as triggers of microgliosis. High mobility group box 1 (HMGB1), a well-characterized DAMP, induces inflammatory responses from several cell types when released into the extracellular space. Mitochondrial transcription factor A (TFAM), a structural and functional homolog of HMGB1, has been implicated as a possible DAMP. However, the effects of TFAM on glial and neuronal cells of the central nervous system remain unknown. This thesis demonstrates that extracellular TFAM acts as a DAMP capable of inducing pro-inflammatory and cytotoxic responses in glial cells by engaging receptors similar to those activated by HMGB1. Stimulation of THP-1 cells (microglia model) with TFAM in combination with interferon (IFN)- γ , resulted in activation of these cells, as demonstrated by a significant decrease in SH-SY5Y neuronal cell viability after their exposure to the supernatants from stimulated THP-1 cells. Similar results were obtained using the U-118 MG astrocytic cell line and primary human astrocytes. The induced neurotoxicity was accompanied by the release of monocyte chemoattractant protein-1 (MCP-1), reactive oxygen species (ROS), and novel intercellular signaling agents called microparticles (MPs). These MPs, in turn, induced THP-1 cell activation in an autocrine manner. Furthermore, my data demonstrate that the receptor for advanced glycation endproducts (RAGE) and the macrophage antigen complex-1 (Mac-1) receptor are engaged by TFAM, as blocking these receptors with specific inhibitors (heparin and soluble RAGE) or antibodies attenuated glial toxicity towards neuronal cells, and decreased the secretion of MCP-1 and ROS. Lastly, TFAM

expression in U-373 MG astrocytic cells and primary human astrocytes was upregulated in response to treatment with hydrogen peroxide. This research provides insight into glial activation by TFAM, and the role of endogenous intercellular signaling molecules in communication between different central nervous system cell types. Moreover, identification of the glial receptors targeted by TFAM may provide novel therapeutic targets for pathologies involving sterile neuroinflammatory processes including Alzheimer's disease.

Preface

To date, part of my research has been described in two manuscripts. One of them was accepted for publication in the Molecular and Cellular Neurosciences (see Appendix B), while the other was accepted for publication in BioMed Research International.

Some of the data presented in this thesis was also presented as posters at the Interdisciplinary Health Conference in Kelowna, BC and at a UBC Okanagan Biology Departmental seminar.

I completed the required training and obtained the appropriate certification to work with Biosafety Level 1 and Level 2 materials including various human cell lines and primary human astrocytes.

I am responsible for all the experimental data and writing presented in this thesis, except for the stimulation of THP-1 cells with IL-6+IL-1 β +TNF- α (part of the data presented in Figure 5), which was performed by Lindsay Spielman. In addition, priming of the HL-60 cells with full-length TFAM, TFAM Box A and TFAM Box B as part of the respiratory burst experiments (Figure 21) were performed by Laurie Moring. Lastly, for the publication included in Appendix B, I performed ~10% of the experiments. Dr. Jonathan Little performed all other experiments and was the lead author of the manuscript.

Table of Contents

Abstract	ii
Preface	iv
Table of Contents	v
List of Tables	x
List of Figures	xi
List of Abbreviations	xiv
Acknowledgements	xviii
Dedication	xix
Chapter 1. Introduction	1
1.1. Alzheimer’s disease	1
1.2. Alzheimer’s disease and inflammation	2
1.3. Damage-associated molecular patterns and inflammation	5
1.4. Mitochondrial transcription factor A	6
1.4.1. Structure of TFAM	6
1.4.2. TFAM and inflammation	7
1.5. High mobility group box 1 and inflammation	8
1.5.1. Macrophage antigen complex-1	9
1.5.2. Receptor for advanced glycation endproducts	11
1.6. Microparticles and inflammation	12
1.7. Cell culture model of neuroinflammation	15
1.8. Research overview and hypothesis	17
Chapter 2. Materials and Methods	20

2.1. Chemicals and reagents	20
2.2. Equipment and supplies	21
2.3. Cell culture models	22
2.4. Establishing toxicity of TFAM-stimulated glial cell supernatants	
towards SH-SY5Y neuronal cells	23
2.4.1. Plating and stimulating THP-1 promonocytic and U-118 MG astrocytic	
cells	23
2.4.2. Plating and treating SH-SY5Y neuronal cells	24
2.5. Cell viability assay: Lactate dehydrogenase (LDH)	25
2.6. Cell viability assay: MTT	26
2.7. Identifying the active domain of TFAM	28
2.8. Identifying the receptors engaged by TFAM: Inhibiting THP-1 promonocytic cell	
responses with heparin, anti-RAGE antibody or anti-Mac-1 antibody	29
2.9. Effects of TFAM on the secretion of pro-inflammatory cytokines by	
glial cells	29
2.10. Effects of TFAM on the release of superoxide by glial cells	32
2.10.1. Plating and differentiating HL-60 cells	32
2.10.2. Respiratory burst assay	33
2.11. Effects of biochemical stressors on the TFAM mRNA expression levels by	
astrocytic cells	34
2.11.1. mRNA extraction from U-373 MG astrocytic cells and	
primary human astrocytes	34
2.11.2. mRNA spin column protocol	35

2.11.3. cDNA synthesis	36
2.11.4. Quantitative polymerase chain reaction (qPCR)	37
2.12. Effects of TFAM on microparticle release by glial cells	39
2.12.1. Isolating microparticles from THP-1 promonocytic cells	39
2.12.2. Determining the neurotoxic properties of microparticles	42
2.13. Statistical analyses	44
Chapter 3. Results	45
3.1. Toxicity of TFAM-stimulated THP-1 promonocytic cells towards SH-SY5Y neuronal cells	45
3.2. Toxicity of TFAM-stimulated U-118 MG astrocytic cells towards SH-SY5Y neuronal cells	47
3.3. Toxicity of TFAM-stimulated primary human astrocytes towards SH-SY5Y neuronal cells	50
3.4. Toxicity of TFAM Box A- and Box B-stimulated glial cells towards SH-SY5Y neuronal cells	53
3.4.1. The effect of TFAM Box A and Box B on THP-1 cells	54
3.4.2. The effect of TFAM Box A and Box B on U-118 MG cells	55
3.4.3. The effect of TFAM Box A and Box B on primary human astrocytes	58
3.5. Inhibition of TFAM-induced microglial toxicity by blocking the RAGE and Mac-1 receptors	61
3.5.1. Targeting the RAGE receptor	61
3.5.2. Targeting the Mac-1 receptor	67
3.6. TFAM-primed release of superoxide by glial cells	72

3.6.1. Inhibition of the respiratory burst by blocking the Mac-1 receptor	75
3.7. Effects of biochemical stressors on TFAM mRNA expression levels by	
astrocytic cells	78
3.7.1. TFAM mRNA expression in U-373 MG cells	78
3.7.2. TFAM mRNA expression in primary human astrocytes	79
3.8. Toxicity of TFAM-induced microparticles towards SH-SY5Y neuronal cells	80
Chapter 4. Discussion	87
4.1. TFAM induces toxicity of glial cells towards neuronal cells	87
4.1.1. Identifying the neurotoxic domain of TFAM	89
4.2. Mechanism underlying TFAM-induced glial activation	93
4.2.1. TFAM enhances the secretion of pro-inflammatory cytokines by	
glial cells	93
4.2.2. TFAM primes the secretion of ROS by glial cells	95
4.2.3. TFAM acts by engaging RAGE and Mac-1	97
4.3. Hydrogen peroxide enhances TFAM mRNA expression levels by	
astrocytic cells	105
4.4. Effects of TFAM-induced microparticles on toxicity of glial cells towards	
neuronal cells	106
Chapter 5. Conclusions and future work	109
5.1. Limitations of research	109
5.2. Future work	110
5.3. Significance of findings	110
References	112

Appendices	128
Appendix A: Enzyme-linked immunosorbent assay (ELISA) reagents	128
Appendix B: Publication: Mitochondrial transcription factor A (Tfam) is a pro-inflammatory extracellular signaling molecule recognized by brain microglia. 2014. Mol. Cell. Neurosci. 60C, 88-96.	129

List of Tables

Table 1: Primer sequences used in qPCR experiments	37
Table 2: Variation in the number of MPs isolated from differentially treated THP-1 cells	81

List of Figures

Figure 1: Chronic self-perpetuating inflammation in Alzheimer's disease	4
Figure 2: TFAM primer efficiency data	38
Figure 3: Example of MPs stained with Annexin-V-FITC visualized under the Olympus fluorescence microscope	40
Figure 4: Example of flow cytometry data	42
Figure 5: TFAM plus IFN- γ induces THP-1 toxicity towards SH-SY5Y cells	46
Figure 6: TFAM plus IFN- γ induces U-118 MG toxicity towards SH-SY5Y neuronal cells	48
Figure 7: TFAM has no effect on IL-6 or TNF- α secretion by U-118 MG cells	50
Figure 8: TFAM plus IFN- γ induces primary human astrocyte toxicity towards SH-SY5Y neuronal cells	51
Figure 9: TFAM induces the secretion of IL-6 by primary human astrocytes	53
Figure 10: Box A and Box B domains of TFAM are equipotent at inducing THP-1 toxicity towards SH-SY5Y cells	55
Figure 11: Box A and Box B domain of TFAM are equipotent at inducing U-118 MG toxicity towards SH-SY5Y cells	56
Figure 12: TFAM Box B is less potent than full-length TFAM or TFAM Box A at inducing primary human astrocyte toxicity towards SH-SY5Y cells	59
Figure 13: Box A and Box B of TFAM have no effect on the secretion of IL-6 by primary human astrocytes	61
Figure 14: Heparin attenuates TFAM plus IFN- γ -induced THP-1 cell toxicity towards SH-SY5Y neuronal cells	62
Figure 15: Heparin decreases MCP-1 secretion by TFAM plus IFN- γ -stimulated	

THP-1 cells	64
Figure 16: sRAGE inhibits MCP-1 secretion by THP-1 cells stimulated with TFAM or TFAM plus IFN- γ	66
Figure 17: Blocking RAGE by a specific antibody inhibits MCP-1 secretion by TFAM plus IFN- γ -stimulated THP-1 cells	67
Figure 18: Blocking the Mac-1 receptor attenuates TFAM plus IFN- γ -induced THP-1 cell toxicity towards SH-SY5Y neuronal cells	68
Figure 19: Blocking RAGE and Mac-1 inhibits MCP-1 secretion by TFAM plus IFN- γ -stimulated THP-1 cells	71
Figure 20: TFAM primes the fMLP-induced release of ROS from HL-60 cells	73
Figure 21: Box A, Box B and full-length TFAM prime the fMLP-induced release of ROS from HL-60 cells	75
Figure 22: Blocking Mac-1 attenuates the TFAM-primed release of ROS from HL-60 cells	77
Figure 23: H ₂ O ₂ induces TFAM mRNA expression in U-373 MG astrocytic cells	79
Figure 24: H ₂ O ₂ induces TFAM mRNA expression in primary human astrocytes	80
Figure 25: TFAM induces the release of MPs from THP-1 cells	82
Figure 26: MPs isolated from stimulated THP-1 donor cells induce toxicity of THP-1 cells towards SH-SY5Y neuronal cells	83
Figure 27: MPs isolated from IFN- γ plus LPS-stimulated THP-1 donor cells increase MCP-1 secretion by THP-1 cells	85
Figure 28: The potential receptors and signaling pathways underlying glial activation by TFAM	98

Figure 29: TFAM-mediated NADPH oxidase priming and ROS production 104

List of Abbreviations

A β - Amyloid beta protein

AD- Alzheimer's disease

AGEs- Advanced glycation end products

APP- Amyloid precursor protein

ANOVA- Analysis of variance

BBB- Blood brain barrier

β -NAD- Beta-nicotinamide adenine dinucleotide

BSA- Bovine serum albumin

cDNA- Complementary DNA

CBS- Calf bovine serum

CI- Confidence interval

CNS- Central nervous system

CpG DNA- Cytosine and guanine enriched DNA

CSF- Cerebrospinal fluid

Ct- Cycle threshold

DAMP- Damage-associated molecular patterns

DMEM-F12- Dulbecco's modified Eagle medium nutrient mixture F-12 Ham

DMF- N-dimethylformamide

DMSO- Dimethyl sulfoxide

DNA- Deoxyribonucleic acid

EDTA- Ethylenediaminetetraacetic acid

ELISA- Enzyme-linked immunosorbent assay

ERK- extracellular signal-regulated kinase

EtOH- Ethanol

F0- DMEM-F12 media without calf bovine serum

F5- DMEM-F12 media supplemented with 5% calf bovine serum

F10- DMEM-F12 media supplemented with 10% calf bovine serum

HL-60- Human promyelocytic leukemia cell line (microglial NADPH oxidase model)

HMGB1- High mobility group box 1

HSD- Honestly significant difference

HSP- Heavy strand promoter

IDT- Integrated DNA technologies

I κ B - Inhibitor of nuclear factor kappa B

I κ B β - Inhibitor of nuclear factor kappa B kinase subunit beta

IL- Interleukin

INT- Iodonitrotetrazolium chloride

JNK- c-Jun terminal kinase

Lactate- Sodium L-lactate

LAL- Limulus ameocyte lysate

LDH- Lactate dehydrogenase

LPS- Lipopolysaccharide

LSD- Least-significant difference

LSP- Light strand promoter

MAC-1- macrophage antigen complex- 1

MAPK- Mitogen-activated protein kinase

MCP- Monocyte chemotactic protein

MIP- Macrophage inflammatory protein

MIQE- Minimum information for publication of quantitative real-time PCR experiments

MMP- Matrix metalloproteinase

MPs- Microparticles

mRNA- Messenger RNA

MTT- 3-(4,5-dimethylthiazol-2-yl)-2,5-diphenyl tetrazolium bromide

NADPH- Nicotinamide adenine dinucleotide phosphate

NCBI- National centre for biotechnology information

NF κ B- Nuclear factor kappa B

NFTs- Neurofibrillary tangles

NO- Nitric oxide

NRT- No reverse-transcriptase

NTC- No template control

O₂^{•-} - Superoxide anion radical

O.D.- Optical density

[•]OH- Hydroxyl radical

P- Probability

PAMP- Pathogen-associated molecular pattern

PAGE- Polyacrylamide gel electrophoresis

PBS- Phosphate-buffered saline

PCR- Polymerase chain reaction

PD- Parkinson's disease

PI3K- Phosphoinositide-3 kinase

PIP₃- Phosphatidylinositol (3,4,5)-trisphosphate

PRR- Pattern recognition receptor

qPCR- Quantitative polymerase chain reaction

RAGE- Receptor for advanced glycation endproducts

ROS- Reactive oxygen species

RT-PCR- Reverse transcription-polymerase chain reaction

S.D.- Standard deviation

SDS- Sodium dodecyl sulphate

S.E.M.- Standard error of the mean

SH-SY5Y- Human neuroblastoma cell line (neuronal model)

STAT- Signal transducers and activators of transcription

TCA- Trichloroacetic acid

TEMED- Tetramethylethylenediamine

TFAM- Mitochondrial transcription factor A

THP-1- Human monocytic cell line (microglia model)

TLR- Toll-like receptor

TNF- Tumor necrosis factor

U-118 MG- Human astrocytoma cell line (astrocyte model)

U-373 MG- Human astrocytoma cell line (astrocyte model)

Acknowledgements

I would like to express my sincerest appreciation and gratitude to my supervisor, Dr. Andis Klegeris for the guidance and advice that he provided me over the past two years. Thank you for your continuous support and patience, especially during my early writing projects, and for showing me that hard work and perseverance always pay off in the end. I am truly fortunate to have had the opportunity to work with you.

I would like to thank my committee members, Dr. Deanna Gibson and Dr. Bruce Mathieson for their friendly guidance and their insightful comments and suggestions. Thank you to Dr. Kirsten Wolthers for providing us with the recombinant protein samples, and to Dr. Mark Rheault for the use of his qPCR equipment, but more importantly for his qPCR expertise. I would also like to thank my fellow colleagues at the Laboratory for Cellular and Molecular Pharmacology for helping me with my project. A special thanks to Lindsay Spielman. I could not have asked for a better lab mate and friend to share these past two years with. Thank you for all the hours you spent editing my writing and for being my sounding board when I needed it the most.

Lastly, I would like to thank my family for their love and endless support. I would not be able to maintain my permanent student status without your help. A special thanks to Jamie Powell. Thank you for always being there for me, encouraging me, and for tirelessly listening to my presentations over and over again.

For my parents

Chapter 1. Introduction

1.1. Alzheimer's disease

Alzheimer's disease (AD) is the most common progressive form of fatal dementia, usually diagnosed in people over the age of 65¹. Currently, over 40 million people worldwide are affected by AD, and unfortunately no effective treatments nor a cure are available for this condition². Moreover, the prevalence of AD continues to rise mainly due to the aging world population. This will place an enormous burden on the health care systems in Canada and worldwide, as treatment already costs approximately \$47,000 per patient per year³. Therefore, it is imperative that effective therapeutic strategies for AD are developed soon.

The two major pathophysiological hallmarks of AD are senile plaques and neurofibrillary tangles (NFTs) in the brain⁴. The plaques are caused by the abnormal accumulation of amyloid- β protein ($A\beta$), which is released from an amyloid precursor protein (APP) upon limited proteolysis⁵. The NFTs are mainly composed of a cytoskeletal microtubule-associated protein, called tau, which becomes hyperphosphorylated, dissociates from the microtubules and consequently self-aggregates in the cytosol⁵. These pathological structures are responsible for the extensive loss of neurons, which in turn leads to the observed decline in cognitive abilities, memory loss, and eventual loss in motor function that causes death in AD. The absence of effective treatments may be in part due to the fact that the exact molecular mechanisms underlying the pathogenesis of AD remain unclear. This makes it difficult to pinpoint accurate molecular targets for drug treatment.

There are several hypotheses, which attempt to explain the cause of the disease; however, the "A β cascade hypothesis" remains the most popular among researchers, which assumes A β to be the main factor driving AD pathogenesis^{6,7}. This hypothesis, however, does not provide a

clear explanation for the observed neuronal loss. It has been suggested that extracellularly released A β binds to neuronal surface receptors leading to the activation of proapoptotic intracellular signaling cascades leading to their death⁵. Other hypotheses focus on the dysregulation of glial cells⁸ and the resulting neuroinflammation⁹ as possible causes for the onset of AD. The dysregulation hypothesis states that glial cell impairment leads to a decreased capacity to clear A β ¹⁰. As a result, A β accumulates and activates microglia, which in turn induces a chronic inflammatory response resulting in neurotoxic effects, due to the non-specific nature of the innate immune system¹⁰.

1.2. Alzheimer's disease and inflammation

Increasing evidence supports the involvement of glial cells and inflammation in the onset and progression of neurodegenerative diseases such as AD^{11,12} and Parkinson's disease (PD)¹³. Microglial cells, in particular, have been the focus of research over the past years, trying to establish their role in the neurodegenerative disease progression.

Microglia originate from the myeloid lineage and invade the central nervous system (CNS) prior to formation of the blood brain barrier (BBB)¹⁴. They are the primary immune effector cells in the CNS, representing the innate immune system, thus providing the first line of defense against injury and invading pathogens. In addition, they play fundamental roles in normal tissue maintenance and homeostasis, despite making up only 5-12% of the total cell population in the brain¹⁵. It is now widely accepted that microglia exist in two basic states: resting and reactive¹⁶.

Previously, microglia in the resting state were considered to be relatively inactive. More recent studies, using two-photon imaging, have revealed, however, that the cells are in a dynamic

state, continuously surveying the environment using cellular processes, which extend and retract to touch elements in their surroundings^{16,17}. Therefore, microglia constantly exercise a neuroprotective function, ‘patrolling’ their surroundings, prepared to react to any foreign agents. When microglia encounter certain stressors or immunological stimuli, they become activated and undergo a morphological transformation, expressing an increased number of surface proteins, including the major histocompatibility complex (MHC) II^{18,19}. This activation results in the clearing of potentially toxic cellular debris and the secretion of both pro-inflammatory mediators, as well as neurotrophic factors, which are essential to neuronal survival and maintaining homeostasis in the brain¹⁸.

Therefore, microglial activation, in itself, cannot be considered a detrimental process. On the contrary, mounting an immune response is required for fighting invading foreign agents and clearing damaged cells. However, it is the dysregulation and over-activation of microglia, termed microgliosis, which has been implicated as a major contributing factor to the neurodegeneration observed in AD. Specifically, the A β plaques in the AD brain have been shown to contribute to the onset of microgliosis¹⁶, as autopsies of AD brains reveal the presence of large numbers of reactive microglia associated with the A β plaques compared to healthy controls²⁰.

This microglia activation is accompanied by the excessive secretion of multiple pro-inflammatory cytokines including; interleukin (IL)-1 β , IL-6, tumor necrosis factor (TNF)- α , as well as chemokines such as monocyte chemotactic protein (MCP)-1²¹. In addition, microglia produce superoxide anion radical (O₂⁻), other reactive oxygen species (ROS) and nitric oxide (NO)²²⁻²⁵, which can be neurotoxic. Furthermore, the cytotoxic factors secreted by microglia can stimulate surrounding astrocytes to release their own neurotoxic substances, which in turn further

stimulate microglia. Ultimately, this creates a chronic and self-perpetuating neuroinflammatory milieu, which contributes to the neuronal cell death observed in AD (Figure 1) ²⁶.

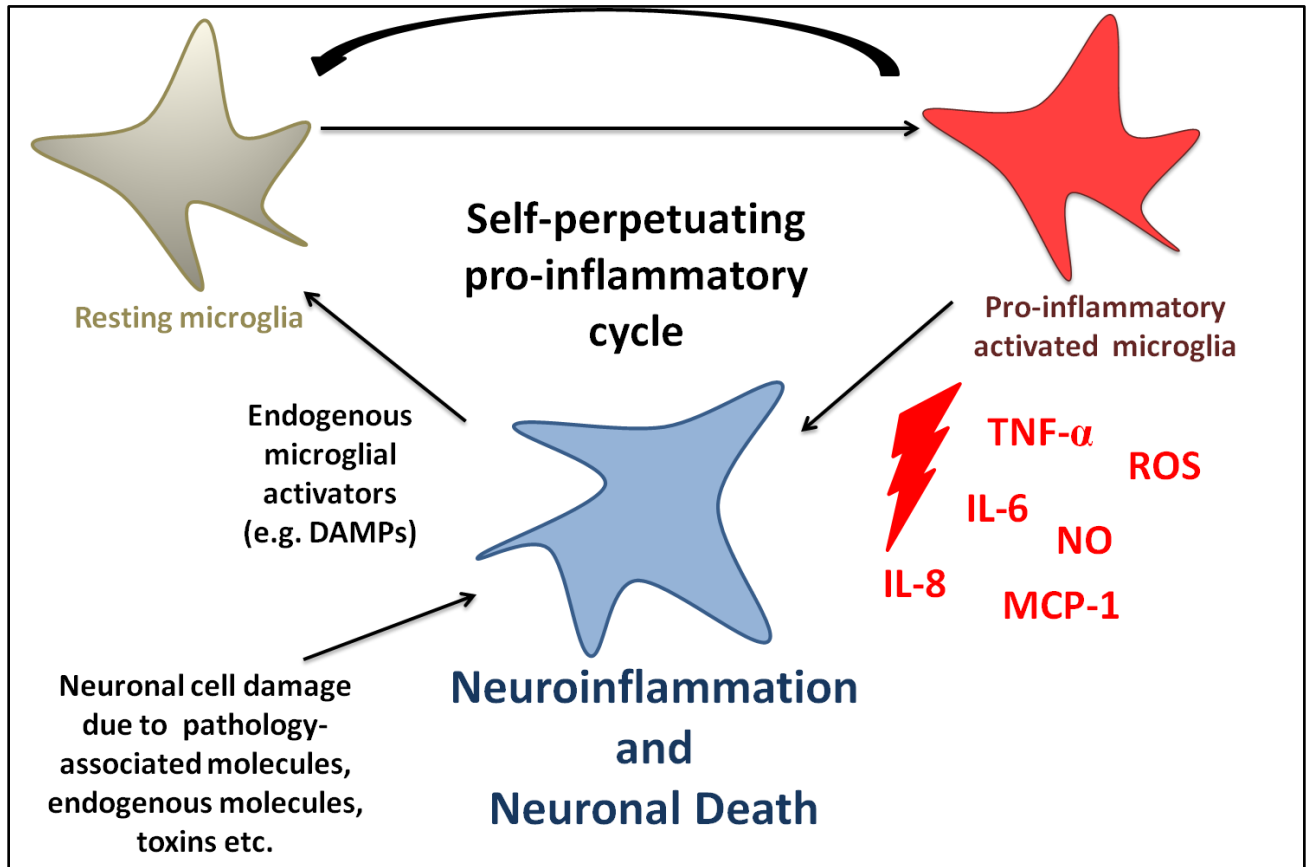


Figure 1. Chronic self-perpetuating inflammation in Alzheimer’s disease. A variety of molecules can activate microglia leading to the excessive release of pro-inflammatory mediators, which can contribute to neuronal death.

1.3. Damage-associated molecular patterns and inflammation

Microglia can be stimulated by a diverse set of molecules²⁷. In addition to A β , other misfolded proteins, such as P301S mutated tau²⁸ and α -synuclein²⁹ have been shown to activate microglia leading to the increased secretion of pro-inflammatory cytokines resulting in neuronal loss.

Microglial cells are also capable of initiating an immune response as a result of activation of pattern recognition receptors (PRRs), such as toll-like receptors (TLRs), the receptor for advanced glycation end products (RAGE) or the macrophage antigen complex-1 (Mac-1) receptor expressed on their surface³⁰⁻³². These PRRs recognize pathogen-associated molecular patterns (PAMPs), as well as damage-associated molecular patterns (DAMPs). PAMPs are exogenous molecules, recognized as non-self, which alert the body to microbial invasion³³. In contrast, DAMPs act as endogenous danger signals that can be released or secreted extracellularly by damaged or dying cells, and are able to trigger inflammatory immune responses in the absence of infection^{34,35}. More recently, DAMPs derived from mitochondria have been recognized as potent triggers of the inflammatory response^{36,37}. It is assumed that the immune activity of these particular DAMPs is due to the bacterial origin of mitochondria. Despite successful symbiosis between mitochondria and the eukaryotic cell, the mitochondria have retained many structural and biochemical features of their bacterial ancestors capable of triggering an inflammatory response³⁷.

Several research groups have attempted to establish a link between mitochondrial DAMPs and the development of neuroinflammatory and neurodegenerative disorders^{38,39}. Mathew et al.³⁸ showed that degraded mitochondrial DNA, acting as a DAMP, is strongly immunogenic to astrocytes. It is capable of eliciting a strong pro-inflammatory cytokine

response, which is relevant to neurodegenerative diseases, such as AD. It is important to determine which other mitochondrial DAMPs may act as activators of glial cells.

1.4. Mitochondrial transcription factor A

Mitochondrial transcription factor A (TFAM) is an example of a mitochondrial protein that has been implicated as a potential novel DAMP. Each human mitochondrion has several copies of its own genome, consisting of a closed circle of double-stranded DNA that encodes 37 genes⁴⁰.

Transcription of these genes begins from three promoters, namely the light-strand promoter (LSP) and the heavy strand promoters 1 and 2 (HSP1 and HSP2), which are located in the major non-coding region termed the displacement-loop regulatory region (D-loop region)⁴¹. An essential regulator of human mitochondrial transcription is the binding protein TFAM. It binds specifically to a 22-bp region upstream from either LSP or HSP1⁴². Upon binding, TFAM causes a sharp U-turn in the DNA, exposing a specific binding site upstream from the transcription initiation site. This prepares the DNA template for recognition by the transcription machinery^{42, 43}. As a result, TFAM is able to regulate mitochondrial transcription initiation (from LSP and HSP1, but not HSP2), mitochondrial gene expression and mitochondrial DNA copy number⁴⁴. In addition, TFAM plays a structural role related to DNA maintenance and DNA compaction into nucleoid structures, which is integral for genome transmission^{45, 46}.

1.4.1. Structure of TFAM

TFAM is a 246 amino acid protein with a molecular weight of around 25kDa, containing several well-defined domains. These include a ~45 amino acid N-terminal mitochondrial targeting sequence, two DNA-binding sites arranged in tandem, namely the high-mobility group (HMG)

box domains (Box A and Box B), followed by a charged C-terminal tail ⁴⁴. The HMG box domains make TFAM a member of the ubiquitous HMGB family of DNA binding factors, and thus a highly conserved protein. HMG box A appears to be the dominant DNA binding domain, while HMG box B does not bind to LSP DNA by itself ⁴⁷. Rather, HMG box B is suggested to be involved in stabilizing interactions between TFAM and the DNA complex, while the C-terminal tail is critical for transcription activation by TFAM ⁴⁷.

1.4.2. TFAM and inflammation

Under normal conditions, TFAM is localized to the inner mitochondrial membrane. Damage to tissues or cells can cause the extracellular release of TFAM, leading to a change in its physiological role. Several studies have shown that after its release from damaged or dying cells in the periphery, TFAM becomes a pro-inflammatory mediator and DAMP ⁴⁸⁻⁵⁰. One particular study observed that TFAM, in combination with mitochondrial N-formyl peptides, was able to significantly increase IL-8 release from human peripheral blood monocytes ⁴⁸. The authors concluded that the mitochondrial components of the cell, particularly TFAM, significantly contributed to the induction of the innate immune response. They further suggested that due to the structural and functional similarities between TFAM and high mobility group box 1 (HMGB1), it might be possible that extracellularly released TFAM was recognized by TLRs and/or RAGE contributing to inflammation ⁴⁸. A recent study investigated the receptors activated by TFAM in the periphery. The authors showed that TFAM, in combination with cytosine and guanine enriched DNA (CpG DNA), acted via RAGE and TLR9 receptors to activate plasmacytoid dendritic cells, and to induce the release of TNF- α from splenocytes ⁵¹. The role of TFAM in the CNS, however, has not been explored. Its receptors and signaling pathways remain

to be established. However, studies performed with HMGB1, a well-studied DAMP, may provide some potential avenues for TFAM research.

1.5. High mobility group box 1 and inflammation

HMGB1 also known as amphoterin, is a ubiquitous nuclear DNA-binding protein with a structure very similar to human TFAM (sequence homology 76%). HMGB1 also contains two DNA-binding motifs, called Box A and Box B, as well as an acidic tail⁵². HMGB1 is found in almost all vertebrate cells and possesses two functions depending on its location: in the nucleus, HMGB1 acts as a regulator for gene transcription and homeostasis in a manner similar to TFAM, while extracellularly it acts as a signaling molecule with pro-inflammatory activity^{52,53}. The latter role has been the focus of many studies, which have established that HMGB1 may act as a DAMP and pro-inflammatory mediator capable of upregulating microglia activation⁵⁴⁻⁵⁶.

In the periphery, a variety of cells including monocytes, macrophages and dendritic cells have been shown to actively secrete HMGB1 in response to biological stressors such as lipopolysaccharide (LPS), TNF- α and IL-1 β ⁵⁷⁻⁵⁹. This secretion of HMGB1 results in an activation/perpetuation of an inflammatory state as shown by the production of pro-inflammatory mediators, including cytokines and chemokines, as well as the recruitment of antigen-presenting cells⁵². In the CNS, HMGB1 is also actively secreted from neurons, microglia and astrocytes⁶⁰⁻⁶². Moreover, upon CNS injury, HMGB1 presence has been correlated with the induction of chronic inflammation and neurodegeneration^{53,63}. This is, in part, due to the ability of HMGB1 to activate glial cells resulting in an inflammatory response. HMGB1 released into the media of cultured neurons was able to activate microglia and elicit an inflammatory response characterized by the release of cytokines such as TNF- α and IL-1 β ⁶⁴. Moreover, media depleted

of HMGB1 through treatment with an anti-HMGB1 antibody were not able to induce microglial activation, thus pointing to HMGB1 as a key trigger of neuroinflammation⁶⁴. The receptors, such as Mac-1 and RAGE, and associated signaling pathways engaged by HMGB1 have been the focus of many studies, as these provide possible molecular targets to achieve modulation of microglial activation^{62, 65-67}.

1.5.1. Macrophage antigen complex-1

Mac-1 also known as CD11b/CD18 or complement receptor 3 is a member of the leukocyte β_2 -integrin family. Mac-1 is expressed primarily by phagocytic cells and natural killer cells⁶⁸ in the peripheral tissues, and by microglia⁶⁹ in the CNS. Mac-1 plays an important role in innate immunity as it regulates important phagocytic cell functions including adhesion, phagocytosis and oxidative burst (ROS production)^{70, 71}. Interestingly, Mac-1 expression is elevated in the brains of AD patients, suggesting its involvement in neurodegeneration⁶⁹. Moreover, Mac-1 has been shown to function as a PRR with the ability to interact with multiple ligands resulting in microglial activation, which is followed by the induction of cytotoxic reactions⁷²⁻⁷⁴. Mac-1 has been shown to mediate both LPS-induced⁷³ and A β -induced production of O₂^{•-} in microglia⁷². Specifically, Zhang et al.⁷² demonstrated that the Mac-1-mediated release of O₂^{•-} was due to the activation of NADPH oxidase in the mouse microglial cells. NADPH oxidase is a multi-subunit enzyme complex that is activated during host defense in immune cells, such as microglia⁷⁵, and catalyzes the production of O₂^{•-} from oxygen. Since NADPH oxidase has been shown to be upregulated in brains of AD and PD patients, it has been associated with neurodegenerative disease^{76, 77}. This has prompted studies to investigate NADPH oxidase as a potential therapeutic target for neurodegenerative diseases^{24, 75}. Therefore, characterizing the signaling pathways

leading to NADPH oxidase activation is essential for finding targets to inhibit the enzyme complex. Thus, Zhang et al.⁷² investigated the signaling pathway induced by Mac-1-mediated activation of NADPH oxidase. They demonstrated that Mac-1 signaled through phosphoinositide-3 kinase (PI3K) when activating the NADPH oxidase complex⁷². Western blotting showed that A β stimulation of Mac^{+/+} microglia resulted in increased p110 membrane translocation (a catalytic subunit of PI3K), while in Mac^{-/-} microglia this translocation was significantly reduced⁷². Moreover, staining for phosphatidylinositol (3,4,5)-trisphosphate (PIP₃), a product of activated PI3K, was significantly reduced in Mac^{-/-} microglia, further confirming the role of Mac-1 in A β -induced PI3K activation⁷².

A recent study, using 1-Methyl-4-phenylpyridinium, LPS, and rotenone, which are common toxins used to create PD models, investigated the role of Mac-1 in HMGB1-mediated activation of NADPH oxidase⁶². Primary microglia cultures from Mac-1^{+/+} or Mac-1^{-/-} mice were treated with HMGB1 and the membrane translocation of the cytosolic subunit of NADPH oxidase, p47^{phox}, was measured⁶². It was determined that Mac-1 was required for membrane translocation and thus activation of the NADPH complex, as Mac-1^{-/-} microglia showed no membrane translocation. Furthermore, O₂^{•-} release by these microglia was significantly reduced⁶². The same study showed that HMGB1 activated microglia from Mac^{+/+} mice, which led to a decreased viability of the dopaminergic neurons as indicated by dendrite degeneration and a reduction in dopamine uptake. Moreover, the release of TNF- α , IL-1 β and nitrite was increased⁶². In contrast, Mac^{-/-} microglia promoted the survival of the dopaminergic neurons and produced significantly less pro-inflammatory cytokines⁶². All together these data indicate that HMGB1-induced microglial activation and inflammation may be mediated by Mac-1. However, the effects of HMGB1 were not mediated by Mac-1 alone, as the attenuation of neurotoxicity and

production of cytotoxic substances was only partial. This suggested the involvement of other additional receptors, such as RAGE.

1.5.2. Receptor for advanced glycation end products (RAGE)

RAGE is a multi-ligand receptor, and has emerged as a central mediator in the inflammatory response. It signals through several mitogen activated protein kinase (MAPK) pathways including p38 and c-Jun N-terminal kinase (JNK)⁷⁸, which feed into the downstream activation of nuclear factor- κ B (NF- κ B). NF- κ B is a transcription factor that is involved in the initiation of the transcription of certain pro-inflammatory cytokines, as well as in the induction of inducible nitric oxide synthase (iNOS). This, in turn, leads to the production of nitric oxide (NO), another pro-inflammatory mediator⁷⁹.

Pedrazzi et al.⁶⁶ demonstrated that extracellular HMGB1 triggered pro-inflammatory activation of astrocytes *in vitro* by engaging RAGE and by signaling through the MAPK and extracellular signal-regulated kinases 1 and 2 (ERK1/2) pathways. This pro-inflammatory state was characterized by the increased release of chemokines, including MCP-1, macrophage inflammatory protein (MIP)-1 α , MIP-2 α and RANTES, which act to attract microglia and circulating monocytes⁶⁶. Another study showed that RAGE expressed on glial cells was required for the pro-inflammatory effects of HMGB1 to occur *in vitro*, as in the absence of RAGE, HMGB1 could not induce significant neuronal cell death⁸⁰. The interaction between HMGB1 and RAGE provides a potential target for inhibiting glial cell activation. Several studies have successfully applied specific anti-RAGE antibodies^{81,82} or soluble RAGE (sRAGE)^{80,83}, the truncated form of the receptor, as inhibitors of HMGB1 activity.

Other studies have used heparin as an inhibitor of RAGE. Xu et al.⁸⁴ showed that heparan sulfate on the cell surface of endothelial cells is required for HMGB1 interaction with RAGE. Cell surface heparan sulfate forms a complex with RAGE prior to HMGB1 binding, a step that is essential for facilitating HMGB1 signaling and activity⁸⁴. As a result, heparin, the fractionated form of heparan sulfate, has been applied as an inhibitor of RAGE. Heparin has been shown to inhibit the binding of heparan sulfate ligands. This may be due to heparin competing against these other ligands for binding sites on the surface of heparan sulfate. In addition, heparin has been shown to specifically inhibit the interaction of RAGE with HMGB1 by altering the conformation of HMGB1. Thus heparin decreases the interaction of HMGB1 with RAGE achieving an anti-inflammatory effect⁸⁵.

Overall, many of the abovementioned studies have shown that the interaction between DAMPs, such as TFAM and HMGB1, and their receptors is one of the initial steps in microglial activation. Moreover, these studies have also demonstrated that inhibition of select DAMP receptors (RAGE and Mac-1) represents a promising therapeutic approach for attenuating the microglial-mediated neuroinflammation and the production of pro-inflammatory mediators. Consequently, this knowledge can be applied to the development of therapeutic interventions for certain neurodegenerative diseases involving sterile inflammation, including AD and PD to prevent neuronal death.

1.6. Microparticles and inflammation

In addition to targeting the receptors engaged by TFAM or HMGB1, it may be possible to specifically target the pro-inflammatory mediators that are released by the microglia upon activation, to inhibit their actions and attenuate the induced neurotoxicity. Consequently, studies

have focused on identifying additional components of the pro-inflammatory cocktail released by activated microglia. Over the recent years, microparticles (MPs) have emerged as novel intercellular signaling agents that appear to have immunomodulatory and biological activities similar to HMGB1^{86,87}. Following activation, apoptosis or necrosis both MPs and HMGB1 are released from a variety of cell types, including monocytes, microglia, astrocytes and neurons^{88,89}.

Originally MPs were considered “platelet dust”, an inert by-product of platelet activation⁹⁰. Recent studies, however, have unveiled that MPs are, in fact, a heterogeneous population of membrane-derived vesicles, ranging in size from 0.1-1 μ m, that regulate various biological and physiological processes, including cell-cell communication, cell proliferation, coagulation and inflammation⁹¹. It is becoming increasingly evident that MPs can contribute to the progression of some neurodegenerative and neuroinflammatory diseases^{88,89,92}. This statement is based on two observations: 1) elevated MP levels have been detected in the cerebrospinal fluid (CSF) and plasma of individuals suffering from CNS disorders, including multiple sclerosis⁹³ and cerebral malaria⁹⁴, and 2) MPs isolated from patients affected by CNS disorders often carry inflammatory mediators and other bioactive molecules within them or embedded on their surface⁹². It is possible that the inflammatory mediators can be liberated from the MPs, and subsequently bind to surrounding cells, such as microglia or neurons, thus contributing to the neurotoxic environment seen in neuroinflammatory diseases. The exact triggers and mechanisms underlying MP release remain to be fully elucidated. A variety of stimuli, including TNF- α ⁹⁵ and LPS^{96,97}, have been shown to stimulate MP shedding by monocytes. A study by Cherri et al.⁹⁸ investigated the effects of MPs from calcium ionophore A23187-stimulated human monocytes on human airway epithelial cells. The released MPs were able to induce the release of IL-8 and

MCP-1 from the human A549-(epithelial)-cell line. Expression levels of both of these pro-inflammatory mediators were also increased compared to unstimulated cells⁹⁸. Based on this evidence, it is possible that pro-inflammatory molecules released by activated cells may, in turn, induce MP release from other surrounding cells, thus contributing to a pro-inflammatory cycle.

To date, the role of DAMPs, such as HMGB1 or TFAM, as triggers of MP release has not been investigated. However, recent studies have shown that HMGB1 can be bound to or even contained within MPs^{87, 99, 100}. The HL-60 (human promyelocytic leukemia cells) and the Jurkat (human T lymphocytes) cell lines were treated with either staurosporine or etoposide to induce apoptosis, or subjected to freeze-thaw cycles to induce necrosis, after which the MPs in the cultured media were quantified using flow cytometry and assessed for the expression of HMGB1⁹⁹. Western blotting indicated that increased HMGB1 was present on the MPs induced by the apoptotic agents compared to the unstimulated control MPs, demonstrating the importance of cell death as an inducer of HMGB1 and MP release⁹⁹. The association of HMGB1 and MPs may lead to amplification of the pro-inflammatory effects that each of these two agents could induce on their own. Due to the structural and functional homology between HMGB1 and TFAM, it is possible that TFAM is released from damaged cells in a similar fashion in association with MPs. Interestingly, if TFAM acts as a DAMP and microglial activator, it may also trigger MP release from glial cells. This insight into MP release would provide an additional therapeutic target for treating neuroinflammatory disorders.

In summary, the activity of HMGB1 as a cytokine and DAMP has been studied quite extensively in both the periphery and the CNS. In comparison, there are fewer studies assessing the role of TFAM in the CNS and neuroinflammation. However, due to the high homology between TFAM and HMGB1 along with research demonstrating the ability of TFAM to act as a

DAMP in peripheral tissues, it is essential to confirm the role of TFAM in the CNS, as well. Characterizing the effects of TFAM on glial cells may provide further insight into the physiological function of microglial activation. Specifically, identifying the receptors and signaling pathways involved in microglial activation by TFAM will provide new insights into the role of endogenous intercellular signaling molecules in communication between different CNS cell types. Moreover, this thesis studies the novel intercellular signaling agents, MPs, as potential DAMPs of the CNS. An increased number of studies have demonstrated the role of MPs as inflammatory triggers and immune regulators in the periphery; therefore it is important to establish their role in the CNS, as this would further expand the knowledge on microglia-mediated neurotoxicity.

1.7. Cell culture model of neuroinflammation

The experiments described in this thesis were conducted *in vitro* using human immortalized cell lines as models for the glial cells and the neurons of the brain. These cells have undergone a mutation allowing them to proliferate indefinitely. The cell lines are inexpensive, readily available, easy to maintain, and can be used for high throughput assays, which makes them ideal for use in laboratory research.

However, due to the accumulation of genomic mutations, which occur during multiple passages, the cell lines may differ in function and morphology from the original cell types. As such, primary, tissue-derived cells are considered better models of glial cells compared to the immortalized cell lines¹⁰¹. Therefore, some of the key findings obtained using cell lines were replicated in this thesis using primary human cells. As primary human microglia and neurons do not readily proliferate *in vitro*, only primary human astrocyte data could be obtained. Availability

of primary human glial cells is limited, as they are obtained directly from human tissues; these cells have decreased proliferation rates and a limited life span, all of which restricted the use of primary cells in the experiments described in this thesis.

To model neuroinflammation *in vitro* the following human cell lines were employed: THP-1 pro-monocytic cells to model microglia, as they possess functional characteristics and receptors similar to microglia including complement receptor 1 (CR1, also known as C3b/C4b receptor)^{102, 103} and Mac-1^{69, 104}. U-373 MG and U-118 MG astrocytoma cells to model astrocytes, as they express specific astrocyte markers similar to their primary astrocyte counterparts, such as glial fibrillary acidic protein (GFAP)^{105, 106}. Instead of THP-1 cells, HL-60 promyelocytic cells were used to model phagocytes expressing NADPH oxidase, which is required for the respiratory burst. Unlike THP-1 cells, HL-60 cells express NADPH oxidase at levels that are sufficient to generate detectable ROS levels^{107, 108}. Formyl peptide N-formyl-methionine-leucine-phenylalanine (fMLP) was used as the widely accepted trigger of ROS production by HL-60 cells¹⁰⁹. And lastly, the human SH-SY5Y neuroblastoma cell line served as the neuronal model, as these cells display characteristics of primary neurons¹¹⁰. All of these cell lines were chosen as they have been successfully used before to model their respective *in vivo* counterpart cell types^{108, 111-113}.

It has been shown that both THP-1 cells and human microglia become activated upon stimulation with LPS and interferon (IFN)- γ in a manner similar to the activation observed in microglia in pathological states¹¹⁴. In order to achieve similar activation of the astrocyte cell lines, U-373 MG cells only require stimulation with IFN- γ , while U-118 MG cells need to be stimulated with a combination of IFN- γ and IL-1 β to induce a neurotoxic response¹¹³. Although IFN- γ and LPS are not present in most CNS inflammatory conditions, the type of activation and

the cytotoxic responses that the combination of these mediators induces from glial cells *in vitro* is very similar to that induced by A β in the brain^{115, 116}.

1.8. Research overview and hypothesis

The role of microglia in the onset and progression of neurodegenerative diseases such as AD and PD has now been widely accepted^{12, 30, 117, 118}. As such, microglia present attractive therapeutic targets to treat the above mentioned CNS disorders. In order to do so, however, it is essential to gain a better understanding of the molecules capable of triggering microgliosis, as well as the mechanisms underlying this activation. Over the recent years, endogenous molecules have been recognized as potential microglial activators. HMGB1, one of the best characterized DAMPs has been shown to interact with various cell types resulting in a potent inflammatory response both in peripheral tissues, as well as in the CNS^{53, 119}. Therefore, TFAM, which is a structural and functional homolog of HMGB1, was explored through this thesis work as a potential DAMP. Since recent studies have demonstrated the ability of TFAM to activate immune cells in peripheral tissues⁴⁹⁻⁵¹, and since the effects of extracellular TFAM in the CNS, particularly those on glial and neuronal cells, remain unknown, this thesis focused on the CNS role of TFAM as a DAMP.

The **central hypothesis** of this thesis is that extracellular TFAM is a novel intercellular signaling molecule of the CNS, which can act as a specific DAMP capable of inducing pro-inflammatory and cytotoxic responses in microglial cells through cellular mechanisms similar to those used by HMGB1 (due to their structural similarities).

To study the effect of TFAM on glial cells and to determine its ability to induce a neurotoxic response *in vitro*, cell culture experiments were performed. Glial cells, or their

surrogate cell lines, were cultured in the presence of TFAM and their supernatants transferred onto neurons to establish whether TFAM could induce glial neurotoxicity. Similar supernatant transfer experiments were performed using Box A and Box B of TFAM as stimulants, to determine which specific TFAM domain is responsible for the glial-mediated neurotoxicity induced by TFAM. Quantitative polymerase chain reaction (qPCR), enzyme-linked immunosorbent assay (ELISA) techniques, as well as flow cytometry were used to characterize the induced glial responses. Flow cytometry was specifically used to assess and quantify the MPs released from TFAM-stimulated microglia-like cells. Finally, changes in TFAM mRNA expression levels in glial cells responding to different biochemical stressors, such as hydrogen peroxide, were measured by qPCR.

Ultimately, the identification of novel intercellular signaling molecules will contribute to broadening the understanding of the mechanisms underlying microglial activation. By expanding the fundamental knowledge on CNS functioning, this research may have practical applications through the identification of novel molecular and therapeutic targets for a variety of pathologies that involve sterile neuroinflammatory processes, including AD.

The five **main research objectives** addressed in this thesis are:

1. To demonstrate the ability of TFAM to elicit neurotoxic responses from human glial cells.
2. To determine the specific domain of the structure of TFAM responsible for triggering glial activation.
3. To identify the key glial receptors engaged by TFAM.
4. To measure changes in the TFAM mRNA expression levels by glial cells in response

to different stressors.

5. To determine whether glial cells release MPs upon TFAM exposure, and if so, to verify whether MPs induce neurotoxic responses in an autocrine manner.

Chapter 2. Materials and Methods

2.1. Chemicals and reagents

The following reagents were obtained from Sigma-Aldrich (Oakville, ON, Canada): 3-(4,5-dimethylthiazol-2-yl)-2,5-diphenyl tetrazolium bromide (MTT), ammonium persulphate, beta-nicotinamide adenine dinucleotide (β -NAD), diaphorase (from *Clostridium kluyveri*), dimethyl sulfoxide (DMSO), ExtrAvidin alkaline phosphatase, fMLP, heparin sodium salt (from porcine intestinal mucosa), iodonitrotetrazolium chloride (INT), LPS (from *Escherichia coli* 055:B5), luminol sodium salt, sodium L-lactate (lactate), 10 mM tris-HCl, tetramethylethylenediamine (TEMED) and Triton X-100.

Acrylamide/bis (29:1, 30% solution), bovine serum albumin (BSA), calf bovine serum (CBS), diethanolamine, Dulbecco's modified Eagle medium nutrient mixture F-12 Ham (DMEM-F12), ethylenediaminetetraacetic acid (EDTA) sodium salt, GeneRuler DNA ladder, hydrogen peroxide, hydrochloric acid, N,N-dimethylformamide (DMF), penicillin/streptomycin, phosphatase substrate tablets, Pierce BCA protein assay kit, Pierce High Capacity Endotoxin Removal Spin Columns, Pierce LAL Chromogenic Endotoxin Quantification Kit, sodium dodecyl sulphate (SDS), sodium chloride, sodium carbonate, sodium bicarbonate, monobasic sodium phosphate, dibasic sodium phosphate, sodium tris (hydroxymethyl)aminomethane (Tris), trichloroacetic acid (TCA), 0.05% and 0.25% trypsin/EDTA solutions, and Zeba Spin Desalting Columns 40K were purchased from ThermoFisher Scientific (Ottawa, ON, Canada).

Human recombinant IFN- γ , human recombinant IL-1 β , as well as the ELISA kits for IL-6, TNF- α and MCP-1 were purchased from Peprotech (Rocky Hill, NJ, USA). Ssofast qPCR reaction mix, Aurum RNA extraction kit and iScript complementary DNA (cDNA) synthesis kit were purchased from Bio-Rad (Mississauga, ON, Canada). Anti-Mac-1 (CD11b) antibody and

the FITC Annexin-V Apoptosis Detection Kit II were purchased from BD Biosciences (Mississauga, ON, Canada). Anti-RAGE antibody (N16) was purchased from SantaCruz Biotechnology (Dallas, TX, USA). Phosphate-buffered saline (PBS) tablets were purchased from Ambresco (Solon, OH, USA). Recombinant human TFAM full-length, Box A and Box B were a generous gift from Dr. Kirsten Wolthers of the University of British Columbia Okanagan campus (Kelowna, BC, Canada).

2.2. Equipment and supplies

All cell culture experiments were performed in a class 2, type IIA biological safety cabinet (BSC). Most cell culture experiments were conducted in sterile 96-well plastic cell culture plates (Corning Inc., Corning, NY, USA). The sterile 96-well plastic cell culture plates were also used to collect small volumes of supernatants for ELISA, MTT and LDH experiments and treatments for the respiratory burst assay. Tissue culture dishes (10 cm², Corning) were used for the cell differentiation. Cell cultures were grown in T-75 flasks (Sarstedt, Montreal, QC, Canada) and incubated in a Steri-Cycle HEPA Class 100 CO₂ incubator (Model#370, ThermoScientific). To observe changes in cell morphology, a VistaVision phase contrast inverted microscope was used (Model#82026-630, VWR International, Edmonton, AB, Canada). A Motic inverted microscope (Model AE31) with an attached Moticam 3000 camera (Motic, Richmond, BC, Canada) was used for taking phase contrast digital pictures. A hemocytometer (ChangBioscience, Castro Valley, CA, USA) was used to count cells. The Sorvall RT1 Centrifuge (Cat#75002384, ThermoScientific) was used for centrifugation of cell cultures, their supernatants, as well as for MP collection. The Spectra Shell plate reader (SLT Labinstruments, Salzburg, Austria) was used to measure absorbance for the cell viability experiments. The FLUOstar Omega microplate

reader (BMG Labtech, Nepean, ON, Canada) was used for measuring chemiluminescence in the respiratory burst experiments.

Sterile 6-well plastic cell culture plates (Corning) were used for growing U-373 MG cells and primary human astrocytes required for the qPCR experiments. Extracted RNA was quantified using the NanoDrop 100 (ThermoScientific) and reverse transcribed to cDNA using a C1000 Thermal Cycler (Model#185-1048, Bio-Rad). The qPCR experiments were carried out in white 96-well plates (Bio-Rad) using a CFX96 Real Time System (Model# 185-5201, Bio-Rad).

Sterile 24-well plastic cell culture plates (Corning) were used for growing THP-1 cells for the MP isolation experiments. The fluorescence microscope used for the detection of the MPs was from Olympus (Model #IX81) and the images were analyzed using MetaMorph Advanced (Version 7.7.8.0, Molecular Devices, Sunnyvale, CA, USA). The Flow Cytometer used for the detection and quantification of the microparticles was the MACSQuant Analyzer (Model#130-092197, Miltenyi Biotec, Bergisch Gladbach, Germany).

2.3. Cell culture models

The THP-1 human promonocytic cell line and the U-373 MG and U-118 MG human astrocytoma cell lines were used to model microglia and astrocytes, respectively. The HL-60 human promyelocytic cell line was used as a neutrophil model, and the human SH-SY5Y neuroblastoma cell line served as the neuronal model. The THP-1 cells, the U-373 MG and U-118 MG cells, as well as the HL-60 cells were obtained from the American Type Culture Collection (ATCC, Manassas, VA, USA), while the SH-SY5Y cells were donated by Dr. Robert Ross (Department of Biological Sciences, Fordham University, Bronx, NY, USA). Primary human astrocytes were isolated from human surgical tissues by Dr. Sadayuki Hashioka at the

Kinsmen Laboratory of Neurological Research at the University of British Columbia Vancouver campus. The cell lines were kept frozen in liquid nitrogen in DMEM-F12 media supplemented with 20% CBS, 10% DMSO to act as a cryoprotectant, as well as penicillin (100 U/ml) and streptomycin (100 µg/ml) to inhibit bacterial growth. They were thawed when needed. Cell cultures were grown in DMEM-F12 media supplemented with 10% CBS (F10 media) in T-75 flasks and incubated at 37°C, 100% humidity and 5% CO₂.

2.4. Establishing toxicity of TFAM-stimulated glial cell supernatants towards SH-SY5Y neuronal cells

2.4.1. Plating and stimulating THP-1 promonocytic, U-118 MG astrocytic cells and primary human astrocytes

Previously described supernatant transfer experiments¹²⁰ were used to establish the TFAM-induced toxicity of glial cells towards SH-SY5Y cells. The experiments using THP-1 monocytic cells and U-118 MG astrocytoma cells were performed on at least three independently grown populations of cells. The experimental procedures described by Little et al.¹²⁰ were modified as follows.

Any potential endotoxin contamination of TFAM was removed using the Pierce High Capacity Endotoxin Removal Columns (ThermoScientific), which contain resin and cellulose beads with polylysine chains on their surface that have high affinity for endotoxins. The resulting endotoxin levels were measured to be less than 2 pg/µg protein using the Pierce LAL Chromogenic Endotoxin Quantification Kit (ThermoScientific). Such endotoxin levels are generally acceptable for tissue culture experiments^{48, 50, 66}. Only these TFAM samples were used for subsequent experiments.

For use in experiments, THP-1 cells were harvested from T-75 flasks and counted using a hemocytometer. The cells were then centrifuged at 450 g for 7 min and re-suspended in DMEM-F12 media supplemented with 5% CBS, penicillin (100 U/ml) and streptomycin (100 µg/ml) (F5 media) to a final concentration of 0.5 million cells/ml. The cells were plated at 250 µl per well into a sterile 96-well plate. Following 30 min recovery time in the incubator, the cells were treated with TFAM (2.5 µg/ml) in the presence or absence of IFN- γ (150 U/ml) or its vehicle solution (PBS) and incubated for 48 h at 37°C.

U-118 MG cells and primary human astrocytes, which adhere to plastic, had to be harvested in a different manner than the THP-1 cells. U-118 MG cells and primary human astrocytes were detached from the flask by removing the media and incubating the cells with 1.5 ml of 0.25% trypsin/EDTA solution for 2 min at 37 °C, followed by gentle tapping of the T-75 flask to aid in detachment of cells from the flask surface. Trypsin was neutralized by adding 10 ml of F10. Cells were then counted using a hemocytometer, centrifuged at 450 g for 7 min and re-suspended to a final concentration of 0.2 million cells/ml. For use in supernatant transfer experiments, U-118 MG cells and primary human astrocytes were plated at 250 µl per well into a sterile 96-well plate, and incubated for 24 h at 37°C to allow the cells to adhere to bottom of the wells. Following the incubation period, the cells were stimulated with TFAM (2.5 µg/ml) in the presence or absence of IFN- γ (150 U/ml) and IL-1 β (100 U/ml) or its vehicle solution (PBS) and incubated for an additional 48 h at 37°C.

2.4.2 Plating and treating SH-SY5Y neuronal cells

Following the 48 h incubation THP-1 or U-118 MG cells, 150 µl of supernatants per well were transferred onto SH-SY5Y cells, which had been plated 24 h earlier. Adherent SH-SY5Y cells

were harvested in a manner similar to that used for harvesting U-118 MG cells, except 0.05% trypsin/EDTA solution was used instead of 0.25% trypsin/EDTA solution. After being counted and centrifuged at 450 g for 7 min, the cells were re-suspended to a final concentration of 0.2 million cells/ml. They were plated at 150 μ l per well into a sterile 96-well plate and incubated for 24 h at 37°C before receiving supernatants from either the THP-1 or the U-118 MG cells.

For the supernatant transfer, the SH-SY5Y supernatants were aspirated and replaced with 150 μ l of either the THP-1 or U-118 MG (stimulated and unstimulated) supernatants. SH-SY5Y cells were incubated for an additional 72 h, after which their viability was tested using the LDH¹²¹ and the MTT assays¹²². Viability of the THP-1 and U-118 MG cells was assessed by conducting the MTT assay on the 100 μ l of cell cultures remaining in the wells. Due to the limited volume of remaining supernatant only the MTT assay and not the LDH assay was conducted to measure the viability of THP-1 or U-118 MG cells.

2.5. Cell viability assay: Lactate dehydrogenase (LDH)

Supernatants from stimulated glial cells and neurons were collected for use in the LDH assay to measure cell death. LDH is a cytoplasmic enzyme that is essential for catalyzing the conversion of lactate to pyruvate. Upon cell damage or lysis LDH is released into the extracellular space. Therefore, the LDH assay can be considered a measure of membrane disruption and cell death¹²¹. The assay is a coupled enzymatic reaction of pyruvate with the tetrazolium salt INT, which changes color to red and can be spectrophotometrically detected by measuring absorbance at 492 nm. The LDH released by dying cells can be quantified and expressed as percent cell death by comparing the optic density (O.D.) values of the stimulated cells to those obtained from a 100%

lysis control, in which unstimulated cells have been lysed with 1% Triton X-100. Previously published experimental procedures for the LDH assay^{29, 123} were modified as follows.

To perform the assay, 100 µl of cell supernatants were collected into a 96-well plate and INT (260 µg/ml) was added to each well. An initial measurement was taken at 492 nm; designated O.D._{initial}. This was followed by the addition of 30 µl of working solution containing lactate (750 µg/ml), β-NAD (60 µg/ml) and diaphorase (55 µg/ml) in PBS to each well. After an incubation time of 15-30 min at 37°C, when the lysis control well appeared dark red, a final measurement was taken at 492 nm, designated O.D._{final}. The following two equations were used to determine percent cell death:

1.) Corrected absorbance (cA) of each sample = O.D._{final} - O.D._{initial}

$$2.) \% \text{ cell death} = \left(\frac{(cA_{\text{sample}} - cA_{\text{media}})}{(cA_{\text{lysis}} - cA_{\text{media}})} \right) \cdot 100\%$$

Where cA_{media} represents the corrected absorbance of the well containing only F5 media and cA_{lysis} represents the corrected absorbance of the cells treated with 1% Triton X-100 (100% cell death control).

2.6. Cell viability assay: MTT

Viability of glial cells and neurons during supernatant transfer experiments was assessed using the MTT assay^{122, 124}. This assay measures cellular metabolic activity via NADPH-dependent cellular oxidoreductase enzymes, thus reflecting the number of viable cells present. The enzymes reduce the tetrazolium dye, MTT, to its insoluble formazan form, which is purple in color and

can be measured spectrophotometrically at a wavelength of 570 nm. Cells with intact metabolic activity have high reduction rates of MTT compared to dying cells. Thus, there is a positive correlation between the formation of the purple formazan dye and cell viability. The MTT assay has been used to accurately measure cell viability of microglial and neuronal cells^{22, 29, 120}. These previously published experimental protocols were modified as follows.

The MTT solution (5mg/ml) was added at a 10x dilution to the wells containing the cells and remaining cell cultures after the partial removal of supernatants for the LDH and ELISA assay. The plates were then incubated for 1-2 h at 37°C, at which point 20% SDS/50% DMF in milli-Q water was added at a 1:1 ratio to each well to solubilize the formazan dye. After an additional incubation period of 3-4 h in a wetbox (Tupperware containing wet paper towel) at 37°C, the O.D. measurement was taken at 570 nm. The percent cell viability was calculated based on the following two equations:

1.) Corrected absorbance (cA) of each sample = $O.D._{sample} - O.D._{media}$

2.) % cell viability = $\left(\frac{cA_{sample}}{cA_{control}} \right) \cdot 100\%$

Where $O.D._{sample}$ represents the absorbance measurement in each well, $O.D._{media}$ represents the absorbance measurement in the media only well, and cA_{sample} represents the corrected absorbance of each sample well. $cA_{control}$ refers to the corrected absorbance measurement of the untreated cells (100% cell viability control).

2.7. Identifying the active domain of TFAM

In addition to isolating full-length TFAM, Dr. Kirsten Wolthers' laboratory, here at UBC Okanagan, also isolated the two high mobility group (HMG) domains of TFAM referred to as Box A and Box B. In order to determine which of the two boxes was mainly responsible for the neurotoxicity induced by TFAM, supernatant transfer experiments were performed, similar to those described by Little et al.¹²⁰.

Any potential endotoxin contamination of Box A and Box B was removed using the Pierce High Capacity Endotoxin Removal Columns (ThermoScientific) and the resulting endotoxin levels were measured to be less than 2 pg/ μ g protein using the Pierce LAL Chromogenic Endotoxin Quantification Kit (ThermoScientific). Only these endotoxin free Box A and Box B samples were used for subsequent experiments.

THP-1 cells were harvested from T-75 flasks and plated at a final concentration of 0.5 million cells/ml in sterile 96-well plates, as described in section 2.4.1.; while the U-118 MG cells and primary human astrocytes were seeded at a final concentration of 0.2 million cells/ml in sterile 96-well plates, as described in section 2.4.1. After 30 min recovery time in the incubator at 37°C, the cells were stimulated with full-length TFAM (2.5 μ g/ml), Box A (2.5 μ g/ml) or Box B (2.5 μ g/ml) in the presence or absence of IFN- γ (150 U/ml). Following 48 h incubation THP-1 cell supernatants were transferred onto SH-SY5Y cells, which had been plated 24 h earlier (see section 2.4.3.). At this time, 100 μ l were collected for ELISA and the remaining THP-1 cell cultures were tested for viability using the MTT assay. The SH-SY5Y cells were incubated for additional 72 h at which point the LDH and MTT assays were performed to assess their viability.

2.8. Identifying the receptors engaged by TFAM: Inhibiting THP-1 promonocytic cell responses with heparin, anti-RAGE or anti-Mac-1 antibody

In order to determine the glial receptors engaged by TFAM, heparin or specific blocking antibodies for RAGE and Mac-1 were used to pre-treat the THP-1 cells. The previously published experimental procedures using heparin⁵¹ and the blocking antibodies^{82, 125} were modified as follows.

THP-1 cells were harvested from T-75 flasks and plated at a final concentration of 0.5 million cells/ml in sterile 96-well plates, as described in section 2.4.1. After 30 min, the cells were pre-treated with either heparin (250 µg/ml), anti-RAGE antibody (10 µg/ml), soluble RAGE (10 µg/ml) or anti-Mac-1 antibody (20 µg/ml). Following 30 min in the incubator at 37°C, the cells were stimulated with TFAM (2.5 µg/ml) in the presence or absence of IFN-γ (150 U/ml). After 48 h incubation, THP-1 supernatants were transferred onto SH-SY5Y cells, which had been plated 24 h earlier (see section 2.4.). At this time, THP-1 supernatants were collected also for ELISA. THP-1 cell viability was assessed by the MTT assay. SH-SY5Y viability was measured using the LDH and MTT assays following an additional 72 h incubation period.

2.9. Effects of TFAM on the secretion of pro-inflammatory cytokines by glial cells

The concentrations of MCP-1, IL-6 and TNF-α secreted by THP-1 cell, U-118 MG cells or primary human astrocytes were measured using ELISA development kits from Peprotech, according to the manufacturer's instructions. This assay relies on the specific interaction between antigens and antibodies, and utilizes the "sandwich" technique. The primary antibody is attached to the well surface and interacts with the MCP-1, IL-6 or TNF-α cytokines (antigens) present in the cell supernatants. Next, an enzyme-conjugated secondary antibody is added, which binds to

the antibody-antigen complex. Upon addition of the enzyme's alkaline phosphatase substrate, the yellow colored break-down product, p-nitrophenol, can be measured spectrophotometrically.

Cell-free supernatants from THP-1 cells, U-118 MG cells and primary human astrocytes were collected from each experiment and stored at -20°C in 96-well plates. The composition of all the reagents and solutions required for the ELISA are listed in Appendix A. The assay was performed as follows: Day 1: 50 μl of primary antibody diluted 1:400 (MCP-1) or 1:100 (IL-6 and TNF- α) in coating buffer (Na_2CO_3 - $\text{NaHCO}_3/\text{H}_2\text{O}$ solution, $\text{pH}=9.6$) were added to each well of a 96-well plate. The plate was then covered with Parafilm and incubated at 4°C overnight. Day 2: The coating buffer was discarded and 180 μl blocking solution (0.5% BSA and 0.5% skim milk powder in PBS) were added to each well, and the plate was incubated in a wetbox for 1 h at 37°C . After discarding the blocking solution the plate was washed twice with PBS-Tween (0.05% Tween in PBS v/v), leaving the solution in the wells after the second wash. The solution was removed from individual wells using the suction system, followed by adding 100 μl of the corresponding samples or standards to the appropriate wells. The concentration of the standards ranged from 0.032 – 10 ng/ml. Four additional media only control wells were also prepared. The plate was covered with Parafilm and incubated at 4°C overnight.

Day 3: The samples were discarded, and the plate was washed three times with PBS-Tween before adding 100 μl of secondary antibody diluted in blocking solution (1:200 for MCP-1 and IL-6, 1:400 for TNF- α) to each well. The plate was then incubated in a wet-box for 45 min at 37°C . After incubation, the secondary antibody solution was discarded and the plate was washed four times with PBS-Tween. 100 μl of extravidin-alkaline phosphatase diluted 1:10,000 in blocking solution were added to the wells. The plate was incubated in a wet-box at 37°C for additional 45 min. Following five washes with PBS-Tween, 100 μl of alkaline phosphatase

substrate solution (5 mg phosphatase substrate tablets dissolved in 5 ml diethanolamine substrate buffer) were added to each well. The absorbance was measured at 405 nm immediately after the addition of the substrate solution and subsequently every hour until the color change could be observed (max O.D. for the blank wells at 0.2 and for the highest standards at 1.2).

The analysis was performed according to the manufacturer's instructions (Peprotech). The change in absorbance of the samples (ΔA_{sample}) and the corrected change in absorbance values (ΔA_{corr}) for each sample were calculated using the following formulas:

- 1.) Absorbance of the samples $\Delta A_{\text{sample}} = \text{O.D.}_{\text{final}} - \text{O.D.}_{\text{initial}}$
- 2.) Corrected change in absorbance values $\Delta A_{\text{corr}} = \Delta A_{\text{sample}} - \Delta A_{\text{blank}}$

To determine the cytokine concentration in each sample, a calibration curve was plotted using the ΔA_{corr} values of the standards (0.032 – 10 ng/ml) and a linear trendline ($y=mx+b$, where m is the slope) was fitted to the curve. The following equations were used to calculate the cytokine concentrations in each sample and the detection limit of the assay:

$$3.) \text{ Cytokine concentration (ng/ml)} = \left(\frac{\Delta A_{\text{corr}}}{m} \right)$$

$$4.) \text{ Detection limit (ng/ml)} = \left(\frac{\text{Average of } \Delta A_{\text{blank}} + 2 \times \text{standard deviation } \Delta A_{\text{blank}}}{m} \right)$$

2.10. Effects of TFAM on the release of superoxide by glial cells

2.10.1. Plating and differentiating HL-60 cells

Differentiated HL-60 cells were used as the microglial model expressing functional NADPH oxidase. Experiments described by Patel et al.¹²⁶ were modified as follows to assess the ability of TFAM to prime ROS release from DMSO-differentiated HL-60 cells.

In order to differentiate the cells, HL-60 were seeded at a concentration of 0.2 million cells/ml into a 10 cm² tissue culture dish in 12 ml of F10 media, and placed in the CO₂ incubator at 37°C for 15 min, following which DMSO was added drop-wise at a concentration of 1.3% (v/v). The cells were allowed to differentiate in the incubator for 5 days before being used in the respiratory burst assay.

Differentiated HL-60 cells were harvested from the 10 cm² tissue culture dish, centrifuged at 450 g for 7 min and plated in 96-well plates at a final concentration of 1 million cells/ml in 250 µl clear (phenol red free) DMEM-F12 media supplemented with 2 % CBS (F2). The cells were allowed to rest for 30 min in the CO₂ incubator at 37°C before being primed with different priming agents. For the first set of experiments, the HL-60 cells were primed with vehicle solution (PBS) or with TFAM (2.5 µg/ml), IFN-γ (150 U/ml) or a combination of the two. For the second set of experiments, the HL-60 cells were primed with TFAM (5 µg/ml), Box A (5 µg/ml) or Box B (5 µg/ml) to determine the domain of TFAM responsible for priming ROS release. For the third set of experiments, the inhibition assays, anti-Mac-1 antibody (20 µg/ml) was added 30 min prior to TFAM (2.5 µg/ml), IFN-γ (150 U/ml) or a combination of the two. For all of the experiments two controls were included, as well: (1) the unprimed control (PBS vehicle control stimulated with fMLP) and (2) the unstimulated control, (primed but not stimulated with fMLP). The plates were then incubated for 24 h before conducting the assay.

2.10.2. Respiratory Burst assay

A variety of cell types, including macrophages and neutrophils, express the subunits of the NADPH oxidase enzyme. Upon cell activation, the subunits assemble and generate a respiratory burst which results in the production of ROS that acts as part of the host defense machinery. Chemiluminescence assays detect the production of light, due to the interaction between the compound luminol and ROS. The light produced can be measured by a plate reader, and can be plotted as light production over time to calculate ROS generation.

To conduct the assay, 85 μ l of each sample were transferred into a new 96-well plate. Luminol was diluted to 50 mM in PBS, pre-heated in the dry incubator at 37°C for 5-10 min and then loaded into the first injector of the FLUOstar Omega plate reader prior to each experiment. To induce the respiratory burst in HL-60 cells, fMLP, a bacterial cell wall component, was used as the stimulant. fMLP was diluted to 20 μ M in PBS, also pre-heated at 37°C for 5-10 min and then loaded into the second injector of the plate reader. The plate containing HL-60 cells was placed into the plate reader, which was pre-heated to 37°C. The plate reader was programmed to take measurements at each cycle over a 60 cycle period, with each cycle lasting 21 s. Luminol and fMLP were injected at different volumes and time points during the assay, 10 μ l at cycle 5 and 5 μ l at cycle 15, respectively. The light measurements taken at each cycle were plotted over time to generate a curve, which was analyzed using the Mars Analysis Software (BMG Labtech). The curve obtained was baseline corrected to adjust for the background production of light, which was calculated as the average values from cycles 40-60. The area under the curve of the light measurements from cycles 15-39 was integrated to produce a chemiluminescent (CHL) value for each well. The data was expressed as % CHL of the PBS (vehicle) control well.

$$1.) \text{ nCHL} = \text{CHL}_{\text{cycles 15-39}} - \text{CHL}_{\text{cycles 40-60}}$$

$$2.) \% \text{ CHL} = \left(\frac{\text{nCHL}_{\text{sample}}}{\text{nCHL}_{\text{control}}} \right) \cdot 100\%$$

Where $\text{CHL}_{\text{cycles}}$ represents the sum of the curve value for each well, and nCHL represents the baseline corrected, normalized CHL signal. The percentage CHL (% CHL) was obtained by dividing the normalized CHL value for the sample well ($\text{nCHL}_{\text{sample}}$) by the normalized CHL value of the control well ($\text{nCHL}_{\text{control}}$).

2.11. Effects of biochemical stressors on the TFAM mRNA expression levels by astrocytic cells

2.11.1. mRNA extraction from U-373 MG astrocytic cells and primary human astrocytes

RNA extraction was performed on at least 3 independently grown populations of U-373 MG cells and at least three different surgical cases of primary human astrocytes. As U-373 MG cells are more resilient to insult, especially oxidative damage, compared to U-118 MG cells, they were chosen for the qPCR experiments. Positive results obtained by using U-373 MG cells were confirmed with the primary human astrocytes. RNA extraction was performed according to the instruction manual of the Aurum Total RNA Mini Kit from Bio-Rad. All the reagents mentioned except for the ice cold PBS and the 70% molecular grade ethanol were provided in the kit.

Adherent U-373 MG cells and primary human astrocytes were removed from the surface of the flask by incubating the cells in 1.5 ml of 0.25% trypsin/EDTA solution for 2 min at 37 °C, followed by gentle tapping of the T-75 flask to aid the detachment of cells from the flask surface. Trypsin was neutralized by adding 10 ml of F10 media. Cells were then counted, centrifuged at

450 g for 7 min and re-suspended to a final concentration of 0.5 million cells/ml. The U-373 MG cells were seeded in 2 ml F10 media per well in sterile 6-well plates, while the primary human astrocytes were seeded in 10 ml F10 per well in sterile 10 cm² tissue culture dishes. Both U-373 MG and primary human astrocytes were left to adhere to the petri dish surface for 24 h in the incubator. Following the incubation period, the U-373 MG cells were treated with IFN- γ (150 U/ml), H₂O₂ (100 μ M), IFN- γ (150 U/ml) plus IL-1 β (100 U/ml), or the PBS vehicle control. Since H₂O₂ was the only stressor to significantly induce the expression of TFAM in U-373 MG cells, and sufficient amounts of RNA are often difficult to obtain from primary human astrocytes, H₂O₂ was the only stimulant investigated for its ability to induce TFAM expression in primary human astrocytes. However, H₂O₂ was added at a concentration of 50 μ M instead of 100 μ M, due to the increased sensitivity of primary cells to stressors such as H₂O₂. After additional 24 h incubation with the stimulants, RNA was extracted from the cells.

2.11.2. mRNA spin column protocol

After the final incubation, all the media was removed from the plates and the cells were washed once with ice-cold PBS. Cells were lysed by adding 350 μ l of the lysis solution provided in the kit, followed by the addition of 350 μ l of 70% molecular grade ethanol. The solutions were pipetted up and down to mix thoroughly, and transferred into a 2 ml microtube containing an RNA binding column. The tube was capped and centrifuged for 30 s at 12,000 g. The lysis/ethanol solution was discarded and 700 μ l of low stringency wash solution was added to the column. The columns were centrifuged for 30 s at 12,000 g and the flow-through was discarded. 80 μ l of DNase I solution was made by combining 5 μ l of DNase I powder reconstituted in 10 mM Tris with 75 μ l of DNase dilution buffer, and was added to each column. The columns were

allowed to incubate with this solution for 15 min at room temperature to remove any potential genomic DNA contamination from the samples. Following incubation, 700 µl of high stringency wash solution was added to the columns. Columns were centrifuged for 30 s at 12,000 g and the flow-through was discarded, followed by addition of 700 µl of low stringency solution and centrifugation at 12,000 g for 1 min. To remove any residual wash solution the columns were centrifuged at 12,000 g for an additional 2 min. The columns were then transferred to 1.5 ml capped Eppendorf tubes and 80 µl of elution solution was added and allowed to incubate for 1 min for columns containing extracts from U-373 MG cells. To elute RNA from primary human astrocytes 40 µl of elution solution was added instead of 80 µl. The columns were centrifuged for 2 min at 12,000 g and the total eluted RNA was collected. The RNA was quantified spectrophotometrically using a NanoDrop 1000 (Thermo Scientific), and the OD_{260/280} values were all within the accepted range of 1.8-2. RNA was stored at -80°C prior to cDNA conversion.

2.11.3. cDNA synthesis

The iScript cDNA synthesis kit (Bio-Rad) was used according to the manufacturer's protocol to convert RNA to cDNA. One µg of each RNA sample was converted to cDNA by combining 4 µl of RT reaction mix and 1 µl of reverse transcriptase enzyme with appropriate volumes of the RNA solution and nuclease-free water to make up a total reaction volume of 20 µl in a 0.2 ml Eppendorf tube. The tubes were finger vortexed, briefly centrifuged, and then placed in a C-1000 thermal cycler (Bio-Rad). The RT reaction was carried out in three stages: 5 min at 25°C, 30 min at 45°C, and 5 min at 85°C. The cDNA samples were diluted 1:5 in nuclease-free water and stored at -20°C.

2.11.4. Quantitative polymerase chain reaction (qPCR)

The TFAM forward and reverse primer sequences were obtained from a previous publication ¹²⁷, and are listed in Table 1. The primers were purchased from Integrated DNA Technologies (IDT) and checked for specificity using the national centre for biotechnology information (NCBI) primer basic local alignment search tool (BLAST).

Table 1: TFAM primer sequences used in qPCR experiments

Forward Primer Sequence (5'-3')	Reverse Primer Sequence (5'-3')	Amplicon (bp)
AAA GAT TCC AAG AAG CTA AGG GTG	CCT AAC TGG TTT CCT GTG CCT A	292

Tests for optimal annealing temperature, primer dimer formation and primer efficiency were conducted on the primer set before its use in the qPCR experiment to ensure that Minimum Information for Publication of Quantitative Real-Time PCR Experiments (MIQE) guidelines were met ¹²⁸. The amplification curve was used to determine the optimal annealing temperature for the primer sets, while the melt curve analysis was performed to demonstrate amplification specificity, which was confirmed by the presence of a single peak in the melt curve. Primer efficiency was evaluated by plotting template dilutions against cycle threshold values (Ct), resulting in a standard curve which was within standard accepted values of 90-110% ¹²⁹. The efficiency curve for the TFAM primer pair is shown in Figure 2.

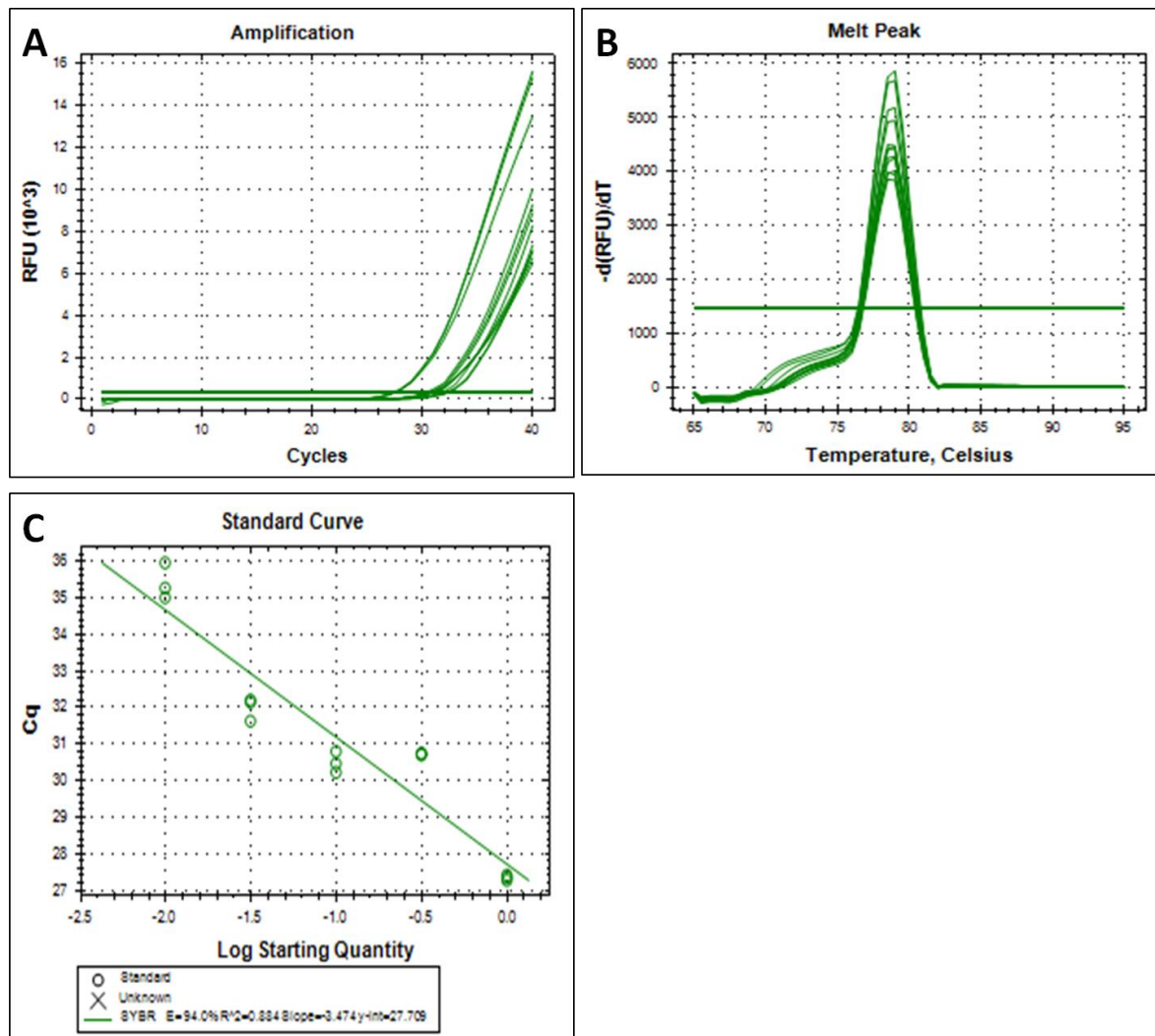


Figure 2. TFAM primer efficiency data. cDNA from U-373 MG cells stimulated with IFN- γ (150 U/ml) for 24 h was used to optimize primers. TFAM primer amplification curve (A), melt curve (B) and standard curve (C) are shown. All values are within standard accepted values for publishing¹²⁹.

qPCR reactions were performed in duplicate on 3-5 independent biological samples and at least three different surgical cases of primary cells in 96-well plates (Bio-Rad). The total reaction volume for each reaction was 10 μ l, containing: 5 μ l Ssofast Evagreen Supermix (Bio-Rad), 0.8 μ l of each primer set (5 μ M), 1 ng of cDNA template and 3.2 μ l of nuclease-free water.

The negative controls: no template control (NTC) and no reverse transcriptase control (NRT) were included to ensure that the observed amplification is not due to DNA contamination in the solutions. The reactions were performed in the CFX96 Real Time System (Bio-Rad) and consisted of the following steps: 95°C for 5 min, followed by 40 cycles of 95°C for 5 s, 59°C for 5 s, followed by a disassociation stage of 95°C for 10 s, 65°C for 5 s, and 95°C for 5 s. The gene expression in each sample was normalized to the reference gene beta-actin expression level. The relative quantification of RNA in each stimulated sample was calculated using the $\Delta\Delta C_t$ method with the unstimulated samples serving as the control.

2.12. Effects of TFAM on microparticle release by glial cells

2.12.1. Isolating microparticles from THP-1 promonocytic cells

MPs were isolated using previously published protocols^{88, 130, 131}, which were modified as follows. THP-1 cells were counted using the hemocytometer, centrifuged at 450 g for 7 min and re-suspended at a concentration of 0.5 million cells/ml in sterile 24-well plates (see section 2.4.1.). The cells were incubated for 30 min at 37°C. Then, they were stimulated with TFAM (2.5 µg/ml), IFN- γ (150 U/ml), LPS (0.5 µg/ml) or the vehicle control and incubated for 24 h. Following the incubation period, the cultured supernatants from each well were collected in separate 50 ml centrifuge tubes and differentially centrifuged in three steps at 4°C: (1.) 5 min at 300 g, (2.) 20 min at 1,200 g, (3.) 30 min at 10,000g. After each centrifugation step, the supernatants were collected and transferred into new 50 ml tubes. After the third step, however, the supernatants were discarded. The pellets were re-suspended in 1 ml of sterile PBS and transferred into 1.5 ml Eppendorf tubes. Tubes were centrifuged for 30 min at 10,000 g to wash the MPs. Following the wash step, PBS was discarded and the pellet was re-suspended in 500 µl

1X Annexin-V binding buffer, diluted 10X in sterile miliQ water from the Annexin-V Apoptosis Detection Kit (BD Biosciences). The samples were kept at -20°C .

MPs were identified under the Olympus fluorescence microscope (Figure 3) and analyzed using MetaMorph (Molecular Devices, Sunnyvale CA). However, the size of the visible MPs suggested that they were aggregates. Therefore, the flow cytometer was used to quantify the MPs instead.

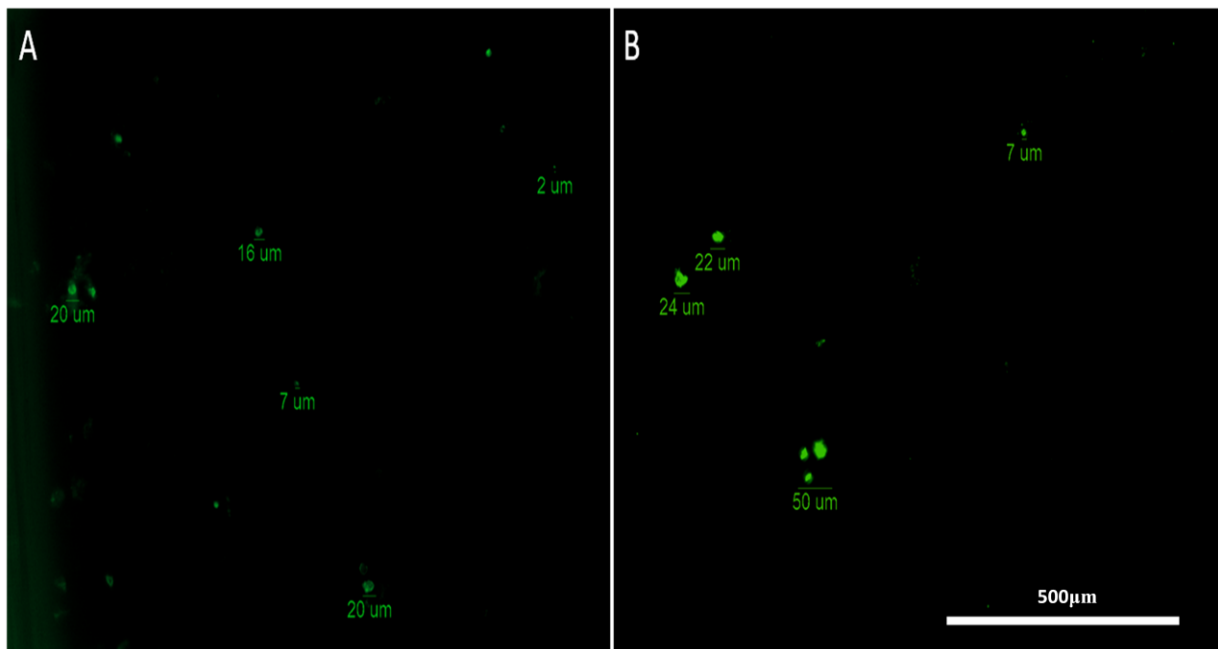


Figure 3. Example of MPs stained with Annexin-V-FITC visualized under the Olympus fluorescence microscope (100 x total magnification).

For use in the flow cytometer, 100 μl of PBS containing MPs were transferred into 1.5 ml Eppendorf tubes and 5 μl of Annexin-V-FITC were added. Annexin-V was selected as it binds to the externalized phosphatidylserine on the surface of MPs. The tubes were incubated at room temperature, in the dark for 15 min. Next, the tubes were centrifuged for 30 min at 10,000g to

remove any unbound Annexin-V-FITC. The pellet was re-suspended in 100 μ l 1X Annexin-V binding buffer and analyzed using the MACSQuant Analyzer (Miltenyi Biotec) (Figure 3).

The flow cytometer was calibrated using beads of a predetermined size (1-900 nm). These were passed through the flow cytometer. As a result, a calibration gate (see arrow in Figure 4A) could be drawn in the MACSQuant Analyzer program to characterize the MPs that were in the 1-900 nm size range. Once the flow cytometer had been calibrated, 20 μ l of each sample were taken up and analyzed for the presence of MPs. If MPs are present within the sample solution, they scatter light of the laser beam within the flow cytometer. Detectors then pick up the forward- and side-scattered light to detect and quantify the MPs in the sample suspension. Forward-scattered light determines the size, while side-scattered light determines the granularity/complexity of the particles.

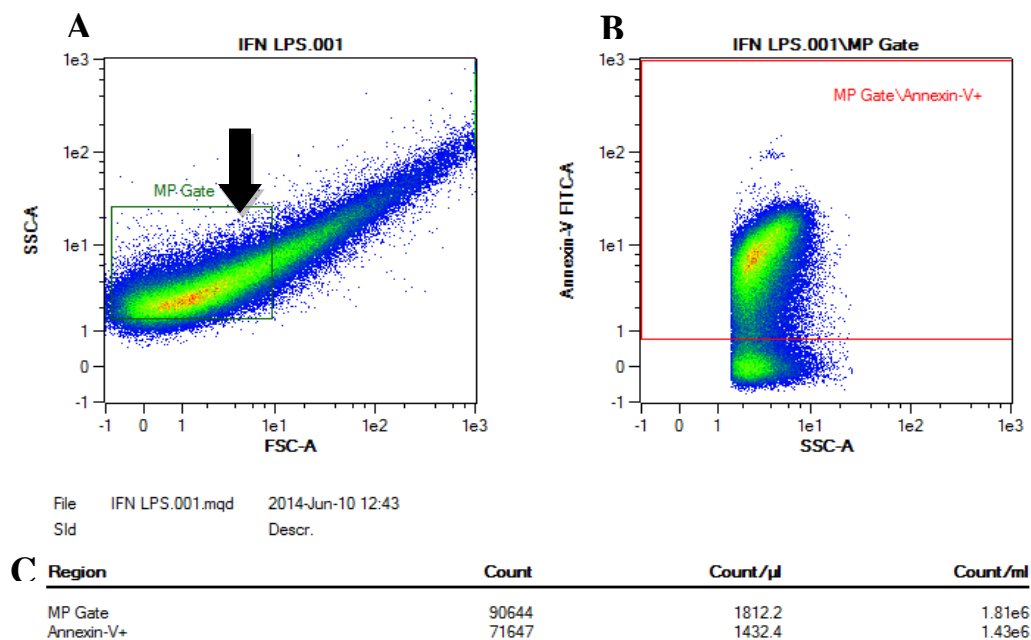


Figure 4. Example of flow cytometry data. THP-1 cells were stimulated with IFN- γ (150 U/ml) plus LPS (0.5 μ g/ml) for 24 h. Cultured supernatants were differentially centrifuged to isolate MPs. MPs were stained with Annexin-V-FITC and quantified by flow cytometry. (A) indicates the gate used to calibrate the flow cytometer. (B) illustrates the number of MPs that fall within the gate and stain positive for Annexin-V. (C) The table shows the MP counts recorded in each region (MP Gate and Annexin-V+).

2.12.2. Determining the neurotoxic properties of microparticles

To assess the neurotoxic properties of the isolated MPs previously published experimental procedures¹³² were modified as follows. The isolated MPs were used to stimulate THP-1 cells to determine whether MPs affect THP-1 cell viability. Subsequently, THP-1 cell supernatants were transferred onto SH-SY5Y neuronal cells to assess their potential neurotoxicity. In addition, the isolated MPs were investigated for their ability to induce ROS release from HL-60 cells using the respiratory burst assay.

In order to use the MPs as stimulants in the transfer and respiratory burst experiments, the protein concentrations present in each MP sample were determined, to ensure that the THP-1 cells and the HL-60 cells were stimulated with equal amounts of MPs. The Pierce BCA Protein Assay Kit (ThermoScientific) was used according to the manufacturer's instructions. A dilution series of BSA standards ranging from 0.025 to 2 mg/ml was prepared by diluting the BSA stock solution in dH₂O. Then 10 µl of MP samples were pipetted in duplicate into a 96-well plate. 200 µl of working reagent (50 : 1, Reagent A:B from the kit) were added to each sample, after which the plate was placed on the plate shaker and mixed thoroughly for 30 s. The plate was covered with Parafilm and incubated at 37°C in the dry incubator for 30 min, followed by the absorbance (O.D.) measurement at 570 nm. The average O.D. for each standard was plotted as a function of the protein concentration used to generate a standard curve, which was required to calculate the protein concentration in the unknown MP samples.

For the transfer experiments, THP-1 cells were counted, centrifuged at 450 g for 7 min and re-suspended at a concentration of 0.5 million cells/ml in sterile 96-well plates (see section 2.4.1.). After 30 min recovery time in the incubator, the cells were stimulated with the THP-1-derived MPs (10 µg of protein/ml) and incubated at 37°C for 48 h. Following the incubation period, the cultured supernatants were transferred onto SH-SY5Y cells that had been plated 24 h earlier (see section 2.4.2.). In addition, 100 µl were collected for IL-6, TNF-α and MCP-1 ELISA assays and the remaining supernatants were tested for THP-1 cell viability using the MTT assay. The SH-SY5Y cells were incubated for an additional 72 h at which point the LDH and MTT assays were performed.

For the respiratory burst experiments, HL-60 cells were differentiated with DMSO for 5 days, as described in section 2.10.1. Differentiated HL-60 cells were harvested from the 10 cm²

tissue culture dish, centrifuged at 450 g for 7 min and plated in 96-well plates at a final concentration of 1 million cells/ml in 250 µl clear (phenol red free) F2. The cells were allowed to rest for 30 min in the CO₂ incubator at 37°C before being primed with the THP-1 cell-derived MPs (10 µg of protein/ml) and incubated at 37°C for 24 h. Following incubation, the respiratory burst assay was performed (see section 2.10.2.).

2.13. Statistical Analyses

SPSS software (version 22.0, IBM SPSS, Chicago IL, USA) and GraphPad PRISM software (version 6.0, GraphPad Software Inc, La Jolla CA, USA) were used to conduct statistical analyses of the data. Randomized block design-analysis of variance (ANOVA) was used to test for significance, as it accounts for the high variability between different experimental days by organizing data from each day into a block. The ANOVA was followed by Fisher's least significant difference (LSD) post hoc test for multiple comparisons to evaluate the significance of individual differences. Data are presented as means ± standard error of the mean (SEM) and significance was established at P<0.05. Significant differences from the unstimulated control is indicated on the graphs as follows: *P<0.05, **P<0.01. Significant differences between uninhibited and inhibited cells or between different treatments is indicated on the graphs as follows: #P<0.05, ##P<0.01 or &P<0.05, &&P<0.01.

Chapter 3. Results

3.1. Toxicity of TFAM-stimulated THP-1 promonocytic cells towards SH-SY5Y neuronal cells

TFAM was tested for its ability to induce THP-1 cytotoxicity towards SH-SY5Y neuronal cells. Experiments were performed as described in the Materials and Methods section 2.4.1. TFAM was tested at a concentration of 2.5 $\mu\text{g/ml}$ in the presence or absence of IFN- γ (150 U/ml), as this combination has previously been shown to successfully induce THP-1 cell activation¹²⁰. The results were compared to the data obtained from the PBS-vehicle treated cells. In addition, as a positive control, THP-1 cells were treated with IFN- γ plus LPS (0.5 $\mu\text{g/ml}$), as well as a pro-inflammatory cocktail composed of IL-6 (1 ng/ml), IL-1 β (100 U/ml) and TNF- α (2 ng/ml), as these combinations of stimulants have previously been shown to induce the activation of microglial cells and subsequent neurotoxicity²². Following 48 h stimulation, the viability of THP-1 cells was measured by the MTT assay (Figure 5A). TFAM and IFN- γ on their own, as well as TFAM plus IFN- γ did not significantly affect the viability of THP-1 cells. The pro-inflammatory cocktail and IFN- γ plus LPS decreased the viability of the THP-1 cells, which has been observed before with potent monocytic cell stimuli^{22, 120}.

THP-1 supernatants were transferred onto SH-SY5Y cells and following a 72 h incubation period the viability of the SH-SY5Y cells was measured by the MTT assay (Figure 5B). Stimulation of THP-1 cells with TFAM or IFN- γ on their own did not induce THP-1 toxicity towards SH-SY5Y cells, and no decrease in neuronal cell viability was measured. In contrast, TFAM plus IFN- γ induced microglial toxicity towards neuronal cells, as demonstrated by a decrease in viability to ~60% (Figure 5B). Furthermore, the pro-inflammatory cocktail, as

well as IFN- γ plus LPS induced THP-1 toxicity towards SH-SY5Y cells and caused a decrease in neuronal cell viability, thus demonstrating that the assay performed as expected.

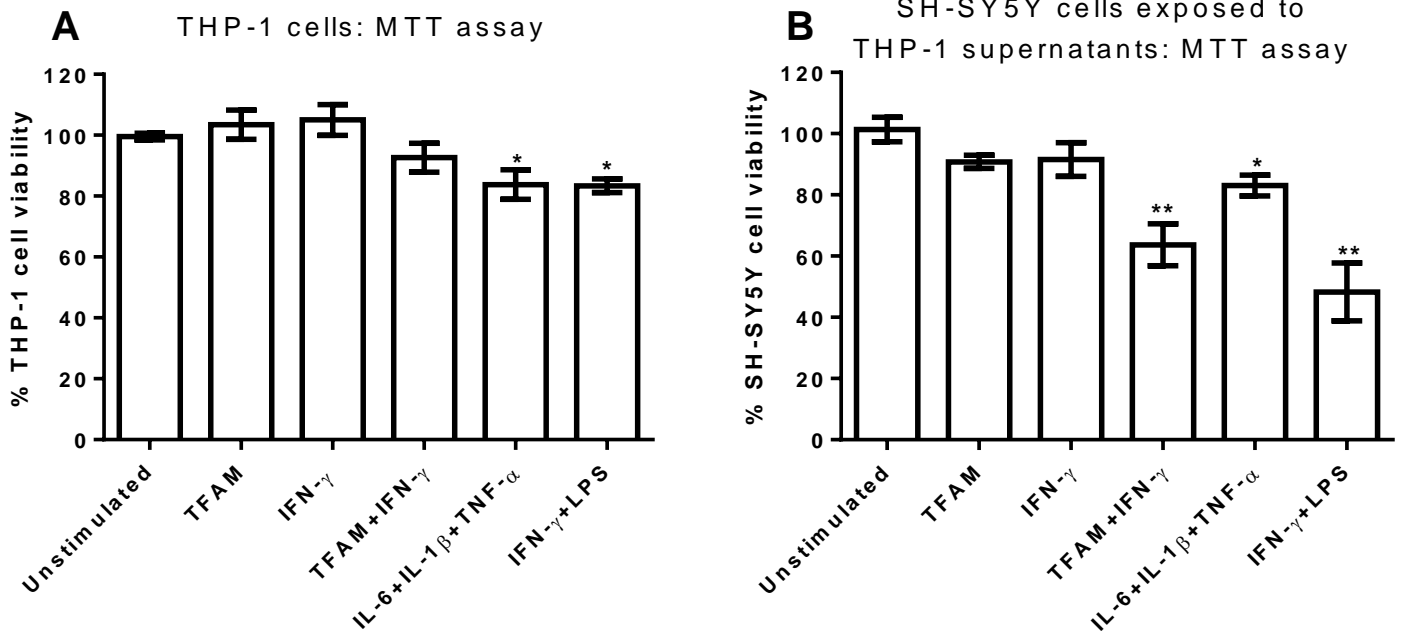


Figure 5. TFAM plus IFN- γ induces THP-1 toxicity towards SH-SY5Y cells. (A) THP-1 cells were treated with TFAM (2.5 μ g/ml), IFN- γ (150 U/ml), LPS (0.5 μ g/ml), IL-6 (1 ng/ml), IL-1 β (100 U/ml), TNF- α (2 ng/ml) or combinations of these stimulants as shown on the abscissa. THP-1 cell viability was measured by the MTT assay at the end of the 48 h incubation period with the stimuli. (B) The MTT assay was used to test the viability of SH-SY5Y cells exposed for 72 h to conditioned media from unstimulated THP-1 cells or THP-1 cells differentially treated as described on the abscissa. Data from 3-10 independent experiments are presented (means \pm SEM). *P<0.05, **P<0.01, significantly different from unstimulated control (ANOVA, followed by Fisher's LSD post-hoc test).

3.2. Toxicity of stimulated U-118 MG astrocytic cells towards SH-SY5Y neuronal cells

To determine the effect of TFAM on a different glial model, the above experiments (see section 3.1.) were repeated in a similar manner using U-118 MG astrocytic cells. TFAM and IFN- γ were again tested for their ability to induce glial activation resulting in toxicity towards the SH-SY5Y neuronal cells. The experiments were performed as described in the Materials and Methods section 2.4.1.

The U-118 MG cells were stimulated with TFAM, IFN- γ , TFAM plus IFN- γ and a combination of IFN- γ plus IL-1 β , as the latter has been shown to be effective at inducing activation of these cells, similar to IFN- γ plus LPS in THP-1 cells^{112, 113}. After 48 h incubation, U-118 MG cell viability was tested using the MTT assay, and no significant decrease in viability could be detected (Figure 6A). Aliquots of the cultured supernatants were collected to be analyzed by ELISA (Figure 7). Supernatants were also transferred onto SH-SY5Y neuronal cells to investigate the neurotoxic potential of TFAM in astrocyte-like cells. After 72 h incubation of the SH-SY5Y cells with the U-118 MG cell supernatants, the neuronal cell viability was tested by the MTT assay (Figure 6B).

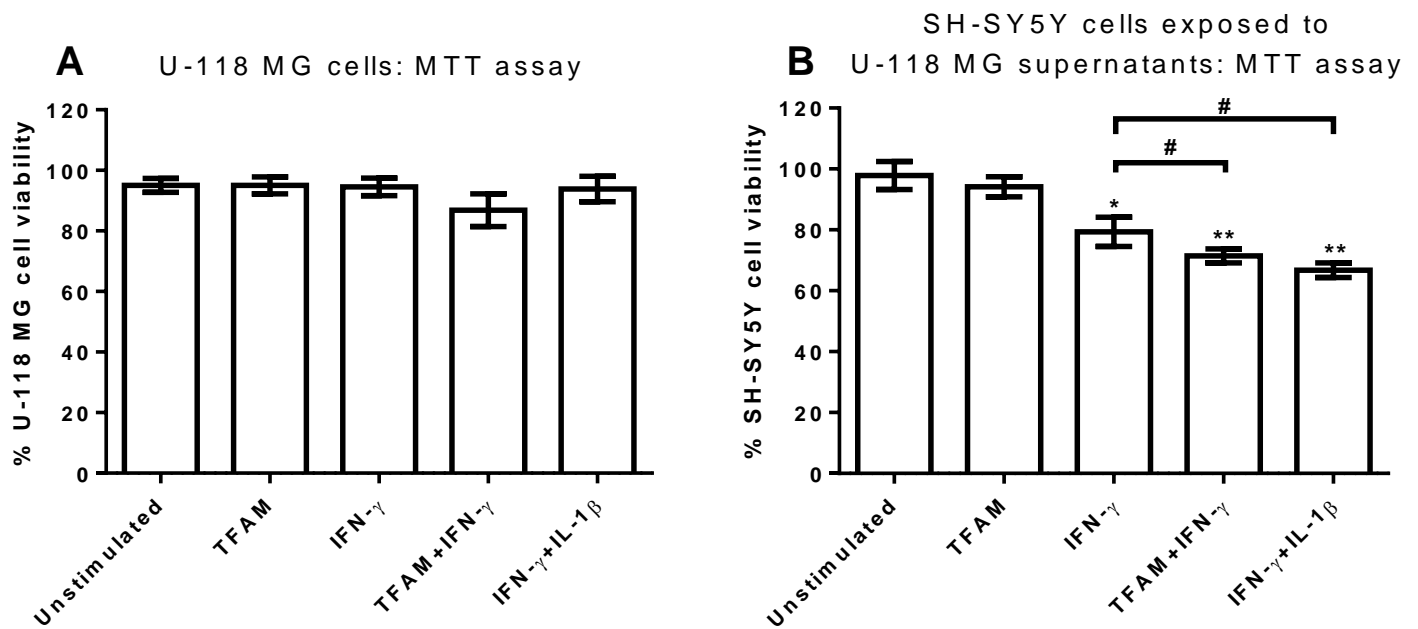


Figure 6. TFAM plus IFN- γ induces U-118 MG toxicity towards SH-SY5Y neuronal cells.

(A) U-118 MG cells were treated with TFAM (2.5 μ g/ml), IFN- γ (150 U/ml), IL-1 β (100 U/ml) or combinations of these stimulants as shown on the abscissa. U-118 MG cell viability was measured by the MTT assay at the end of the 48 h incubation period with the stimuli. (B) The MTT assay was used to test the viability of SH-SY5Y cells exposed for 72 h to conditioned media from unstimulated U-118 MG cells or U-118 MG cells differentially treated as described on the abscissa. Data from 3-10 independent experiments are presented (means \pm SEM).

*P<0.05, **P<0.01, significantly different from unstimulated control; #P<0.05, significant difference between IFN- γ and TFAM plus IFN- γ or between IFN- γ and IFN- γ plus IL-1 β (ANOVA, followed by Fisher's LSD post-hoc test).

Stimulation of U-118 MG cells with TFAM alone did not significantly reduce the viability of SH-SY5Y cells (Figure 6B). However, in combination with IFN- γ , TFAM induced U-118 MG toxicity towards SH-SY5Y cells, observed by a significant decrease in viability of the neuronal cells to ~70% viability (Figure 6B). IFN- γ on its own also induced U-118 MG toxicity towards SH-SY5Y cells, as seen by a similar decrease in the viability of the neurons. However, there was a significant difference between the effect of IFN- γ - and TFAM plus IFN- γ -stimulated

U-118 MG cells on the SH-SY5Y cells (Figure 6B), indicating that the observed neuronal toxicity was due to TFAM stimulation in addition to the effect of IFN- γ stimulation. Moreover, IFN- γ plus IL-1 β , acting as the positive control, induced U-118 MG toxicity, decreasing SH-SY5Y cell viability, thus demonstrating the utility of the assay.

The collected U-118 MG supernatants were analyzed to characterize the induced neurotoxicity. The supernatants were analyzed by IL-6 and TNF- α ELISA. The results showed that TFAM did not significantly induce the release of either IL-6 (Figure 7A) or TNF- α (Figure 7B) from U-118 MG cells. Similarly, TFAM plus IFN- γ were not able to induce measurable secretion of IL-6 or TNF- α from U-118 MG cells, nor did IFN- γ plus IL-1 β .

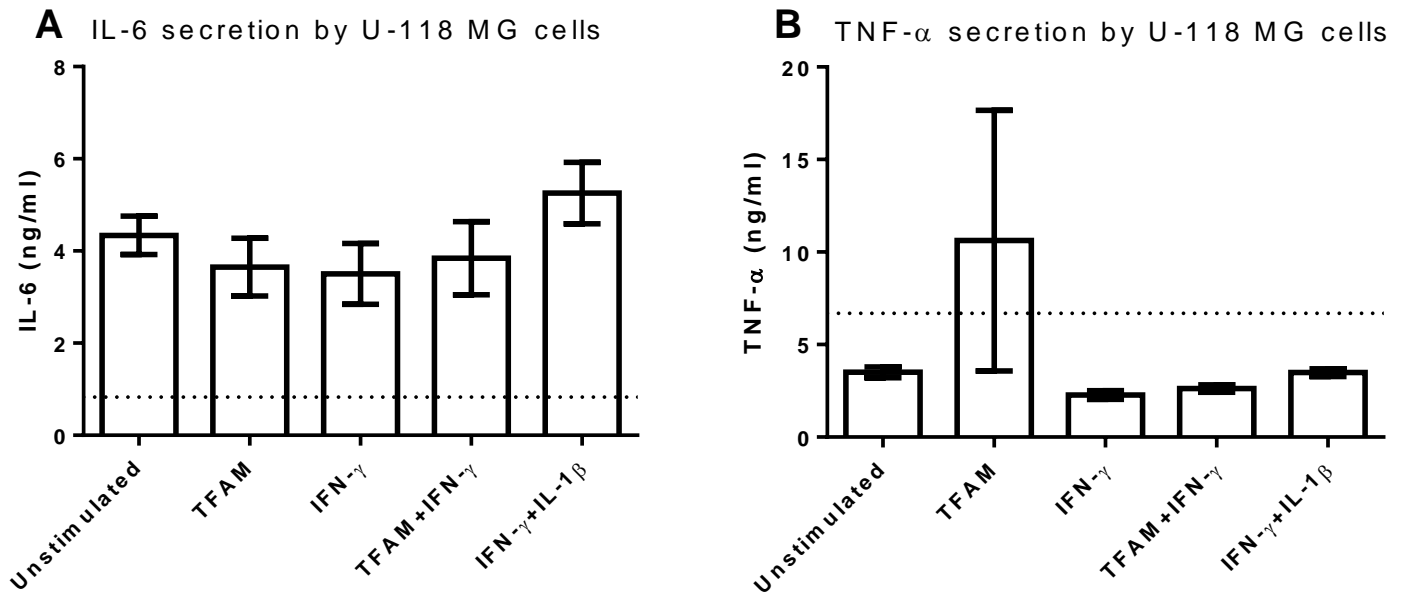


Figure 7. TFAM has no effect on IL-6 or TNF- α secretion by U-118 MG cells. U-118 MG cells were treated with TFAM (2.5 μ g/ml), IFN- γ (150 U/ml), IL-1 β (100 U/ml) or combinations of these stimulants as shown on the abscissa. ELISA was used to measure (A) IL-6 and (B) TNF- α in U-118 MG supernatants after 48 h incubation with stimuli. Data from 3-4 independent experiments are presented (means \pm SEM). No significance could be detected between the different stimulants (ANOVA, followed by Fisher's LSD post-hoc test). Dotted lines represent the ELISA detection limits.

3.3. Toxicity of stimulated primary human astrocytes towards SH-SY5Y neuronal cells

TFAM was tested for its ability to induce primary human astrocyte toxicity towards SH-SY5Y neuronal cells to confirm the results obtained with the U-118 MG astrocytic cells (see section 3.2.). The experiments were performed as described in the Materials and Methods section 2.4.1.

Primary human astrocytes were treated with TFAM, IFN- γ , TFAM plus IFN- γ or IFN- γ plus IL-1 β for 48 h. After the incubation period, viability of the primary human astrocytes was assessed by using the MTT assay (Figure 8A). Similar to the results obtained with the U-118 MG cells, none of the stimulants significantly affected the viability of the primary human astrocytes.

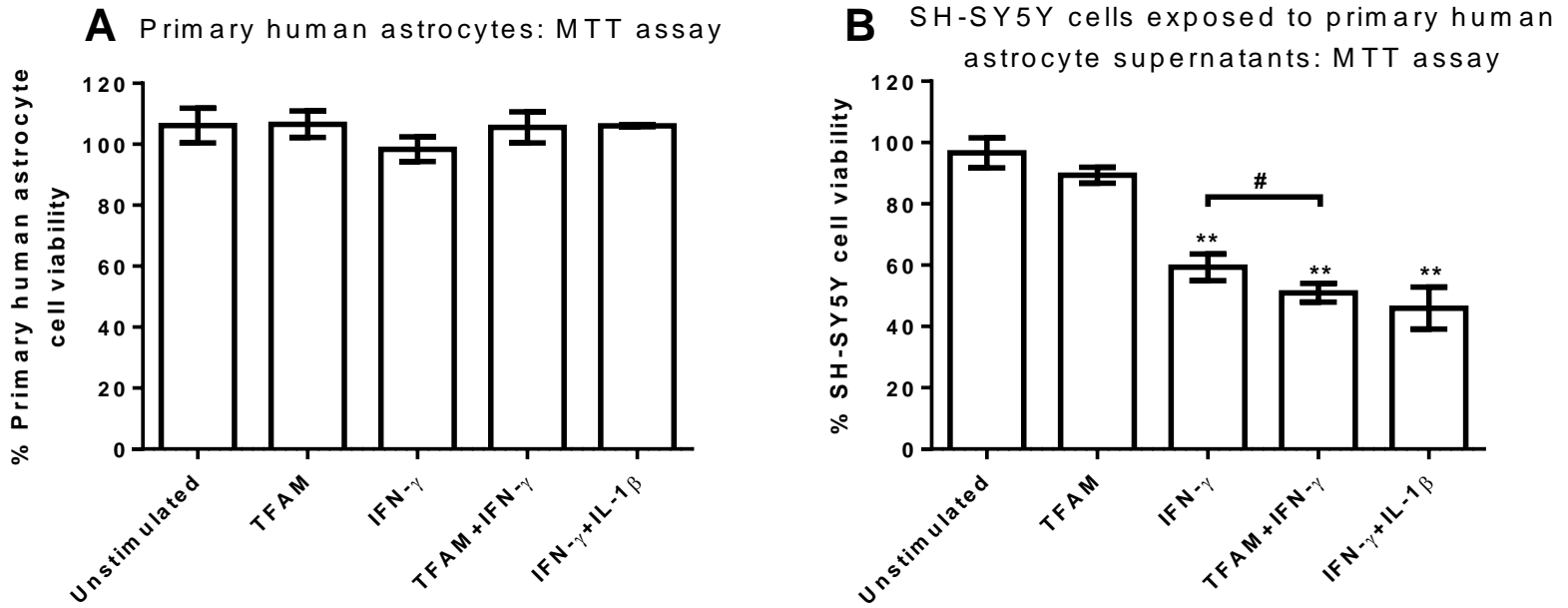


Figure 8. TFAM plus IFN- γ induces primary human astrocyte toxicity towards SH-SY5Y neuronal cells. (A) Primary human astrocytes were treated with TFAM (2.5 μ g/ml), IFN- γ (150 U/ml), IL-1 β (100 U/ml) or combinations of these stimulants as shown on the abscissa. Primary human astrocyte viability was measured by the MTT assay at the end of the 48 h incubation period with the stimuli. (B) The MTT assay was used to test the viability of SH-SY5Y cells exposed for 72 h to conditioned media from unstimulated primary human astrocytes or primary human astrocytes differentially treated as described on the abscissa. Data from 3-4 independent experiments are presented (means \pm SEM). **P<0.01, significantly different from unstimulated control; #P<0.05, significant difference between IFN- γ and TFAM plus IFN- γ (ANOVA, followed by Fisher's LSD post-hoc test).

The supernatants from the primary human astrocytes were transferred onto the SH-SY5Y neuronal cells to assess their cytotoxic potential. The neuronal cells were incubated for 72 h, following which their viability was tested with the MTT assay (Figure 8B). TFAM did not induce glial cell activation resulting in observed toxicity towards the neuronal cells. In the presence of IFN- γ , however, primary human astrocytes became activated, which resulted in a

decrease in the viability of the SH-SY5Y cells (Figure 8B). Moreover, similar to the results obtained from the IFN- γ -stimulated U-118 MG cells, the primary human astrocytes stimulated with IFN- γ alone also showed a negative effect on the viability of the SH-SY5Y cells. However, there was a significant difference between IFN- γ alone and TFAM plus IFN- γ (Figure 8B) indicating that TFAM in addition to the effects caused by IFN- γ is responsible for the observed neurotoxicity in these cells, as well. The utility of the assay was once more confirmed by the positive control IFN- γ plus IL-1 β , which elicited primary human astrocyte toxicity towards SH-SY5Y cells.

The primary human astrocyte supernatants that had been collected after the 48 h incubation period with the different stimuli were analyzed by IL-6 ELISA (Figure 9). TFAM alone increased the secretion of IL-6 by primary human astrocytes above the level of unstimulated control cells. TFAM plus IFN- γ significantly increased IL-6 secretion by primary human astrocytes compared to the secretion by the unstimulated control (Figure 9). Furthermore, the IL-6 secretion induced by TFAM plus IFN- γ was significantly higher compared to the IL-6 secretion induced by TFAM alone (Figure 9). IFN- γ plus IL-1 β (positive control) also significantly increased IL-6 release by primary human astrocytes compared to the levels released by unstimulated control cells, indicating that the ELISA successfully detected differences in cytokine secretion ¹²⁰.

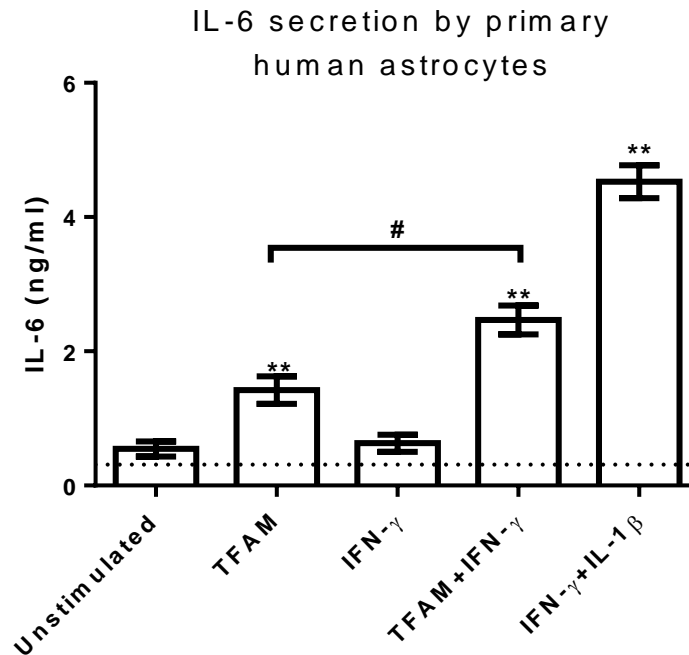


Figure 9. TFAM induces the secretion of IL-6 by primary human astrocytes. Primary human astrocytes were stimulated with TFAM (2.5 μ g/ml), IFN- γ (150U/ml), TFAM plus IFN- γ or IFN- γ plus IL-1 β (100 U/ml) as shown on the abscissa. ELISA was used to measure IL-6 in primary human astrocyte supernatants after 48 h incubation with the stimuli. Data from 3-4 independent experiments are presented (means \pm SEM). ** P <0.01, significantly different from unstimulated control; # P <0.05, significant difference between TFAM and TFAM plus IFN- γ (ANOVA, followed by Fisher's LSD post-hoc test). Dotted line represents the ELISA detection limit.

3.4. Toxicity of TFAM Box A- and Box B-stimulated glial cells towards SH-SY5Y neuronal cells

The TFAM domain responsible for the induction of glial cell toxicity towards neuronal cells was investigated. The effects of the individual HMG boxes of TFAM, Box A (2.5 μ g/ml) and Box B (2.5 μ g/ml) on microglia and astrocytes were tested in these experiments and compared to the

effects of full-length TFAM (2.5 µg/ml), as well as to unstimulated PBS-vehicle treated cells. The experiments were performed as described in the Materials and Methods section 2.7.

3.4.1. The effect of TFAM Box A and Box B on THP-1 cells

THP-1 cells were stimulated with full-length TFAM, TFAM Box A or TFAM Box B in the presence or absence of IFN- γ for 48 h to determine differences in the toxic potential of these stimulants. After the incubation period, the viability of the THP-1 cells was measured by the MTT assay (Figure 10A). The results showed that none of the stimulants significantly affected the viability of THP-1 cells.

THP-1 cell supernatants were collected for ELISA analysis and transferred onto SH-SY5Y cells to determine their neurotoxicity. After 72 h incubation in the supernatants, the viability of the SH-SY5Y cells was assessed by the MTT assay (Figure 10B). TFAM plus IFN- γ induced the activation of THP-1 cells, leading to a decrease in the viability of the neuronal cells to ~60% (Figure 10B). Similarly, Box A plus IFN- γ - and Box B plus IFN- γ -stimulated THP-1 cells significantly reduced the viability of the neuronal cells (Figure 10B). The difference between the effects on SH-SY5Y cell viability caused by THP-1 cells stimulated with Box A or Box B was not statistically significant. Similarly, the difference between the decrease in neuronal viability caused by Box A plus IFN- γ - or Box B plus IFN- γ -stimulated THP-1 cells and that caused by full-length TFAM plus IFN- γ -stimulated THP-1 cells was not significantly different. Thus the data indicated that Box A and Box B were equipotent at inducing toxicity of THP-1 cells towards SH-SY5H cells. The previously collected THP-1 supernatants were analyzed by ELISA for MCP-1 secretion; however, no significant differences in MCP-1 levels between treatments could be detected; therefore, the data are not presented.

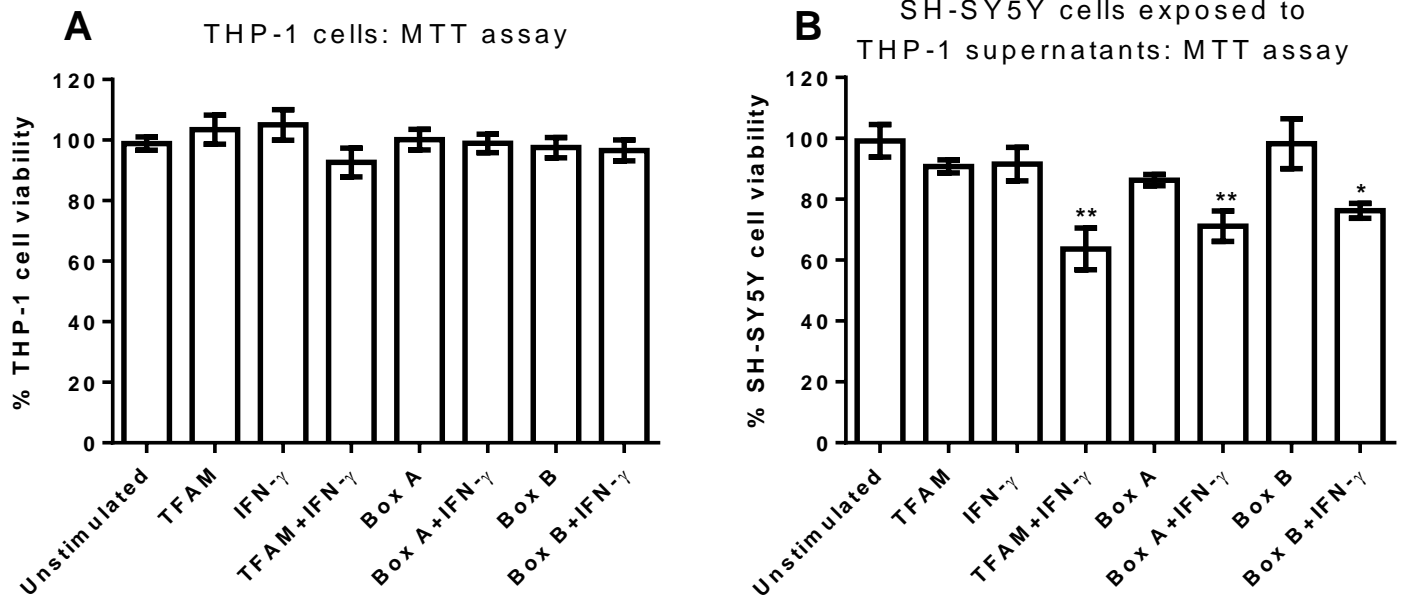


Figure 10. Box A and Box B domains of TFAM are equipotent at inducing THP-1 toxicity towards SH-SY5Y cells. (A) THP-1 cells were treated with TFAM (2.5 $\mu\text{g/ml}$), Box A (2.5 $\mu\text{g/ml}$), Box B (2.5 $\mu\text{g/ml}$), IFN- γ (150 U/ml) or combinations of these stimulants as shown on the abscissa. THP-1 cell viability was measured by the MTT assay at the end of the 48 h incubation period with the stimuli. (B) The MTT assay was used to test the viability of SH-SY5Y cells exposed for 72 h to conditioned media from unstimulated THP-1 cells or THP-1 cells differentially treated as described on the abscissa. Data from 3-8 independent experiments are presented (means \pm SEM). * $P < 0.05$, ** $P < 0.01$, significantly different from unstimulated control (ANOVA, followed by Fisher's LSD post-hoc test).

3.4.2. The effect of TFAM Box A and Box B on U-118 MG cells

The above experiments on THP-1 cells (see section 3.4.1.) were repeated with astrocytic cells to determine whether the observed equipotency of TFAM Box A and Box B at decreasing neuronal viability could also be observed in a different glial cell type.

U-118 MG astrocytic cells were stimulated with full-length TFAM, TFAM Box A or TFAM Box B in the presence or absence of IFN- γ . The combination of IFN- γ plus IL-1 β was used as a positive control. Following 48 h incubation with the stimulants, the viability of the U-118 MG cells was assessed by the MTT assay (Figure 11A).

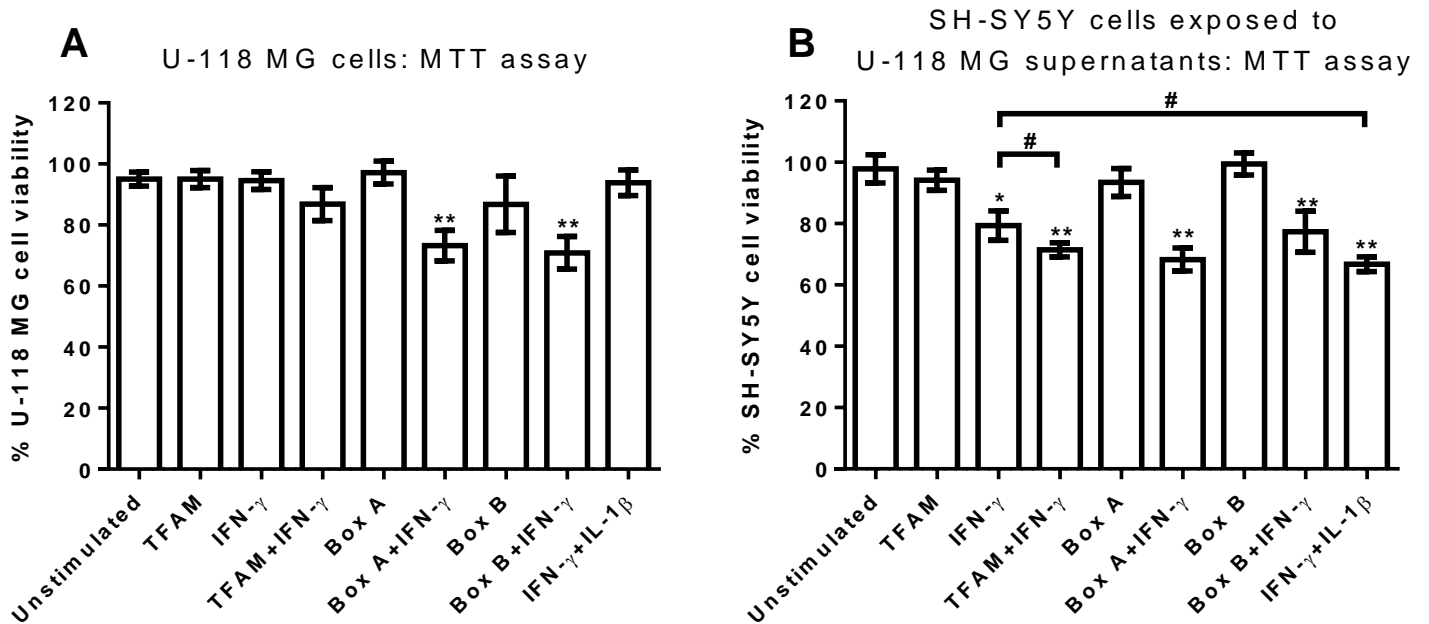


Figure 11. Box A and Box B domain of TFAM are equipotent at inducing U-118 MG toxicity towards SH-SY5Y cells. (A) U-118 MG cells were treated with full-length TFAM (2.5 μ g/ml), Box A (2.5 μ g/ml), Box B (2.5 μ g/ml), IFN- γ (150 U/ml), IL-1 β (100 U/ml) or combinations of these stimulants as shown on the abscissa. U-118 MG cell viability was measured by the MTT assay at the end of the 48 h incubation period with the stimuli. (B) The MTT assay was used to test the viability of SH-SY5Y cells exposed for 72 h to conditioned media from unstimulated U-118 MG cells or U-118 MG cells differentially treated as described on the abscissa. Data from 4-9 independent experiments are presented (means \pm SEM). *P<0.05, **P<0.01, significantly different from unstimulated control; #P<0.05, significant difference between IFN- γ and TFAM plus IFN- γ or IFN- γ and IFN- γ plus IL-1 β (ANOVA, followed by Fisher's LSD post-hoc test).

TFAM Box A plus IFN- γ and Box B plus IFN- γ were the only stimuli to significantly affect the viability of the U-118 MG cells (Figure 11A). Although Box A plus IFN- γ and Box B plus IFN- γ significantly decreased the viability of U-118 MG cells, the viability remained ~70%, thus minimizing the possibility that any effects on the viability of SH-SY5Y cells observed may be due to U-118 MG cell death rather than activation. Moreover, similar effects on astrocyte cell viability have been observed before with potent astrocytic cell stimuli¹¹³.

U-118 MG cell supernatants were collected for ELISA analysis and were transferred onto SH-SY5Y cells. After incubating with the supernatants for 72 h, the viability of the SH-SY5Y cells was measured by the MTT assay (Figure 11B). The results showed that similar to full-length TFAM alone, Box A and Box B on their own did not induce U-118 MG toxicity towards the SH-SY5Y cells. However, in the presence of IFN- γ , Box A and Box B induced significant toxicity of U-118 MG cells towards SH-SY5Y neuronal cells that was comparable to that induced by TFAM plus IFN- γ (Figure 11B). Moreover, the decreases in neuronal viability induced by U-118 MG cells stimulated with Box A or Box B plus IFN- γ or with TFAM plus IFN- γ were not statistically different from each other. This indicated that the boxes were also equipotent in this glial cell line. Although IFN- γ -stimulated U-118 MG cells decreased the viability of the SH-SY5Y cells, there was a statistical difference between IFN- γ and TFAM plus IFN- γ stimulation (Figure 11B), indicating that the decrease in viability was likely due to TFAM in addition to the effect of IFN- γ .

The U-118 MG supernatants were analyzed by ELISA to determine TNF- α secretion induced by TFAM. However, none of the stimulants significantly induced the release of TNF- α above the levels of the unstimulated control cells; as such the data are not presented.

3.4.3. The effect of TFAM Box A and Box B on primary human astrocytes

The experiments with U-118 MG cells were repeated using primary human astrocytes to confirm the results obtained. Primary human astrocytes were stimulated in a similar manner to the U-118 MG cells. Full-length TFAM, TFAM Box A and TFAM Box B were added to the primary human astrocytes in the presence or absence of IFN- γ , and the cells were incubated for 48 h. IFN- γ plus IL-1 β was used as the positive control in these experiments. Following the incubation period, the viability of the primary human astrocytes was measured by the MTT assay (Figure 12A).

The viability of the primary human astrocytes was affected by Box A or Box B in the presence and absence of IFN- γ . However, the viability of the primary human astrocytes did not decrease below ~90%, thus making the possibility unlikely that the effects observed downstream in the SH-SY5Y cells were due to the death of the primary human astrocytes rather than their activation. Moreover, similar effects on primary human astrocyte cell viability have been observed before with potent astrocytic cell stimuli¹¹³.

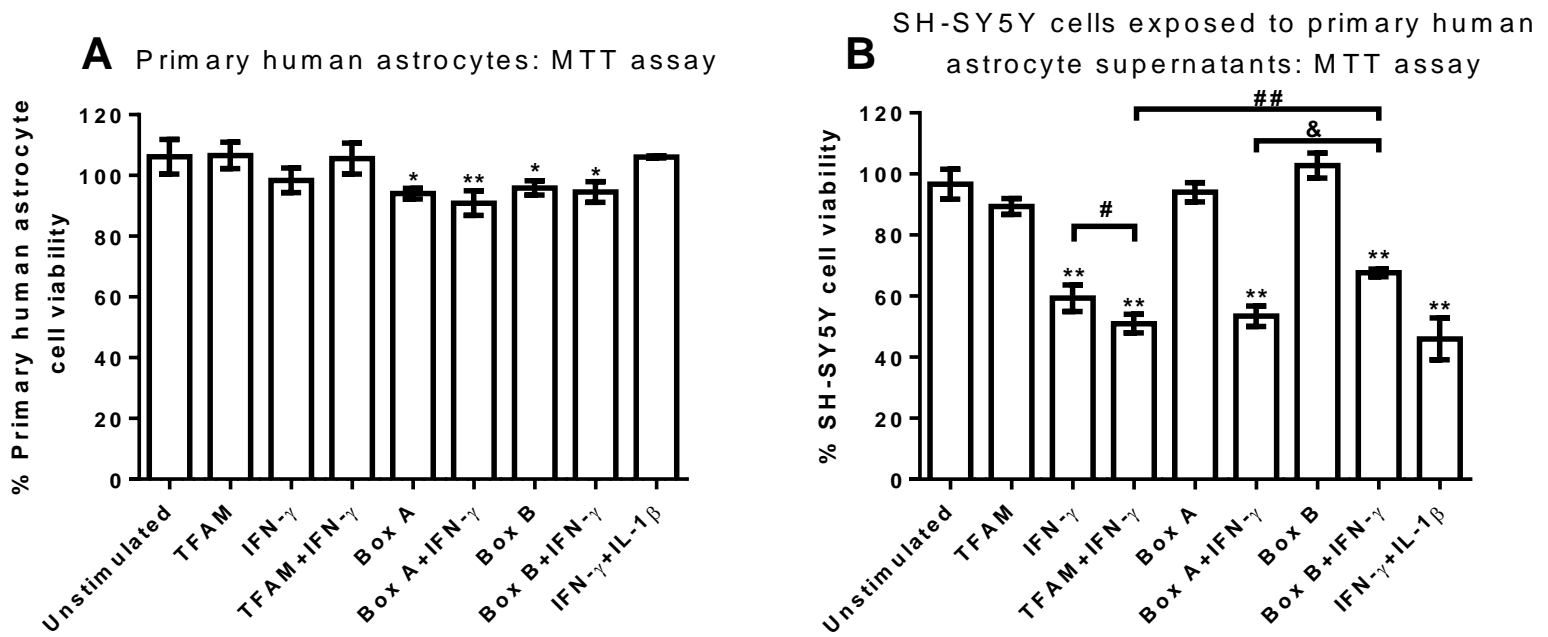


Figure 12. TFAM Box B is less potent than full-length TFAM or TFAM Box A at inducing primary human astrocyte toxicity towards SH-SY5Y cells. (A) Primary human astrocytes were treated with TFAM (2.5 $\mu\text{g/ml}$), Box A (2.5 $\mu\text{g/ml}$), Box B (2.5 $\mu\text{g/ml}$), IFN- γ (150 U/ml), IL-1 β (100 U/ml) or combinations of these stimulants as shown on the abscissa. Primary human astrocyte viability was measured by the MTT assay at the end of the 48 h incubation period with the stimuli. (B) The MTT assay was used to test the viability of SH-SY5Y cells exposed for 72 h to conditioned media from unstimulated primary human astrocytes or primary human astrocytes differentially treated as described on the abscissa. Data from 3-4 independent experiments are presented (means \pm SEM). * $P < 0.05$, ** $P < 0.01$, significantly different from unstimulated control; # $P < 0.05$, significant difference between TFAM plus IFN- γ and IFN- γ ; ## $P < 0.01$, significant difference between TFAM plus IFN- γ and Box B plus IFN- γ ; & $P < 0.05$, significant difference between Box A plus IFN- γ and Box B plus IFN- γ (ANOVA, followed by Fisher's LSD post-hoc test).

The primary human astrocyte supernatants were transferred onto SH-SY5Y cells and collected to be analyzed by ELISA. The SH-SY5Y cells were incubated in astrocyte supernatants for an additional 72 h, after which their viability was assessed by the MTT assay (Figure 12B). The toxicity of the primary human astrocytes towards the SH-SY5Y cells was comparable to that induced by the U-118 MG cells. Full-length TFAM, Box A and Box B in the absence of IFN- γ did not induce primary human astrocyte activation; no decrease in the viability of the SH-SY5Y cells was observed. When primary human astrocytes were stimulated with TFAM or Box A in the presence of IFN- γ , however, the SH-SY5Y viability decreased to ~50% (Figure 12B). Box B plus IFN- γ -stimulated primary human astrocytes also decreased the viability of the SH-SY5Y cells to ~65% (Figure 12B). The difference in primary human astrocyte toxicity induced by Box A plus IFN- γ and Box B plus IFN- γ was statistically significant (Figure 12B). Moreover, Box A plus IFN- γ -mediated activation of primary human astrocytes was not significantly different from full-length TFAM plus IFN- γ -mediated activation. Combined, these results may indicate that, in primary human astrocytes, Box B is less potent than Box A and the full-length TFAM at inducing glial cell toxicity towards neuronal cells.

The IL-6 ELISA data revealed no significant IL-6 release by primary human astrocytes in response to stimulation by TFAM Box A or TFAM Box B. The addition of IFN- γ to Box A or Box B also did not induce a significant release of IL-6 by primary human astrocytes over the level secreted by the unstimulated control cells (Figure 13). The only significant release of IL-6 by primary human astrocytes was induced by stimulation with full-length TFAM, TFAM plus IFN- γ and IFN- γ plus IL-1 β (Figure 13).

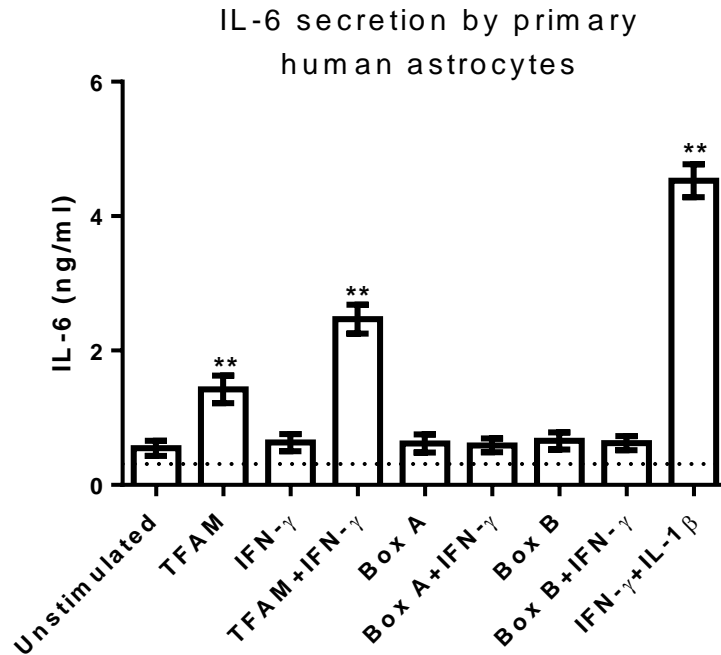


Figure 13. Box A and Box B of TFAM have no effect on the secretion of IL-6 by primary human astrocytes. Primary human astrocytes were stimulated with TFAM (2.5 μ g/ml), Box A (2.5 μ g/ml), Box B (2.5 μ g/ml), IFN- γ (150U/ml), IL-1 β (100 U/ml) or combinations of these stimulants as shown on the abscissa. ELISA was used to measure IL-6 in primary human astrocyte supernatants after 48 h incubation with the stimuli. Data from 3-4 independent experiments are presented (means \pm SEM). **P<0.01, significantly different from unstimulated control (ANOVA, followed by Fisher's LSD post-hoc test). Dotted line represents the ELISA detection limit.

3.5. Inhibition of TFAM-induced microglial toxicity by blocking the RAGE and Mac-1 receptors

3.5.1. Targeting the RAGE receptor

Experiments were performed as described in the Materials and Methods section 2.8.1. THP-1 cells were treated with heparin for 30 min prior to stimulation with TFAM (2.5 μ g/ml), IFN- γ (150 U/ml) or TFAM plus IFN- γ . Following 48 h incubation, viability of the THP-1 cells was

measured by the MTT assay (Figure 14A). At the concentrations tested, neither heparin, nor TFAM in the presence or absence of IFN- γ were toxic to THP-1 cells.

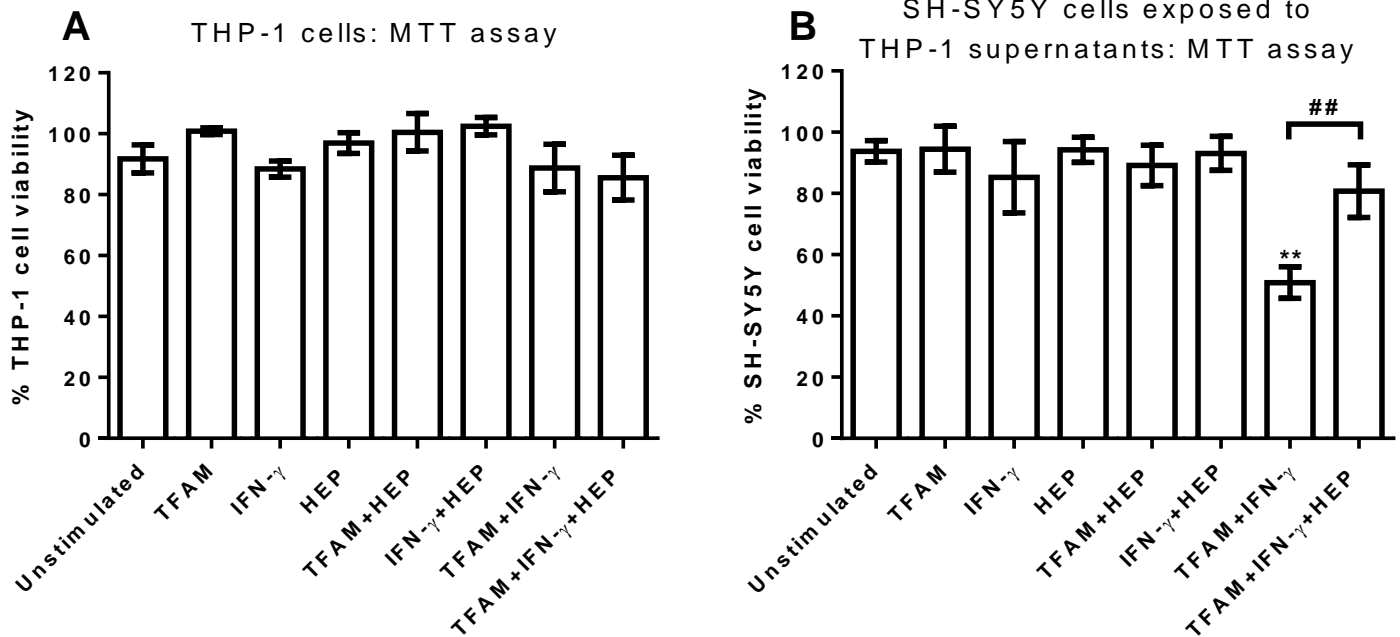


Figure 14. Heparin attenuates TFAM plus IFN- γ -induced THP-1 cell toxicity towards SH-SY5Y neuronal cells. (A) THP-1 cells were pre-treated with heparin (HEP, 250 μ g/ml) and stimulated with TFAM (2.5 μ g/ml), IFN- γ (150 U/ml) or combinations of these stimulants as shown on the abscissa. THP-1 cell viability was measured by the MTT assay at the end of the 48 h incubation period with the various stimuli. (B) The MTT assay was used to test the viability of SH-SY5Y cells exposed for 96 h to conditioned media from unstimulated THP-1 cells or THP-1 cells differentially treated as described on the abscissa. Data from 3-5 independent experiments are presented (means \pm SEM). **P<0.01, significantly different from unstimulated control; ##P<0.01, significant difference between TFAM plus IFN- γ and TFAM plus IFN- γ in the presence of heparin (ANOVA, followed by Fisher's LSD post-hoc test).

After the 48 h incubation period, the supernatants from the THP-1 cells were transferred onto the SH-SY5Y neuronal cells to assess the neurotoxic potential of TFAM in the presence and absence of heparin. The remaining supernatants were collected to be analyzed by ELISA. Following 96 h incubation with THP-1 supernatants, the SH-SY5Y cell viability was tested using the MTT assay (Figure 14B). Only the supernatants from the THP-1 cells treated with TFAM plus IFN- γ induced significant THP-1-mediated toxicity towards SH-SY5Y neuronal cells (Figure 14B). In the presence of heparin (250 μ g/ml), this neurotoxicity was attenuated, suggesting the involvement of RAGE (Figure 14B).

The supernatants that had been collected from the THP-1 cells were analyzed by ELISA for MCP-1 secretion. Stimulation with TFAM plus IFN- γ significantly induced the release of MCP-1 by THP-1 cells (Figure 15). TFAM or IFN- γ alone also increased MCP-1 secretion. The addition of heparin to the TFAM plus IFN- γ -stimulated THP-1 cells significantly decreased the secretion of MCP-1 compared to the secretion by the uninhibited TFAM plus IFN- γ -stimulated cells (Figure 15).

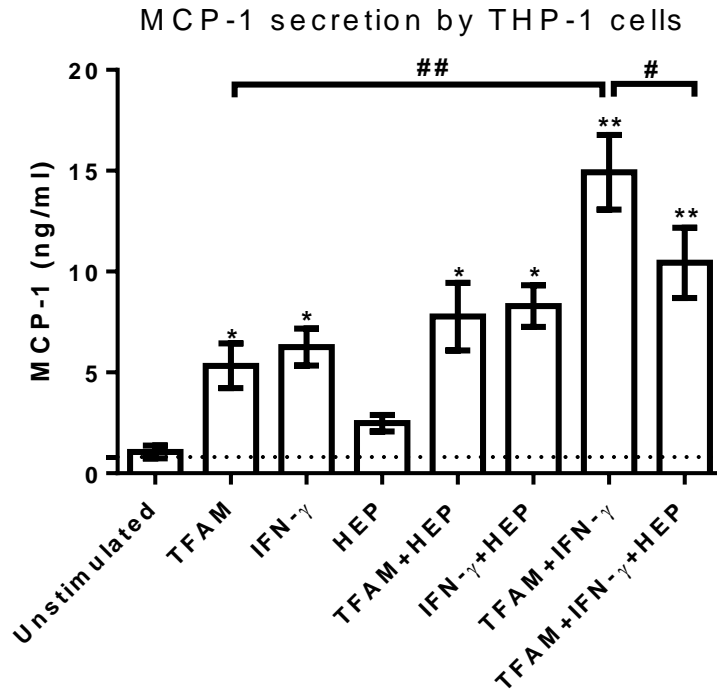


Figure 15. Heparin decreases MCP-1 secretion by TFAM plus IFN- γ -stimulated THP-1 cells. THP-1 cells were pre-treated with heparin (HEP, 250 μ g/ml) and stimulated with TFAM (2.5 μ g/ml), IFN- γ (150 U/ml) or combinations of these stimulants as shown on the abscissa. ELISA was used to measure MCP-1 in THP-1 supernatants after 48 h incubation with the stimuli. Data from 5-7 independent experiments are presented (means \pm SEM). *P<0.05, **P<0.01, significantly different from unstimulated control; #P<0.05, significant difference between TFAM plus IFN- γ and TFAM plus IFN- γ in the presence of heparin; ##P<0.01 significant difference between TFAM plus IFN- γ and TFAM (ANOVA, followed by Fisher's LSD post-hoc test). Dotted line represents the ELISA detection limit.

To test the ability of more specific RAGE inhibitors to attenuate THP-1 toxicity towards SH-SY5Y cells, sRAGE, the truncated form of the RAGE receptor, and anti-RAGE antibodies were used. THP-1 cells were pre-treated with sRAGE (10 μ g/ml) or anti-RAGE (10 μ g/ml) antibodies prior to stimulation with TFAM, IFN- γ or TFAM plus IFN- γ . Following 48 h incubation, the viability of the THP-1 cells was assessed by the MTT assay. In addition, the

THP-1 cell supernatants were transferred onto SH-SY5Y cells to determine the ability of the antibodies to attenuate the induced neurotoxicity, while the remaining supernatants were collected to be analyzed with the MCP-1 ELISA. The SH-SY5Y cells were incubated for additional 72 h before being tested for viability with the MTT and LDH assays. However, these supernatant transfer experiments did not yield any significant differences between treatments; as such the data are not presented in this thesis.

In contrast, the collected THP-1 supernatants were analyzed by ELISA and the results showed that sRAGE (Figure 16) and anti-RAGE antibody (Figure 17), similar to heparin, decreased the secretion of MCP-1 by TFAM plus IFN- γ -stimulated THP-1 cells. This further implicated the involvement of RAGE in mediating the effects of TFAM. RAGE alone, however, was not responsible for all the effects of TFAM, as the attenuation of neurotoxicity and the decreases in MCP-1 secretion were only partial. This suggested the involvement of additional mechanisms in mediating the activity of TFAM.

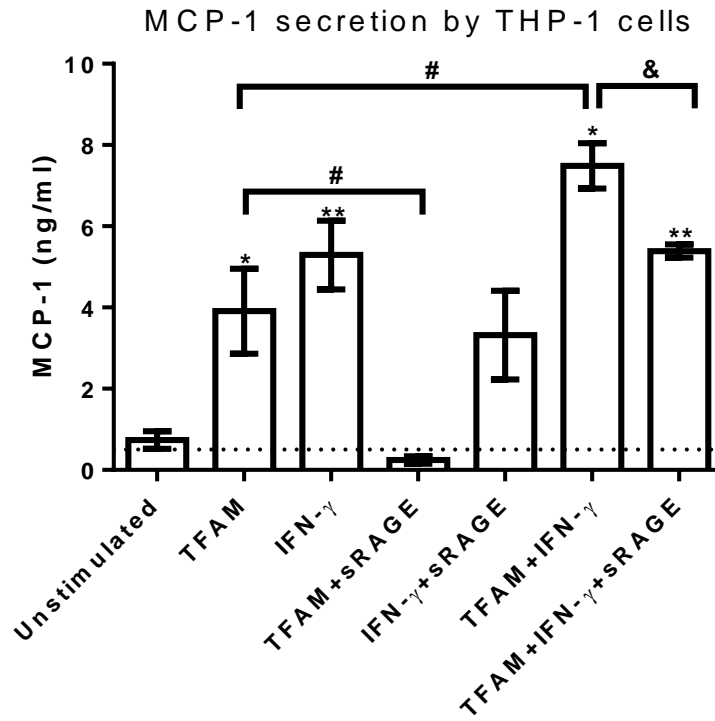


Figure 16. sRAGE inhibits MCP-1 secretion by THP-1 cells stimulated with TFAM or TFAM plus IFN- γ . THP-1 cells were pre-treated with sRAGE (10 μ g/ml) and stimulated with TFAM (2.5 μ g/ml), IFN- γ (150 U/ml) or combinations of these stimulants as shown on the abscissa. ELISA was used to measure MCP-1 in THP-1 supernatants after 48 h incubation with stimuli. Data from 3-10 independent experiments are presented (means \pm SEM). *P<0.05, significantly different from unstimulated control; #P<0.05, significant difference between TFAM and TFAM plus IFN- γ or TFAM and TFAM in the presence of sRAGE; &P<0.05, significant difference between TFAM plus IFN- γ and TFAM plus IFN- γ in the presence of sRAGE (ANOVA, followed by Fisher's LSD post-hoc test). Dotted line represents the ELISA detection limit.

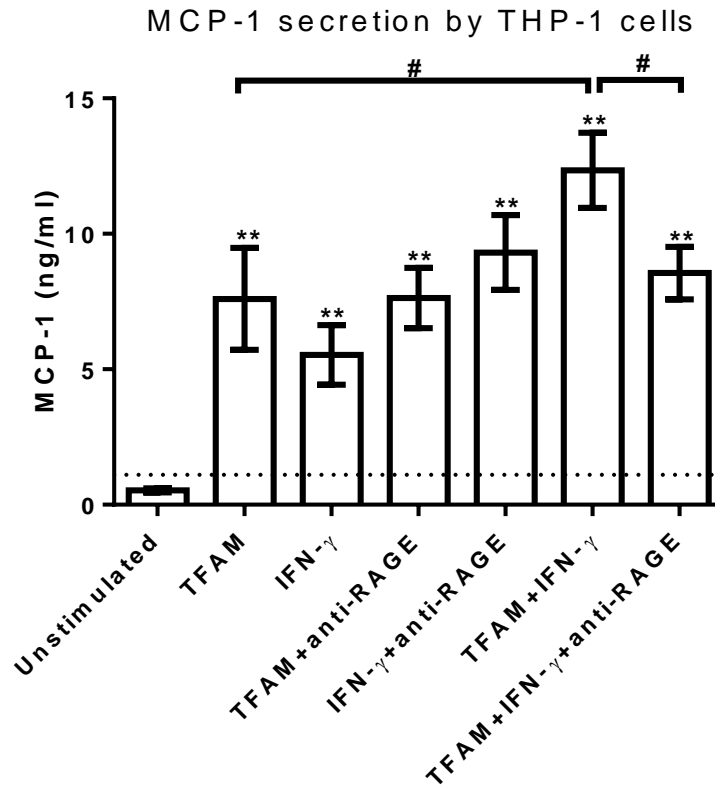


Figure 17. Blocking RAGE by a specific antibody inhibits MCP-1 secretion by TFAM plus IFN- γ -stimulated THP-1 cells. THP-1 cells were pre-treated with anti-RAGE antibody (10 $\mu\text{g/ml}$) and stimulated with TFAM (2.5 $\mu\text{g/ml}$), IFN- γ (150 U/ml) or combinations of these stimulants as shown on the abscissa. ELISA was used to measure MCP-1 in THP-1 supernatants after 48 h incubation with the stimuli. Data from 3-7 independent experiments are presented (means \pm SEM). ** $P < 0.01$, significantly different from unstimulated control; # $P < 0.05$, significant difference between TFAM plus IFN- γ and TFAM or TFAM plus IFN- γ and TFAM plus IFN- γ in the presence of anti-RAGE antibody (ANOVA, followed by Fisher's LSD post-hoc test). Dotted line represents the ELISA detection limit.

3.5.2. Targeting the Mac-1 receptor

THP-1 cells were treated with the anti-Mac-1 antibody for 30 min prior to stimulation with TFAM, IFN- γ or TFAM plus IFN- γ . Following 48 h incubation, THP-1 cells were tested for viability by the MTT assay (Figure 18A). None of the stimulants or the antibody significantly

decreased the viability of the THP-1 cells; similar to the results obtained with the heparin-treated THP-1 cells (Figure 14A).

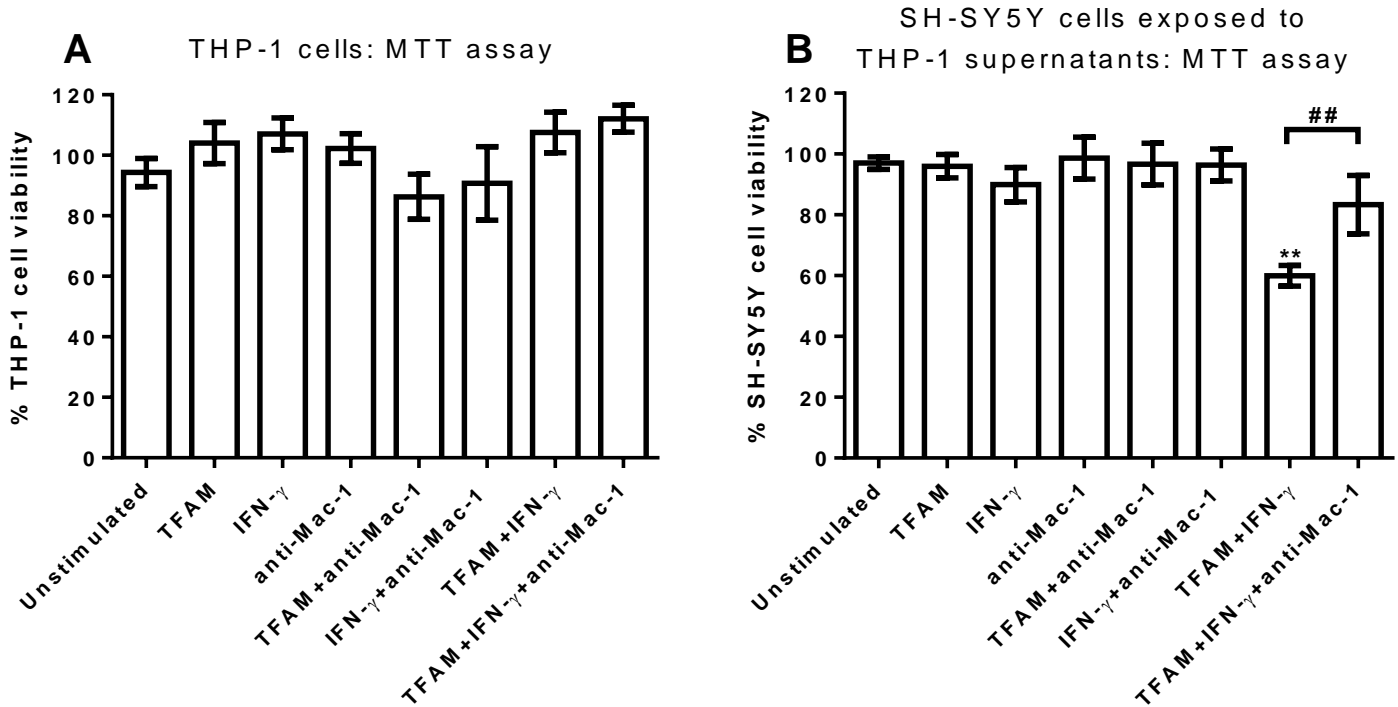


Figure 18. Blocking the Mac-1 receptor attenuates TFAM plus IFN- γ -induced THP-1 cell toxicity towards SH-SY5Y neuronal cells. (A) THP-1 cells were pre-treated with anti-Mac-1 antibody (20 μ g/ml) and stimulated with TFAM (2.5 μ g/ml), IFN- γ (150 U/ml) or combinations of these stimulants as shown on the abscissa. THP-1 cell viability was measured by the MTT assay at the end of the 48 h incubation period with the various stimuli. (B) The MTT assay was used to test the viability of SH-SY5Y cells exposed for 72 h to conditioned media from unstimulated THP-1 cells or THP-1 cells differentially treated as described on the abscissa. Data from 3-7 independent experiments are presented (means \pm SEM). **P<0.01, significantly different from unstimulated control; ###P<0.01, significant difference between TFAM plus IFN- γ and TFAM plus IFN- γ in the presence of anti-Mac-1 antibody (ANOVA, followed by Fisher's LSD post-hoc test).

THP-1 cell supernatants were transferred onto SH-SY5Y neuronal cells to assess their cytotoxic effects and the ability of the anti-Mac-1 antibody to potentially inhibit these effects. Following a 72 h incubation period with the THP-1 cell supernatants, the SH-SY5Y cells were assessed for viability by the MTT assay (Figure 18B). The supernatants from THP-1 cells stimulated with TFAM plus IFN- γ significantly decreased SH-SY5Y cell viability, indicating activation of THP-1 cells (Figure 18B). However, in the presence of the anti-Mac-1 antibody the induced neurotoxicity was significantly attenuated (Figure 18B), suggesting that the TFAM-induced toxicity may be mediated by Mac-1 in addition to RAGE.

Therefore, the next step was to inhibit the RAGE and Mac-1 receptors simultaneously. THP-1 cells were pre-treated with both antibodies for 30 min prior to stimulation with TFAM and IFN- γ . After 48 h, THP-1 cells were tested for viability with the MTT assay. In addition, the THP-1 cell supernatants were transferred onto SH-SY5Y cells and the remaining supernatants were collected to be analyzed by ELISA. The SH-SY5Y cells were incubated for an additional 72 h before being tested for viability with the MTT and LDH assays. These experiments were not successful, as higher concentrations of anti-RAGE antibody may have been required to obtain significant inhibition in the supernatant transfer experiments; as such, the data are not presented in this thesis.

However, the MCP-1 ELISA analysis of THP-1 supernatants that had been collected showed interesting results (Figure 19). Stimulation of THP-1 cells with TFAM plus IFN- γ significantly induced the secretion of MCP-1 by THP-1 cells (Figure 19). When THP-1 cells were pretreated with the Mac-1 or the RAGE antibodies before the TFAM plus IFN- γ stimulation, secretion of MCP-1 decreased compared to the secretion by THP-1 cells stimulated with TFAM plus IFN- γ alone (Figure 19). Furthermore, when both receptors were inhibited

simultaneously there was a significant decrease in MCP-1 secretion compared to the decrease induced by a single antibody (Figure 19). This indicates that both receptors might be involved simultaneously in mediating the activity of TFAM. Moreover, there may be additional receptors involved, as inhibiting both Mac-1 and RAGE did not completely abolish MCP-1 secretion by the THP-1 cells.

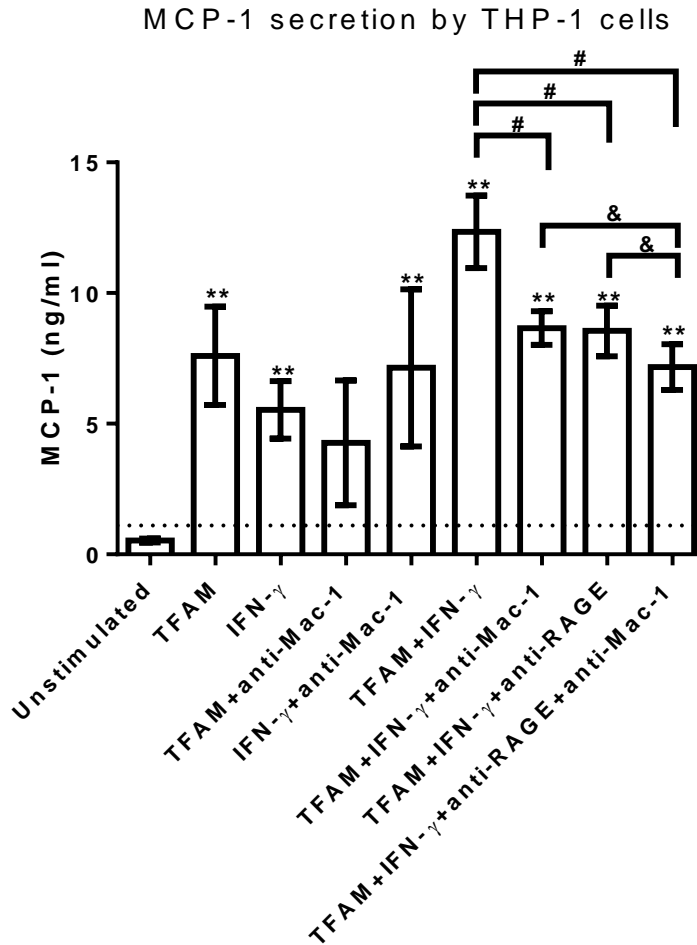


Figure 19. Blocking RAGE and Mac-1 decreases MCP-1 secretion by TFAM plus IFN- γ -stimulated THP-1 cells. THP-1 cells were pre-treated with anti-Mac-1 antibody (20 $\mu\text{g/ml}$), anti-RAGE antibody (10 $\mu\text{g/ml}$) or combinations of the antibodies; followed by stimulation with TFAM (2.5 $\mu\text{g/ml}$), IFN- γ (150 U/ml) or combinations of these stimulants as shown on the abscissa. ELISA was used to measure MCP-1 in cell-free supernatants after 48 h incubation with stimuli. Data from 3-7 independent experiments are presented (means \pm SEM). * $P < 0.05$, ** $P < 0.01$, statistically significant from unstimulated control; # $P < 0.05$, significant difference between TFAM plus IFN- γ and TFAM plus IFN- γ plus one blocking antibody (RAGE or Mac-1); & $P < 0.05$, significant difference between TFAM plus IFN- γ plus blocking antibodies (RAGE or Mac-1) and TFAM plus IFN- γ plus both blocking antibodies (ANOVA, followed by Fisher's LSD post-hoc test). Dotted line represents the ELISA detection limit.

3.6. TFAM-primed release of superoxide by glial cells

Full-length TFAM, TFAM Box A and TFAM Box B were tested for their ability to prime the NADPH oxidase-dependent respiratory burst in glial cells. For these experiments, THP-1 cells were replaced with DMSO-differentiated human HL-60 cells, as THP-1 cells do not express sufficient levels of the NADPH oxidase to generate detectable concentrations of ROS. The experiments were conducted as described in the Materials and Methods section 2.10.

The first set of experiments examined the ability of full-length TFAM to prime the release of ROS from HL-60 cells. To do this, HL-60 cells were differentiated in DMSO (1.3%, v/v) for 5 days, after which the media was replaced and they were either primed with TFAM (2.5 µg/ml), IFN-γ (150 U/ml) or a combination of both priming agents for 24 h. The release of ROS was measured by the respiratory burst assay using fMLP as the respiratory burst-inducing stimulant. The results were compared to the values obtained from cells treated only with PBS vehicle control but that were stimulated with fMLP (unprimed control). The results were expressed as a percentage of the chemiluminescence signal obtained from the unprimed control. As an additional control, HL-60 cells were primed with IFN-γ plus LPS (well-studied priming agents¹³³⁻¹³⁶), but were not stimulated with fMLP (unstimulated control).

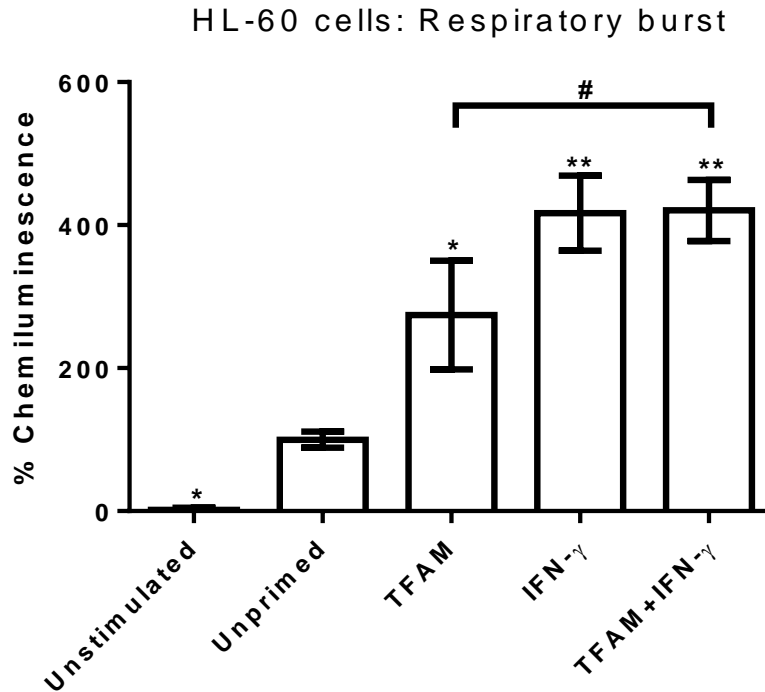


Figure 20. TFAM primes the fMLP-induced release of ROS from HL-60 cells. Cells were differentiated with DMSO prior to use in the experiments. The cells were washed and primed with TFAM (2.5 $\mu\text{g/ml}$), IFN- γ (150 U/ml) or TFAM plus IFN- γ as shown on the abscissa. HL-60 cells that were primed with IFN- γ plus LPS but not stimulated with fMLP (unstimulated), or not primed but stimulated with fMLP (unprimed) were included as controls. After 24 h, the luminol-dependent chemiluminescence response of HL-60 cells was measured following stimulation with 1 μM fMLP. Results were expressed as a percentage of the unprimed control cells. Data from 4-8 independent experiments are presented (means \pm SEM). * $P < 0.05$, ** $P < 0.01$, significantly different from unprimed, fMLP stimulated cells; # $P < 0.05$, significant difference between TFAM and TFAM plus IFN- γ (ANOVA, followed by Fisher's LSD post-hoc test).

TFAM and IFN- γ alone significantly primed the fMLP-induced respiratory burst of HL-60 cells (Figure 20). In addition, TFAM plus IFN- γ also significantly primed the NADPH oxidase-dependent release of ROS from HL-60 cells in response to fMLP stimulation, as shown by the increase in the luminol-dependent chemiluminescence (Figure 20). Moreover, priming

with TFAM plus IFN- γ significantly enhanced the release of ROS from the HL-60 cells above the levels released by TFAM priming on its own.

In the second set of experiments, the ability of TFAM Box A and TFAM Box B to prime the NADPH oxidase-dependent respiratory burst and the release of ROS was investigated. HL-60 cells were primed with full-length TFAM (5 $\mu\text{g/ml}$), Box A (5 $\mu\text{g/ml}$) or Box B (5 $\mu\text{g/ml}$). The results of the primed HL-60 cells were again compared to the results obtained from the unprimed control (PBS vehicle plus fMLP stimulation). The IFN- γ plus LPS-primed but unstimulated (no fMLP) control was included in this experiment, as well.

Similar to the results obtained from the previous experiment, full-length TFAM significantly primed the respiratory burst, which led to enhanced release of ROS from the HL-60 cells, as indicated by the increase in % chemiluminescence above that of the unprimed control (Figure 21). Box A and Box B significantly primed the respiratory burst activity (Figure 21). The priming activity of Box A was significantly higher than that of Box B. However, the priming activity of Box A was not significantly different from that of full-length TFAM. This indicates that Box B might be less efficient than Box A and full-length TFAM at priming the respiratory burst in HL-60 cells.

HL-60 cells: Respiratory burst

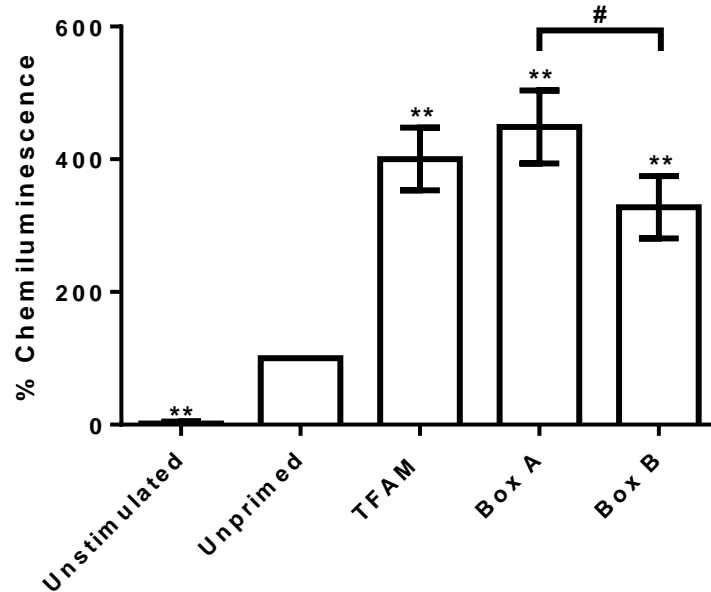


Figure 21. Box A, Box B and full-length TFAM prime the fMLP-induced release of ROS from HL-60 cells. HL-60 cells were differentiated with DMSO prior to use in the experiments. The cells were washed and primed with TFAM (5 $\mu\text{g/ml}$), Box A (5 $\mu\text{g/ml}$) or Box B (5 $\mu\text{g/ml}$) as shown on the abscissa. HL-60 cells that were primed with IFN- γ plus LPS but not stimulated with fMLP (unstimulated) or not primed but stimulated with fMLP (unprimed) were included as controls. After 24 h, the luminol-dependent chemiluminescence response of HL-60 cells was measured following stimulation with 1 μM fMLP. Results were expressed relative to unprimed control cells. Data from 5 independent experiments are presented (means \pm SEM). ** $P < 0.01$, significantly different from unprimed cells; # $P < 0.05$, significant difference between Box A- and Box B-primed HL-60 cells (ANOVA, followed by Fisher's LSD post-hoc test).

3.6.1. Inhibition of the respiratory burst by blocking the Mac-1 receptor

The mechanism of action underlying the TFAM-mediated priming of the respiratory burst was investigated using DMSO-differentiated HL-60 cells. The Mac-1 receptor was blocked using the anti-Mac-1 antibody to determine whether the priming of the respiratory burst by TFAM could

be inhibited. The results from the primed HL-60 cells were compared to those results obtained from the unprimed control (PBS vehicle plus fMLP stimulation).

Anti-Mac-1 antibody was added to HL-60 cells 30 min prior to priming with TFAM, IFN- γ or a combination of the two priming agents. Following 24 h incubation, the release of ROS was measured by respiratory burst assay using fMLP as the inducing stimulant. The results were expressed as a percentage of the luminol-dependent chemiluminescence signal of the unprimed control (PBS vehicle plus fMLP stimulation). Similar to the results presented in Figure 20, IFN- γ , TFAM, and TFAM plus IFN- γ significantly increased the respiratory burst activity of differentiated HL-60 cells, indicating priming activity (Figure 22).

Pre-treatment of the TFAM-, IFN- γ - or TFAM plus IFN- γ -primed HL-60 cells with the anti-Mac-1 antibody significantly attenuated the respiratory burst activity of the HL-60 cells, as indicated by a decrease in % chemiluminescence compared to the % chemiluminescence of the uninhibited counterparts (Figure 22). A significant difference between the Mac-1-inhibited and the uninhibited HL-60 cells was only achieved with the priming by TFAM plus IFN- γ (from ~400% to ~190%). However, the HL-60 cells primed with TFAM or IFN- γ on their own in the presence of the anti-Mac-1 antibody also showed a decreasing trend in % chemiluminescence compared to the % chemiluminescence of the uninhibited counterparts, albeit these effects were not statistically significant. This indicates the potential involvement of Mac-1 in the priming of the NADPH oxidase-dependent respiratory burst by TFAM in HL-60 cells.

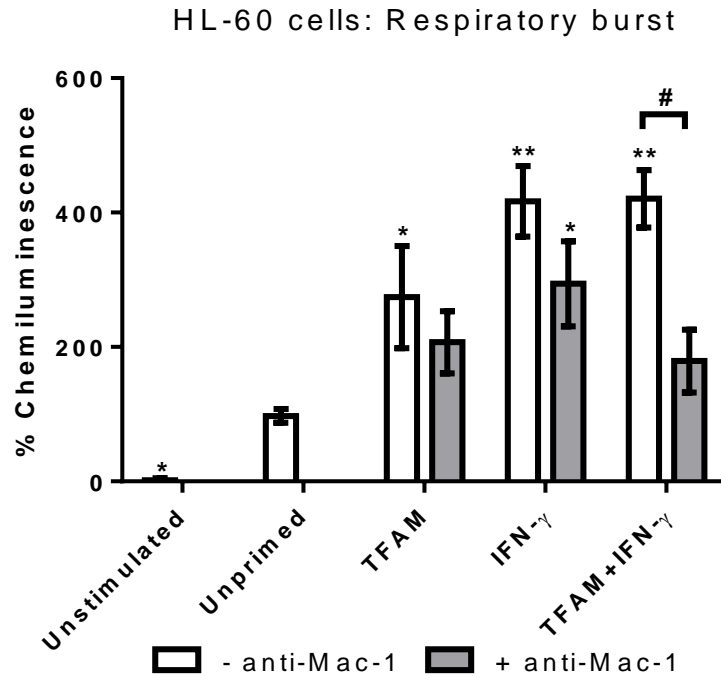


Figure 22. Blocking Mac-1 attenuates the TFAM-primed release of ROS from HL-60 cells.

HL-60 cells were differentiated with DMSO prior to use in the experiments. The cells were washed, pre-treated with the anti-Mac-1 antibody (20 $\mu\text{g/ml}$) and primed with TFAM (2.5 $\mu\text{g/ml}$), IFN- γ (150 U/ml) or TFAM plus IFN- γ as shown on the abscissa. In the absence of anti-Mac-1 antibody, HL-60 cells were also primed with IFN- γ plus LPS but not stimulated with fMLP (unstimulated) or not primed but stimulated with fMLP (unprimed); these cells were included as controls. After 24 h, the luminol-dependent chemiluminescence response of HL-60 cells was measured following stimulation with 1 μM fMLP. Results were expressed relative to unprimed control cells. Data from 4-6 independent experiments are presented (means \pm SEM). * $P < 0.05$, ** $P < 0.01$, significantly different from unprimed cells; # $P < 0.05$, significant difference between TFAM plus IFN- γ and TFAM plus IFN- γ in the presence of anti-Mac-1 antibody (ANOVA, followed by Fisher's LSD post-hoc test).

3.7. Effects of biochemical stressors on TFAM mRNA expression levels by astrocytic cells

The ability of biochemical stressors such as H₂O₂ to up-regulate TFAM mRNA expression in astrocytic cells was investigated. The experiments were performed as described in the Materials and Methods section 2.11.

3.7.1. TFAM mRNA expression in U-373 MG cells

The qPCR assay was used to measure the changes in the expression of TFAM in U-373 MG cells after 24 h stimulation with H₂O₂, IFN- γ or IFN- γ plus IL-1 β . Figure 23 illustrates that TFAM expression by U-373 MG cells was only significantly increased in the cells that had been incubated with H₂O₂. The results indicated a 4-fold increase in TFAM expression compared to the expression in unstimulated control cells (Figure 23). IFN- γ and IFN- γ plus IL-1 β , on the other hand, did not significantly upregulate TFAM expression in the U-373 MG cells.

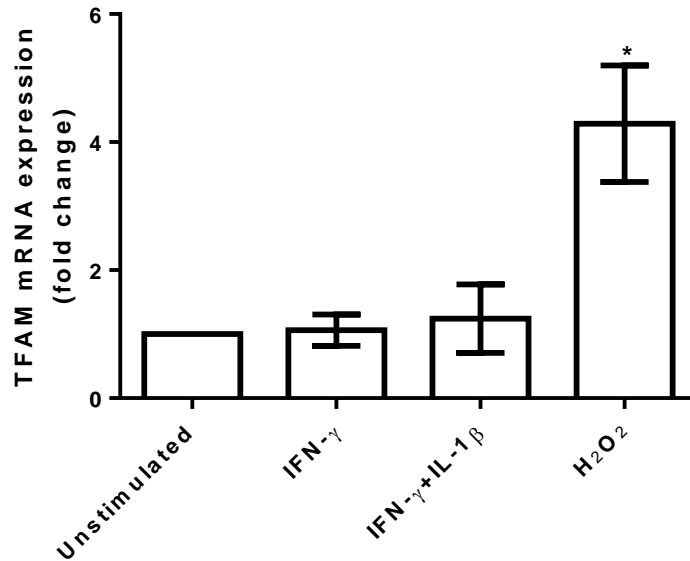


Figure 23. H₂O₂ upregulates TFAM mRNA expression in U-373 MG astrocytic cells.

U-373 MG cells were treated with IFN- γ (150 U/ml), IFN- γ plus IL-1 β (100 U/ml) or H₂O₂ (100 μ M) as shown on the abscissa. Total RNA was extracted 24 h later and TFAM mRNA expression was analyzed using qPCR. Results were normalized to the reference gene β -actin and are presented as a fold increase compared to the TFAM mRNA levels in unstimulated U-373 MG control cells (expression level = 1). Data from 3 independent experiments are presented (means \pm SEM). *P<0.05, significantly different from unstimulated control, (ANOVA, followed by Fisher's LSD post-hoc test).

3.7.2. TFAM mRNA expression in primary human astrocytes

The qPCR experiments were repeated with primary human astrocytes to confirm the positive results obtained with the U-373 MG astrocytic cells. Since H₂O₂ was the only stressor to significantly induce the expression of TFAM in U-373 MG cells, and sufficient amounts of RNA are often difficult to obtain from primary human astrocytes, only the effect of H₂O₂ on primary human astrocyte TFAM expression was investigated. The results showed that 24 h incubation of primary human astrocytes in the presence of H₂O₂ had an effect on the expression of TFAM.

Similar to the results obtained from the experiments with the U-373 MG cells, H₂O₂ significantly upregulated the expression of TFAM in primary human astrocytes (Figure 24).

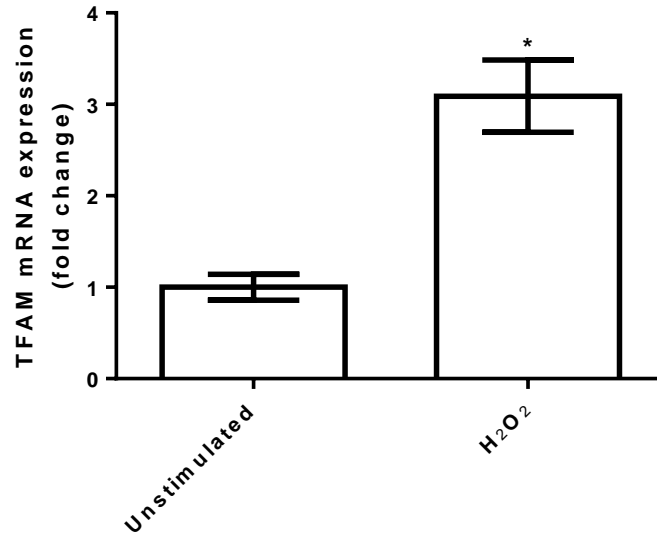


Figure 24. H₂O₂ induces TFAM mRNA expression in primary human astrocytes. Primary human astrocytes were treated with H₂O₂ (50 μM) as shown on the abscissa. Total RNA was extracted 24 h later and TFAM mRNA expression was analyzed using qPCR. Results were normalized to the reference gene β-actin and are presented as a fold increase compared to the TFAM mRNA levels in unstimulated primary human astrocyte controls (expression level = 1). Data from 3 independent experiments are presented (means ± SEM). *P<0.05, significantly different from unstimulated control, (Unpaired parametric T-test with Welch’s correction).

3.8. Toxicity of TFAM-induced microparticles on SH-SY5Y neuronal cells

The ability of TFAM to trigger the release of MPs from THP-1 cells was investigated. The experiments were performed as described in the Materials and Methods section 2.12.1.

THP-1 cells were stimulated with TFAM, IFN-γ or a combination of the two stimulants for 24 h. IFN-γ plus LPS was used as a positive control in these experiments. Following the

incubation period, the THP-1 supernatants were collected and centrifuged step-wise at different speeds to isolate the MPs. Once the MPs were isolated, they were stained with Annexin-V-FITC and visualized under the fluorescence microscope (example image in Figure 3). The flow cytometer was used to quantify the isolated MPs more accurately. These results showed that there was a wide range in the number of MPs obtained from different THP-1 cell populations, despite the same isolation procedures (Table 2). The data in Figure 25 was obtained from the same cells as the data presented in Table 2. There was a significant difference between the number of MPs released by the unstimulated THP-1 cells and by those stimulated with TFAM. Although all stimulants used enhanced the release of MPs, TFAM was the only stimulant to cause a statistically significant induction with the numbers of observations made (Figure 25).

Table 2. Variation in the number of MPs isolated from differentially treated THP-1 cells

Treatments	Minimum to maximum number of MPs/μl obtained from THP-1 cells from three separate isolation experiments
Unstimulated	768-1585 MPs/ μ l
TFAM	1621-2118 MPs/ μ l
IFN-γ	739-1691 MPs/ μ l
TFAM+IFN-γ	521-3467 MPs/ μ l
IFN-γ+LPS	905-2654 MPs/ μ l

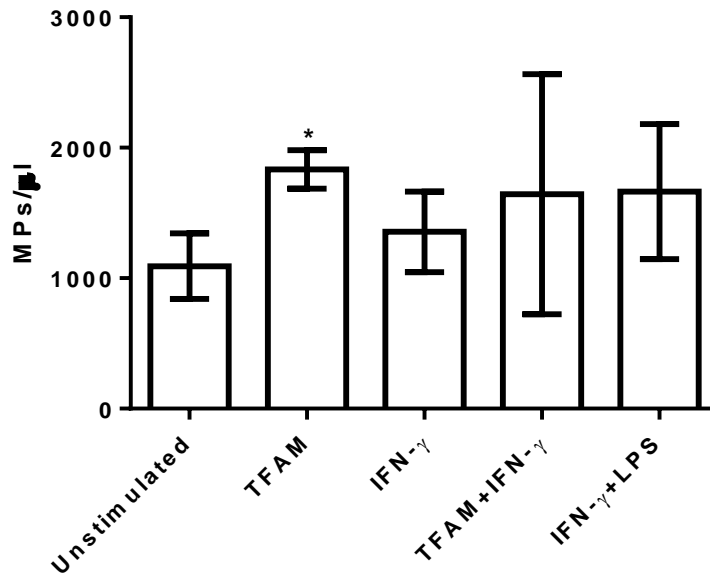


Figure 25. TFAM induces the release of MPs from THP-1 cells. THP-1 cells were stimulated with TFAM (2.5μg/ml), IFN-γ (150U/ml), TFAM plus IFN-γ or IFN-γ plus LPS (0.5 μg/ml) as shown on the abscissa. After 24 h, MPs were isolated by differential centrifugation, stained with Annexin-V FITC and quantified by flow cytometry using side-scatter (SSC) detection settings determined by sizing beads. Data from 3 independent experiments are presented (means ± SEM). *P<0.05, significantly different from unstimulated control (ANOVA, followed by Fisher's LSD post-hoc test).

Next, the ability of the isolated MPs to induce toxicity of THP-1 cells towards SH-SY5Y cells was investigated. The experiments were performed as described in the Materials and Methods section 2.12.2. THP-1 cells were stimulated with MPs (10 μg of protein/ml) isolated from THP-1 cells that had been treated with TFAM, IFN-γ, TFAM plus IFN-γ or IFN-γ plus LPS for 48 h. Following the incubation period, viability of THP-1 cells was assessed by the MTT assay and the results were compared to the results from the unstimulated control cells. At the concentration tested, none of the isolated MPs significantly decreased the viability of the THP-1 cells (Figure 26A).

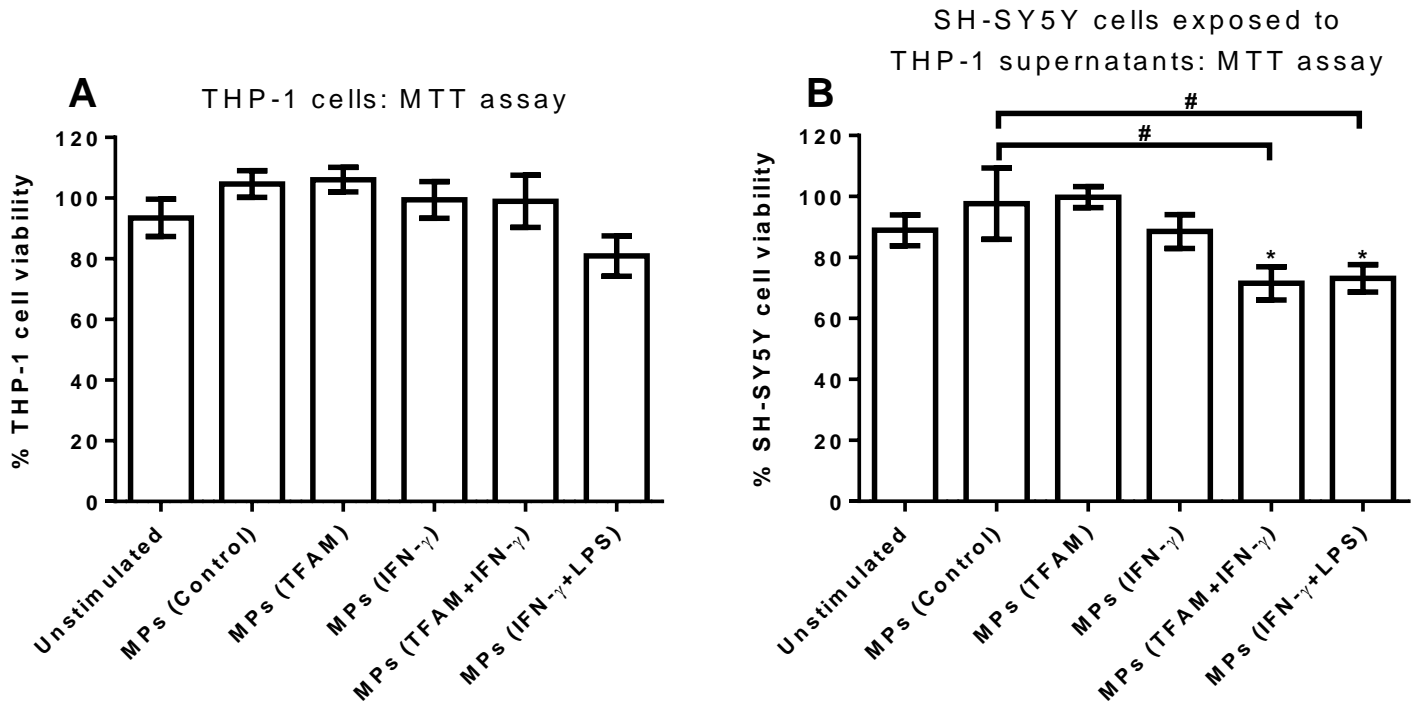


Figure 26. MPs isolated from stimulated THP-1 donor cells induce toxicity of THP-1 cells towards SH-SY5Y neuronal cells. (A) THP-1 cells were treated with media only (unstimulated), MPs (10 μ g of protein/ml) isolated from unstimulated THP-1 cells (control) or from THP-1 cells that had been differentially stimulated with TFAM (2.5 μ g/ml), IFN- γ (150 U/ml), TFAM plus IFN- γ or IFN- γ plus LPS (0.5 μ g/ml) as shown on the abscissa. THP-1 cell viability was measured by the MTT assay at the end of the 48 h incubation period with the various MPs. **(B)** The MTT assay was used to test the viability of SH-SY5Y cells exposed for 72 h to conditioned media from unstimulated THP-1 cells or THP-1 cells differentially treated as described on the abscissa. Data from 3-8 independent experiments are presented (means \pm SEM). * P <0.05, significantly different from unstimulated control; # P <0.05, significant difference between stimulation with MPs isolated from unstimulated THP-1 cells and MPs isolated from TFAM plus IFN- γ -stimulated or IFN- γ plus LPS-stimulated THP-1 cells (ANOVA, followed by Fisher's LSD post-hoc test).

Supernatants from the THP-1 cells treated with the MPs that had been isolated from differentially stimulated THP-1 cells were transferred onto SH-SY5Y cells to determine their cytotoxic potential. The remaining supernatants were collected to be analyzed by ELISA. The SH-SY5Y cells were incubated in the supernatants for 72 h, following which their viability was measured by the MTT assay (Figure 26B). The MPs isolated from unstimulated THP-1 cells, as well as those isolated from TFAM- or IFN- γ -stimulated THP-1 cells did not induce THP-1 cell toxicity towards SH-SY5Y cells. However, the MPs isolated from THP-1 cells that had been stimulated with TFAM plus IFN- γ or IFN- γ plus LPS activated the THP-1 cells, resulting in a significant decrease in the viability of the neuronal cells (Figure 26B). Furthermore, the THP-1 cell toxicity towards the SH-SY5Y neuronal cells induced by these two MP populations was significantly different from the effect of the supernatants from THP-1 cells stimulated with MPs that had been isolated from unstimulated donor THP-1 cells. Therefore, these results demonstrated that the stimulant used to induce MP release from THP-1 cells had an effect on the activity of the MPs released.

The collected THP-1 supernatants were analyzed by ELISA to determine the ability of MPs to induce cytokine secretion by THP-1 cells. Overall the MPs did not induce the secretion of pro-inflammatory cytokines TNF- α and IL-6 by THP-1 cells regardless of the type of stimulation the MP donor THP-1 cells received (data not shown). The only MPs that stimulated the release of MCP-1 above the level of the unstimulated control cells were the MPs isolated from THP-1 cells that had been stimulated with IFN- γ plus LPS (Figure 27).

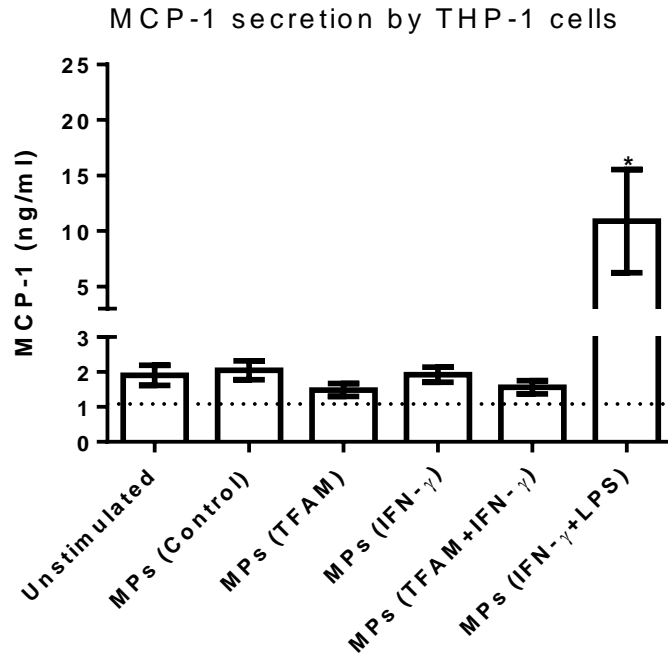


Figure 27. MPs isolated from IFN- γ plus LPS-stimulated THP-1 donor cells increase MCP-1 secretion by THP-1 cells. THP-1 cells were treated with media only (unstimulated), MPs (10 μ g of protein/ml) isolated from unstimulated THP-1 cells (control) or THP-1 cells that had been differentially stimulated with TFAM (2.5 μ g/ml), IFN- γ (150 U/ml), TFAM plus IFN- γ or IFN- γ plus LPS (0.5 μ g/ml) as shown on the abscissa. ELISA was used to measure MCP-1 in THP-1 supernatants after 48 h incubation with MPs. Data from 3 independent experiments are presented (means \pm SEM). * $P < 0.05$, significantly different from unstimulated control (ANOVA, followed by Fisher's LSD post-hoc test). Dotted line represents the ELISA detection limit.

The MPs were also tested for their ability to prime the respiratory burst in DMSO-differentiated HL-60 cells. The experiments were performed as described in the Materials and Methods section 2.12.2. After the five day differentiation period in DMSO, HL-60 cells were primed with the MPs isolated from unstimulated THP-1 cells or THP-1 cells that had been stimulated with TFAM, IFN- γ , TFAM plus IFN- γ or IFN- γ plus LPS. The HL-60 cells were incubated with the MPs for 24 h after which the release of ROS was measured by the respiratory

burst assay using fMLP as the inducing stimulant. The results were compared to those obtained from the PBS vehicle control (unprimed control) cells. The MPs did not prime the respiratory burst activity in HL-60 cells; as such the data are not presented in this thesis.

Chapter 4. Discussion

4.1. TFAM induces toxicity of glial cells towards neuronal cells

TFAM, a novel DAMP of the CNS, was investigated for its potential to induce glial cell activation and subsequent neuronal toxicity. This was investigated using an *in vitro* cell model based on supernatant transfer experiments that have been successfully employed to investigate the glial cell-mediated toxicity towards neurons¹¹¹⁻¹¹³. This toxicity is mediated by a cocktail of cytotoxic factors, including a variety of pro-inflammatory cytokines, ROS and NO and is relevant to the neuroinflammatory processes that occur in neurodegenerative diseases^{18, 137, 138}. In addition to these established pro-inflammatory mediators, increasing numbers of studies have focused on the release of the endogenous signals, the DAMPs, in response to immune cell activation^{34, 35} and the role of DAMPs in neurodegenerative diseases^{38, 139}.

The most investigated and well-characterized DAMP is HMGB1, which can activate immune cells in the peripheral tissues, as well as glial cells in the CNS, triggering an inflammatory response^{61, 62, 140}. Several studies have investigated the mitochondrial protein TFAM as a potential DAMP due to its structural and functional homology to HMGB1. These studies have revealed that TFAM can activate immune cells in the peripheral tissues^{50, 51}; however, its role as a DAMP in the CNS, was previously unknown. Based on these exploratory studies on TFAM as a DAMP in the periphery, as well as the established literature on HMGB1, I hypothesized that TFAM could act as a DAMP in the CNS. Specifically, I hypothesized that TFAM, by interacting with specific receptors (RAGE and Mac-1), could induce activation of glial cells resulting in the subsequent toxicity of their supernatants towards neuronal cells.

To test this hypothesis, THP-1 cells were used as the microglia model and the U-118 MG cells were used as the astrocyte model, as they possess functional characteristics and receptors

similar to their primary microglia/astrocyte counterparts. THP-1 cells express CR1 (also known as C3b/C4b receptor)^{102, 103} and Mac-1^{69, 104}, while U-118 MG express specific astrocyte markers, such as glial fibrillary acidic protein (GFAP)^{105, 106}. The experiments with the U-118 MG cells that showed positive results were confirmed using primary human astrocytes. The SH-SY5Y cells were used as the neuronal model as these cells display certain characteristics of primary neurons¹¹⁰.

THP-1 cells, U-118 MG cells and primary human astrocytes were cultured on their own and stimulated with TFAM in the presence or absence of IFN- γ . THP-1 cells were also stimulated with IFN- γ plus LPS and a cytokine cocktail made up of IL-6, IL-1 β and TNF- α ; used as positive controls previously shown to induce the activation of microglial cells and subsequent neurotoxicity²². Similarly, U-118 MG cells and primary human astrocytes were stimulated with IFN- γ plus IL-1 β , in addition to TFAM and IFN- γ , to induce their activation¹¹³. Following incubation, the supernatants from the stimulated glial cells were transferred onto SH-SY5Y cells and after 72 h the neuronal viability was measured by the MTT assay.

The results showed that stimulation of THP-1 cells and U-118 MG cells with TFAM alone or IFN- γ alone did not result in THP-1 cell toxicity towards the SH-SY5Y cells. These findings were confirmed using TFAM-stimulated primary human astrocytes. In contrast to the THP-1 results, IFN- γ alone induced astrocyte (U-118 MG cells and primary human astrocytes) toxicity towards the SH-SY5Y cells. However, the significant difference between the toxicity induced by IFN- γ stimulation alone and that induced by TFAM plus IFN- γ indicated that TFAM triggered additional glial toxicity above the levels induced by IFN- γ .

TFAM in combination with IFN- γ induced toxicity of the glial cells, which caused a significant decrease in SH-SY5Y cell viability. This was observed in all cell types assayed. This

observation is consistent with studies that investigated the effect of HMGB1 on murine macrophages, which showed that HMGB1 forms immune complexes by binding to IFN- γ , IL-1 β and TNF- α ^{54, 141}. This complex formation resulted in a higher secretion of pro-inflammatory cytokines, such as IL-6 or macrophage inflammatory protein-2 (MIP-2) by macrophages compared to HMGB1 on its own, in the absence of immune complex formation^{54, 141}. The actual mechanism(s) by which HMGB1 enhances the release of pro-inflammatory cytokines requires further investigation. TFAM may act in a similar manner by forming immune complexes with IFN- γ , which would provide an explanation for the observed glial cell activation in the presence of IFN- γ . In addition, the synergism between TFAM and IFN- γ could be explained by the different signaling pathways they engage. In mononuclear phagocytes, IFN- γ activates the JAK/STAT pathway^{22, 142} resulting in the transcription of a variety of cytokines and growth factors that are important for cell proliferation, differentiation and apoptosis¹⁴³. In contrast, TFAM potentially signals through the JNK¹²⁰ and ERK⁵¹ pathways, which regulate the expression of genes involved in apoptosis, inflammation, cytokine and growth factor production^{144, 145}. These different pathways can interact with each other and can also enhance activation of each other^{143, 146}. Therefore, simultaneous activation of these pro-inflammatory signaling pathways by stimulation with TFAM and IFN- γ may potentially enhance microglial activation above the level achieved by activating just one pathway.

4.1.1. Identifying the neurotoxic domain of TFAM

The next research question addressed was which specific domain of TFAM is responsible for activating glial cells resulting in the observed neurotoxicity. Similar to HMGB1, TFAM is composed of two HMG boxes, Box A and Box B, which are arranged in tandem connected by a

27 amino acid linker⁴⁴. Box A and Box B differ in primary sequence, resulting in a difference in their physiological roles. Box A is the predominant mitochondrial DNA binding domain, while Box B does not directly bind DNA itself, but instead, stabilizes the interaction between Box A and DNA^{44,47}. This difference in their physiological functions may translate into a difference in their cytotoxic potential, as is the case with HMGB1. Box B of HMGB1 appears to be the domain responsible for induction of the pro-inflammatory response on target cells, while Box A of HMGB1 possesses no intrinsic pro-inflammatory properties^{52,55,147}. Murine macrophage-like RAW 264.7 cells showed a significant difference in TNF- α release when stimulated with truncated forms of either HMGB1 Box A or Box B. Box B on its own induced the release of TNF- α , IL-6 and IL- β , similar to the full-length HMGB1, while Box A did not induce a significant release of TNF- α ⁵⁵. Moreover, antibodies against the full-length HMGB1 and Box B reduced the secretion of TNF- α from murine macrophages⁵⁵. A separate study provided evidence for the protective properties of HMGB1 Box A. The HMGB1-induced release of TNF- α and IL-1 β by murine macrophages was significantly decreased in the presence of Box A protein¹⁴⁷. Furthermore, *in vivo* experiments using LPS-exposed mice showed that treatment with Box A led to increased survival of the mice compared to the control mice¹⁴⁷.

To answer the question of which domain of TFAM, Box A or Box B, is responsible for the toxicity of TFAM, supernatant transfer experiments similar to those described in the previous section (4.1.) were conducted. In addition to stimulating with full-length TFAM, the truncated forms of TFAM, Box A and Box B, were applied separately to the THP-1 cells, U-118 MG cells or the primary human astrocytes.

The results showed that Box A and Box B on their own did not induce THP-1 or U-118 MG cell-mediated toxicity towards neuronal cells and did not significantly decrease the viability

of the SH-SY5Y cells. In contrast, full length TFAM plus IFN- γ , Box A plus IFN- γ and Box B plus IFN- γ significantly induced THP-1 and U-118 MG cell toxicity towards SH-SY5Y cells. Furthermore, there was no significant difference between the activation induced by Box A or Box B in the presence of IFN- γ , which indicated that these two TFAM domains were equipotent. In contrast to THP-1 cells, supernatants from IFN- γ -stimulated U-118 MG cells significantly decreased the viability of the SH-SY5Y cells. However, the significant increase in toxicity, when comparing the effects of IFN- γ and TFAM plus IFN- γ stimulation of U-118 MG cells, indicates that the added TFAM induced toxicity above the level that was caused by IFN- γ -alone.

These results are consistent with a recent study by Julian et al.^{49, 51} on the effects of TFAM on plasmacytoid dendritic cells and splenocytes. TFAM in combination with CpG DNA triggered a pro-inflammatory response from these cells, which was characterized by a significant release in TNF- α ^{49, 51}. Furthermore, they determined that Box A and Box B of TFAM in combination with CpG were equivalent at promoting the release of TNF- α from the splenocytes⁵¹. They went on to suggest that unlike HMGB1, where the difference in amino acid sequence is responsible for the observed differences in immunogenicity between Box A and Box B, the pro-inflammatory properties of TFAM Box A and Box B, as well as of full-length TFAM itself, are due to molecular surface charge characteristics¹⁴⁸. This conclusion was based on the results from their heparin inhibition experiments⁵¹. Since heparin is a highly negatively charged molecule, it primarily binds other proteins electrostatically^{149, 150}. Therefore, heparin may inhibit the biological activity of TFAM by interacting with the positive surface charge of full-length TFAM and its boxes. A separate study also confirmed that although the difference in residues between Box A and Box B affects the DNA binding ability of Box B, the electrostatic surface potential remains positive in both domains⁴⁷. This may translate into similar physiological functions of

the two box domains and may explain the equipotency of Box A and Box B as inducers of neurotoxicity.

Compared to the THP-1 and the U-118 MG cells, the primary human astrocytes responded differently to Box A and Box B. The viability of the primary human astrocytes decreased upon stimulation with Box A and Box B in the presence and absence of IFN- γ . In addition, similar to the IFN- γ -stimulated U-118 MG cells, there was a significant difference between IFN- γ and TFAM plus IFN- γ stimulation. This indicated that the induced toxicity was due to TFAM in addition to the effect of IFN- γ .

Box A and Box B only induced primary human astrocyte toxicity towards the SH-SY5Y cells in the presence of IFN- γ . Moreover, primary human astrocyte toxicity towards the SH-SY5Y cells induced by Box B plus IFN- γ was lower in magnitude compared to that induced by Box A plus IFN- γ . In addition, there was a significant difference between TFAM plus IFN- γ and Box B plus IFN- γ . This indicated that in primary human astrocytes Box A and Box B were not equipotent, and that Box B was less potent at inducing neurotoxicity.

These results contradict the above mentioned studies indicating the equipotency of both TFAM domains. However, this difference in toxic potential of the two boxes on astrocytes may simply be due to the increased sensitivity of primary cells to stimulation compared to cell lines, which are more robust. Cell lines compared to their primary cell counterparts are inherently more resilient to stimulation due to their cancerous origin²². Moreover, the resilience may be a result of a difference in signaling pathway activation patterns between the cell lines and the primary cells, due to the random mutations that the cell lines may have undergone due to multiple divisions.

4.2. Mechanism underlying TFAM-induced glial activation

Due to the pro-inflammatory and neurotoxicity-inducing activity of TFAM, several potential mechanisms of its action were explored. The ability of TFAM to induce the release of pro-inflammatory cytokines from THP-1 cells, U-118 MG cells and primary human astrocytes was investigated. In addition, priming of the production of ROS by TFAM was studied using the promyelocytic HL-60 cells.

4.2.1. TFAM enhances the secretion of pro-inflammatory cytokines by glial cells

In response to different stimuli, glial cells release a wide variety of cytokines, which act as signaling molecules affecting cell function in an autocrine or paracrine manner. Activated glial cells can release pro-inflammatory cytokines, such as IL-6, IL-1 β or TNF- α , as well as the chemokine MCP-1^{22, 112, 151}. MCP-1 is, primarily, a chemotactic agent, but increased expression and release of MCP-1 has also been associated with inflammation and microglial activation^{152, 153}. Inhibiting the excessive release of IL-6, IL-1 β , TNF- α or MCP-1 could be beneficial in chronic neuroinflammation, as these cytokines perpetuate the pro-inflammatory cycle. Therefore, the release of these pro-inflammatory cytokines by glial cells in response to TFAM stimulation was investigated.

A recent study from our laboratory demonstrated that TFAM significantly induced the expression and secretion of IL-6, IL-1 β and IL-8 by THP-1 cells¹²⁰; therefore, I did not re-test the release of these specific cytokines, but instead focused on MCP-1 secretion by THP-1 cells in response to TFAM stimulation. TFAM alone induced the release of MCP-1 from THP-1 cells. In combination with IFN- γ , however, this release was increased, which is consistent with the supernatant transfer experiments indicating increased glial cell-mediated neurotoxicity in the

presence of TFAM plus IFN- γ . The released MCP-1 may act to recruit and activate additional microglia, as the MCP-1 receptor is expressed by these cells^{152, 154}. Using a neuron/microglia co-culture system Yang et al.¹⁵² demonstrated that MCP-1-induced neurotoxicity required the presence of microglia, as exogenously administered MCP-1 alone, in the absence of microglia, did not directly damage neurons. Moreover, exogenously administered MCP-1 activated microglia and increased expression of IL-1 β and TNF- α by microglia¹⁵². Increase of these cytokines has been associated with neurodegeneration^{137, 155}, and inhibiting their release may enhance neuronal survival.

Supernatants from TFAM-stimulated U-118 MG cells were assessed for the presence of cytokines. Although the SH-SY5Y cells that had been incubated with the supernatants from TFAM plus IFN- γ -stimulated U-118 MG cells showed a decrease in viability, the observed neurotoxicity could not be explained by the release of IL-6 or TNF- α . There was no significant release above the unstimulated control cells of either of these two cytokines upon stimulation with TFAM, IFN- γ or TFAM plus IFN- γ . The absence of increased cytokine secretion, however, may be explained by the high basal cytokine secretion level of the U-118 MG cells, which is a previously described characteristic of glioma cell lines^{112, 156}. As a result, high concentrations of stimulants could be required to achieve an increased cytokine release above the basal level. Thus, the stimulants used in this experiment, including TFAM, may not have been at a high enough concentration to induce IL-6 and/or TNF- α release from the U-118 MG cells. Future investigations could focus on determining the TFAM concentrations necessary to stimulate IL-6 and TNF- α release from U-118 MG cells, but the concentrations will then most likely be above the physiologically relevant range.

In contrast to the U-118 MG cells, the primary human astrocytes showed a significant increase in the release of IL-6 in response to TFAM, which was enhanced in the presence of IFN- γ . Although IL-6 can have beneficial effects in the CNS due to its neurotrophic properties, the overexpression of IL-6 has been linked to neuroinflammation^{5, 157}. IL-6 in combination with other cytokines, such as TNF- α , has been shown to induce microglial toxicity towards neuronal cells²², thus contributing to the propagation of the pro-inflammatory cycle. Therefore, due to the pleiotropic role of IL-6 in the CNS, it is essential to enhance the understanding of IL-6 regulation, as this may provide an additional target for modulating overactivated microglia in sterile neuroinflammatory conditions.

4.2.2. TFAM primes the secretion of ROS by glial cells

Stimulated glial cells may also release ROS through the activity of NADPH oxidase, which is the multi-subunit enzyme complex responsible for the production of ROS by phagocytic cells, including microglia²⁵. The enzyme complex consists of four cytoplasmic subunits that translocate and dock with the two membrane subunits upon the activation of the complex. This forms an electron-transfer system that catalyzes the reduction of molecular oxygen at the expense of NADPH, resulting in the two primary products $O_2^{\bullet -}$ and H_2O_2 ¹⁵⁸ (Figure 29). These oxygen metabolites can give rise to additional ROS that primarily function as antimicrobial agents to destroy invading pathogens. The increased and uncontrolled production of ROS, however, can result in damage to surrounding cells leading to additional inflammatory reactions¹⁵⁸. Oxidative stress has been implicated as one of the central mechanisms of chronic neurodegeneration in AD and PD^{24, 75, 77}. Moreover, NADPH oxidase expression is up-regulated in AD⁷⁶ and has been shown to be essential in amyloid-induced microglial neurotoxicity^{159, 160}.

HMGB1 has also been shown to trigger microglial activation and NADPH oxidase-dependent ROS production leading to dopaminergic neurodegeneration⁶². Therefore, the ability of TFAM to prime ROS release from microglia-like cells was investigated.

Respiratory burst experiments were conducted using HL-60 cells as models of microglia possessing functional NADPH oxidase complexes to measure the effects of TFAM on the release of ROS.

TFAM alone primed the release of ROS. However, TFAM plus IFN- γ enhanced the release of ROS above the levels achieved by TFAM priming alone. This is consistent with the results obtained from the supernatant transfer experiments, as well as the ELISA experiments, as TFAM induced glial cell toxicity towards SH-SY5Y cells and significantly higher levels of cytokine secretion only in the presence of IFN- γ . The results from the respiratory burst experiments indicate that the synergism between TFAM and IFN- γ also affects the priming of the respiratory burst.

Therefore, it appears that, overall, TFAM requires a co-activator in order to induce significant activation of glial cells and to trigger the release of the pro-inflammatory mediators. In the context of developing therapeutic strategies for diseases involving sterile inflammation, blocking the interaction between TFAM and IFN- γ could be an additional strategy.

Next, experiments were conducted to determine which domain of TFAM was responsible for priming the respiratory burst. Full-length TFAM, Box A and Box B, all significantly primed fMLP-dependent respiratory burst activity in HL-60 cells. However, Box B was less efficient than Box A at priming the respiratory burst. This may be explained by the difference in binding affinities that the two domains possess. In contrast to Box A, which is the dominant DNA binding domain of TFAM, Box B lacks the ability to bind DNA on its own⁴⁴. This difference in

binding ability may not be solely applicable to DNA, but possibly to other molecules or receptors, as well. Box B, for example, may not be able to bind as efficiently to the Mac-1 receptor (see section 4.2.3.), which may be responsible for priming and mediating NADPH oxidase activation.

4.2.3. TFAM acts by engaging RAGE and Mac-1

After the ability of TFAM to induce cytotoxic responses from glial cells in the form of pro-inflammatory cytokines, chemokines and ROS had been established (see sections 4.2.1. and 4.2.2.), the next research question addressed was which specific glial receptors were engaged by TFAM when interacting with glial cells. This insight into the possible molecular targets is important, as it may identify new ways of modulating glial cell activation. Previous studies performed with HMGB1 provided some potential receptor targets for TFAM research. HMGB1 has been shown to trigger activation of glial cells by engaging TLR2, TLR4 and TLR9^{67, 161, 162}, as well as RAGE^{66, 80} and Mac-1^{62, 65}, resulting in an increased secretion of pro-inflammatory mediators. RAGE and Mac-1 were investigated as potential glial receptors targeted by TFAM (Figure 28).

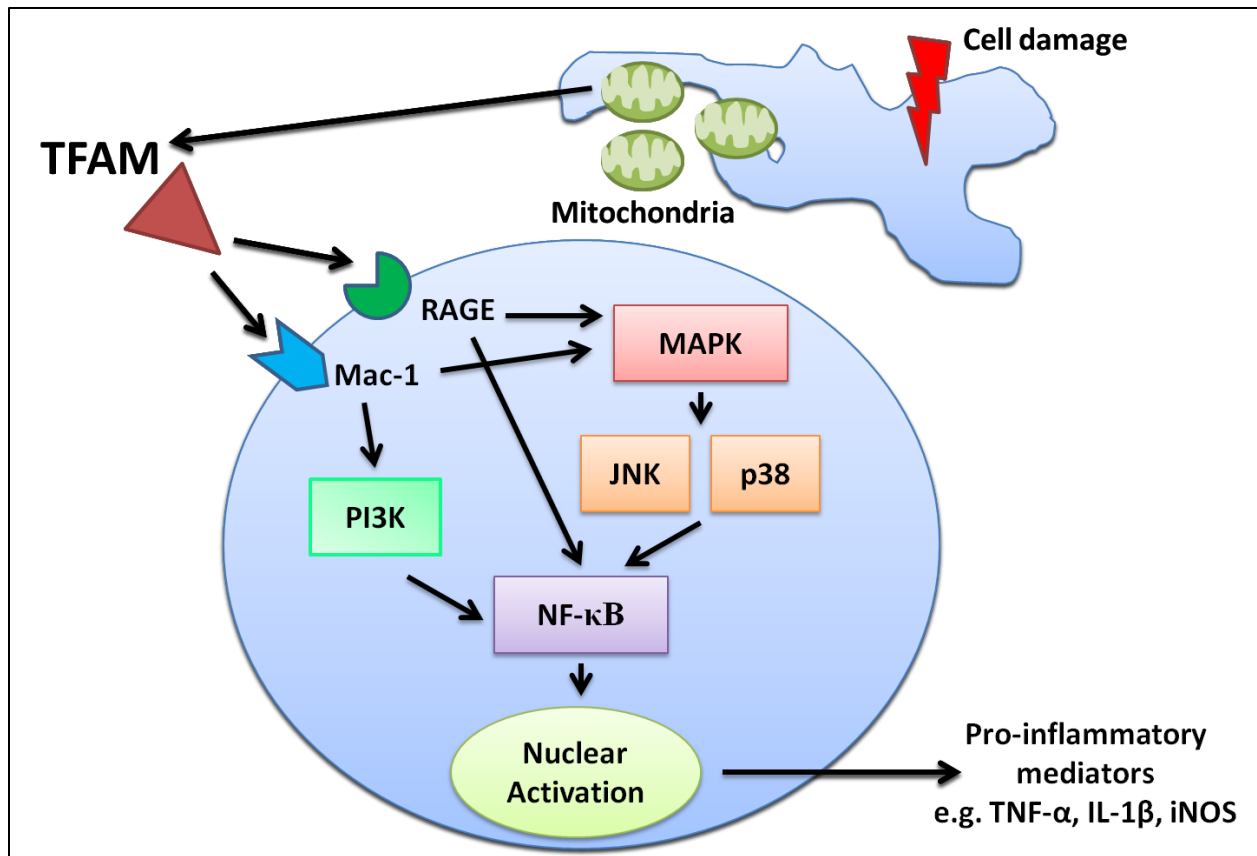


Figure 28. The potential receptors and signaling pathways underlying glial activation by TFAM. Upon cell damage, extracellularly released TFAM engages RAGE and Mac-1 on the surface of glial cells, leading to signal transduction via MAPK and PI3K pathways. This activation induces gene transcription and secretion of pro-inflammatory mediators.

THP-1 cells were incubated for 30 min with different RAGE blocking agents (heparin, sRAGE, anti-RAGE antibody), which have all been shown to successfully inhibit the interaction between RAGE and its ligands^{49, 80-82, 84, 85}; followed by stimulation with TFAM, IFN- γ or TFAM plus IFN- γ .

In the presence of heparin, the toxicity of THP-1 cells towards SH-SY5Y cells induced by TFAM plus IFN- γ was attenuated. Several studies focusing on the HMGB1 interaction with

RAGE have demonstrated that heparan sulfate, which is found on the surface of virtually all animal cells⁸⁴, is required for this specific ligand-receptor interaction^{84,85}. Based on the results from the HMGB1 experiments, heparin may inhibit the interaction between RAGE and TFAM in a similar manner by: (1) competing with TFAM for binding sites on the surface of heparan sulfate, thereby inhibiting the formation of the heparan sulfate-TFAM complex necessary for TFAM activity, or (2) altering the conformation of TFAM, thus inhibiting the interaction between TFAM and RAGE. Therefore, addition of heparin sulfate before cells exposure to TFAM should result in increased SH-SY5Y cell viability, which is consistent with the results obtained. Moreover, the supernatants collected from the TFAM plus IFN- γ -stimulated THP-1 cells treated with heparin showed a decrease in MCP-1 levels compared to the uninhibited counterparts. Similar results were obtained by Ling et al.⁸⁵, who demonstrated that HMGB-1-mediated secretion of IL-6 and TNF- α by RAW264.7 macrophages decreased in the presence of heparin. The decrease in MCP-1 secretion could help explain the observed attenuation in TFAM plus IFN- γ -induced glial cells activation and subsequent neurotoxicity in response to the heparin treatment, as increased levels of MCP-1 are considered to be pro-inflammatory¹⁵². In addition, activated microglia in neurodegenerative disease have been shown to exhibit upregulated mRNA and protein expression of pro-inflammatory chemokines, including MCP-1¹³⁷. Although *in vivo* conditions surrounding microglial activation and neurodegeneration are far more complex than *in vitro*, knowing that MCP-1 secretion can be attenuated by heparin adds to potential targets for glial cell modulation.

The next two blocking agents used to inhibit RAGE were sRAGE and anti-RAGE antibody. THP-1 cells were treated with the truncated form of the RAGE receptor (sRAGE) or a specific anti-RAGE antibody for 30 min prior to stimulation with TFAM, IFN- γ or TFAM plus

IFN- γ . sRAGE and the anti-RAGE antibody did not attenuate TFAM plus IFN- γ -induced THP-1 cell toxicity in the supernatant transfer experiments (data not shown). Use of higher concentrations of the inhibitors may be required to see an effect in the MTT assay. In the ELISA experiments, sRAGE decreased MCP-1 secretion from TFAM and TFAM plus IFN- γ -stimulated THP-1 cells compared to secretion from the uninhibited cells. The decrease in MCP-1 secretion observed in THP-1 cells inhibited by sRAGE should not be over-interpreted, as only three experiments using sRAGE were conducted due to limited availability of this reagent. Nonetheless, another study using TFAM-stimulated splenocytes and plasmacytoid dendritic cells demonstrated that secretion of TNF- α could be attenuated in the presence of sRAGE⁵¹. This led to the conclusion that TFAM partially acted through RAGE⁵¹. The anti-RAGE antibody also decreased MCP-1 secretion from TFAM plus IFN- γ -stimulated THP-1 cells compared to the secretion from uninhibited cells, thus providing further evidence for the involvement of RAGE in the pro-inflammatory activity of TFAM. Similar results were obtained by Pedrazzi et al.⁶⁶, who demonstrated that inhibiting RAGE prior to HMGB1 stimulation of primary rat astrocytes led to a decrease in the level of MAPK and ERK1/2 phosphorylation, which in turn, led to reduced downstream transcription and subsequent secretion of MCP-1.

Overall, these results implicate RAGE as one of the glial receptors targeted by TFAM and as one of the facilitators of the pro-inflammatory activity of TFAM. However, the effects of TFAM are not mediated by RAGE alone, as the attenuation of neurotoxicity and production of MCP-1 by inhibitors of RAGE was only partial. This indicates the involvement of additional receptors.

HMGB1 has been shown to act through Mac-1^{62, 65}, which makes it another potential target for TFAM. Therefore, THP-1 cells were pre-treated with an anti-Mac-1 antibody, which

has been shown to successfully block the Mac-1 receptor ¹²⁵, prior to stimulation with TFAM, IFN- γ or TFAM plus IFN- γ .

The supernatant transfer experiments showed that inhibiting the Mac-1 receptor attenuated the TFAM plus IFN- γ -induced THP-1 cell toxicity towards SH-SY5Y neuronal cells compared to the uninhibited cells. Moreover, MCP-1 secretion by the TFAM plus IFN- γ -stimulated THP-1 cells was decreased in the presence of the anti-Mac-1 antibody compared to the uninhibited cells. Mac-1 has been shown to signal through the MAPK pathways, specifically JNK1/2 and p38 ¹⁶³, leading to induction of the transcription factor NF- κ B. This, in turn, leads to downstream transcription of pro-inflammatory mediators, including MCP-1 ¹⁶⁴. This would explain the attenuation in neurotoxicity and MCP-1 secretion observed in THP-1 cells inhibited by the anti-Mac-1 antibody.

Next, experiments were performed to determine whether inhibiting RAGE and Mac-1 simultaneously would lead to a further decrease or complete abolishment of MCP-1 secretion by the TFAM plus IFN- γ -stimulated THP-1 cells. The results showed that when RAGE and Mac-1 were inhibited simultaneously, MCP-1 release was below the level of MCP-1 secreted by THP-1 cells inhibited by either of the inhibitors alone. A recent study found that RAGE serves as a counter-receptor for Mac-1 by directly binding to Mac-1, and that this interaction plays a role in leukocyte recruitment *in vivo* and *in vitro* ¹⁶⁵. As a chemokine, MCP-1 plays a role in leukocyte recruitment, and its expression and secretion may, therefore, be affected by the RAGE-Mac-1 interaction. Blocking both RAGE and Mac-1 almost completely abolished neutrophil extravasation into the inflamed peritoneum of mice demonstrating that the interaction between these receptors is required for leukocyte recruitment ¹⁶⁵. Consequently, the release of MCP-1 may be lower when both receptors are inhibited compared to inhibiting one receptor at a time.

Moreover, S100B protein, which is another DAMP and RAGE ligand, was found to increase the binding between RAGE and Mac-1, suggesting the formation of a ternary complex between the ligand and the two receptors ¹⁶⁵. It may be possible that a similar ternary complex may exist between RAGE, Mac-1 and TFAM, but this requires further experimental proof.

In addition to investigating the effect of inhibiting Mac-1 on cytokine release, additional experiments were focused on assessing the role of Mac-1 in ROS release by HL-60 cells. Mac-1 has been shown to be involved in mediating ROS release from HMGB-1-stimulated mouse microglia cells ⁶². Treatment of Mac-1^{-/-} mice-derived microglia with HMGB1 resulted in a significant reduction in O₂[•] release compared to microglia from Mac-1^{+/+} mice ⁶². Therefore, respiratory burst experiments using the anti-Mac-1 antibody were performed to determine whether Mac-1 was involved in TFAM priming of ROS production by glial cells.

The results of the respiratory burst experiments showed that inhibiting Mac-1, indeed, attenuated the TFAM-primed ROS release from HL-60 cells. A possible explanation may be provided by the fact that upregulated expression of Mac-1 and the fMLP receptor has been demonstrated in neutrophils in response to LPS priming ¹³³. TFAM priming may have similar effects on Mac-1 and fMLP receptor expression in HL-60 cells. Therefore, inhibiting the Mac-1 receptor would attenuate the priming of the fMLP-induced ROS release by TFAM, but may not completely abolish it, due to the other types of receptors mediating the effects of TFAM. This would be consistent with the results obtained indicating decreased ROS release in the presence of anti-Mac-1 antibody.

An additional argument to support Mac-1 as a mediator of TFAM-primed ROS release by HL-60 cells is the fact that Mac-1 has been shown to activate NADPH oxidase-mediated O₂[•] production and neurotoxicity using mesencephalic mouse neuron-glia cultures ⁷². Priming of the

NADPH oxidase complex has been suggested to be mediated by a cross-talk between serine/threonine kinases and tyrosine kinases¹⁶⁶. Priming agents, such as LPS or TFAM, may induce the activation of tyrosine kinases leading to the phosphorylation and subsequent activation of serine kinases. Stimulating agents, such as fMLP, may then trigger the phosphorylation of additional serine kinases. Once all the necessary serine kinases have been activated, they then phosphorylate the p47^{phox} cytoplasmic subunit of the NADPH oxidase complex, which may be the signal for oxidase activation¹⁶⁶. Thus, priming establishes a baseline level of phosphorylation of the serine kinases, while stimulation is required to increase phosphorylation above a certain threshold and thus initiate activation.

Zhang et al.⁷² described an additional potential signaling pathway, involving a different kinase, which may trigger the activation of the NADPH oxidase complex. They demonstrated that Mac-1 signals through the PI3K pathway to achieve activation of the complex. Therefore, if TFAM engages Mac-1, the activated PI3K could phosphorylate the cytoplasmic components of NADPH oxidase, thus activating the complex. The activated NADPH oxidase would then mediate the production of O₂^{•-} in response to fMLP stimulation (Figure 29). In addition, ROS can act as second messengers that contribute to the activation of NF-κB leading to the expression of pro-inflammatory mediators⁷³. Combined, these mediators contribute to a pro-inflammatory environment that is potentially damaging to surrounding neurons. Therefore, inhibiting Mac-1 could block its interaction with TFAM resulting in a decrease in the production of ROS and an increase in neuronal viability.

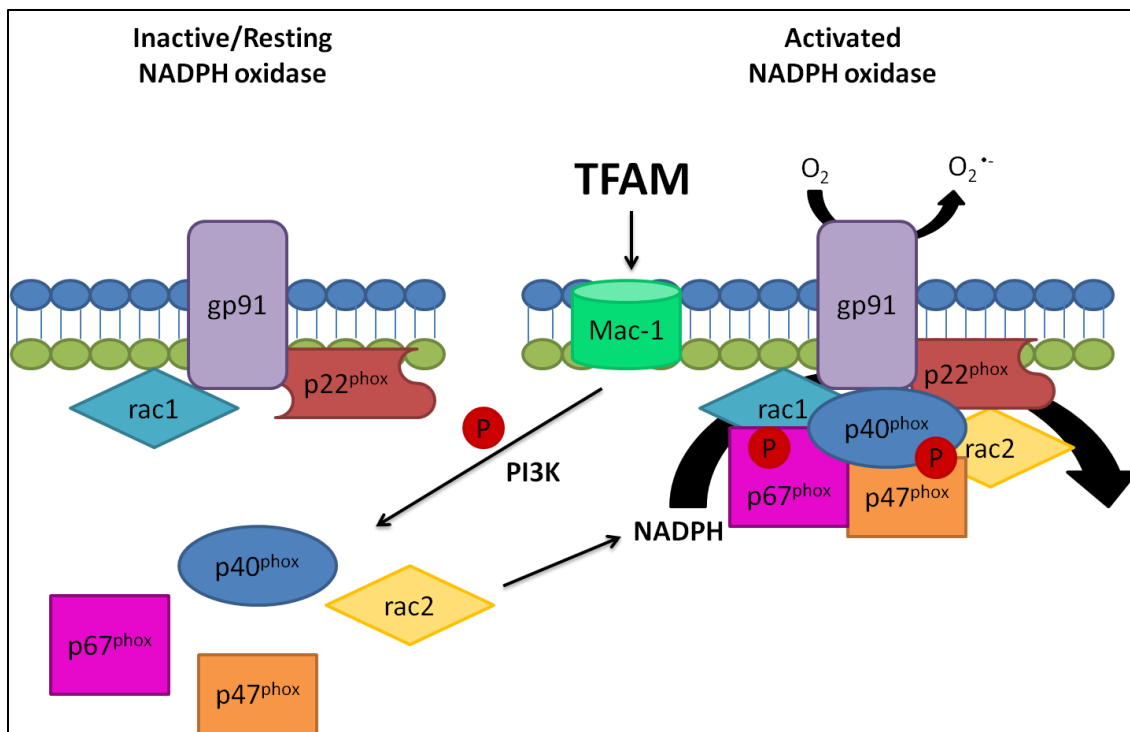


Figure 29. TFAM-mediated NADPH oxidase priming and ROS production. TFAM can bind to the Mac-1 receptor activating downstream kinases such as PI3K, which leads to the phosphorylation (p) of the cytoplasmic components of NADPH oxidase complex (p67^{phox}, p47^{phox}, p40^{phox} and rac2). The cytoplasmic components then translocate and interact with the membrane-bound components (rac1, gp91 and p22^{phox}) forming an activated NADPH oxidase complex. Activated NADPH oxidase transfers electrons from NADPH to molecular oxygen generating O₂^{•-}, which contributes to neurodegeneration.

Overall the above observations indicate the involvement of both RAGE and Mac-1 in the pro-inflammatory activity of TFAM. However, additional receptors appear to be involved as inhibiting RAGE or Mac-1 simultaneously did not completely abolish MCP-1 secretion, but simply attenuated the release. Therefore, future investigations should focus on identifying additional receptors involved in TFAM-mediated signaling to provide additional targets for

modifying microglial activation. These may include TLR2, TLR4 and TLR9^{67, 51, 161, 162}, as HMGB1 and TFAM have been shown to signal through these receptors in peripheral tissues.

4.3. Hydrogen peroxide enhances TFAM mRNA expression levels by astrocytic cells

The next research question that was addressed was how the expression of TFAM in glial cells changes in response to different stimulating agents. qPCR experiments were performed using U-373 MG cells and primary human astrocytes. The glial cells were exposed to IFN- γ , IFN- γ plus IL-1 β or H₂O₂ for 24 h, following which, TFAM expression was determined. The only biochemical stressor to induce TFAM expression by glial cells was H₂O₂.

H₂O₂ has been shown to function as a second messenger in alveolar macrophages activating the major pro-inflammatory MAPK signaling pathways including JNK and ERK, as well as the downstream NF- κ B transcription factor¹⁶⁷⁻¹⁶⁹. These pathways control the inducible expression of pro-inflammatory genes. In addition, ROS, including H₂O₂, are used as communicating agents between mitochondria, by activating signaling pathways¹⁷⁰. For example, ROS has been shown to be part of an important retrograde signal leading to the stimulation of the antioxidant response element (ARE) of cytoprotective genes, including nuclear factor-(erythroid-derived 2)-related factor 2 (Nrf2)¹⁷⁰. In the presence of ROS, Nrf2 translocates to the nucleus where it binds and activates nuclear factor (NRF)-1, which in turn regulates mitochondrial biogenesis and the expression of proteins such as TFAM¹⁷⁰. This signaling pathway would explain the qPCR results obtained, which showed increased TFAM expression upon stimulation with H₂O₂.

Although an increase in TFAM gene expression could be detected in the glial cells, it is unclear whether this increase will be reflected at the protein level, as well. Post-transcriptional

modifications and mRNA degradation may inhibit the translation of the TFAM mRNA into a functional TFAM protein. One study found that TFAM protein expression was significantly elevated in human bladder cancer tissues compared to normal, healthy bladder tissue ¹²⁷. Using western blot analysis, Chung et al. ⁵⁰ demonstrated that serum levels of TFAM are significantly increased after hemorrhagic shock in rats. Additionally, TFAM mRNA and protein levels in the skeletal muscle of aged human subjects increased 11-fold and 2.6-fold, respectively, compared to the levels found in young subjects ¹⁷¹. These differences in TFAM expression levels in peripheral tissues may suggest that similar variation in the expression levels occurs during CNS diseases.

However, in contrast to studies measuring TFAM expression in the periphery, there are fewer studies investigating the expression of TFAM in the CNS. The experiments presented in this thesis are a novel and unexplored area investigating TFAM expression levels by glial cells in the CNS. Future studies should focus on investigating the effect of additional stressors on the expression of TFAM by glial cells, and on determining the levels of TFAM protein to confirm mRNA to protein translation in the CNS cells.

4.4. Effects of TFAM-induced microparticles on toxicity of glial cells towards neuronal cells

The last experiments investigated an additional mechanism of action of TFAM involving the novel intercellular signaling agents; the MPs. Previous studies have shown that MPs have immunomodulatory and other biological activities similar to HMGB1 ^{86, 87}. Following activation, apoptosis or necrosis, MPs and HMGB1 are released from a variety of cell types, including monocytes, microglia, astrocytes and neurons ^{88, 89}. Once released, MPs regulate various biological and physiological processes, including cell-cell communication, cell proliferation, coagulation and inflammation ⁹¹. In addition, it is becoming increasingly evident that MPs can

contribute to the progression of some neurodegenerative and neuroinflammatory diseases^{88, 89, 92, 172}. Levels of circulating MPs are elevated in the CSF and plasma from patients suffering from CNS disorders, including multiple sclerosis⁹³ and cerebral malaria⁹⁴. As such, MPs have been explored as potential biomarkers of neurological disorders, providing a potential early detection method for neurodegenerative diseases that are difficult to diagnose.

To date, studies have demonstrated that pro-inflammatory cytokines, such as TNF- α , IFN- γ and IL-1 β , which are present during these neuroinflammatory disease states, are potent triggers of MP release¹⁷³. In contrast, however, the role of DAMPs, such as HMGB1 or TFAM, as triggers of MP release has not yet been investigated. Since TFAM has the ability to induce microglial activation, which can lead to MP release, the role of TFAM as a trigger for MP release was investigated.

THP-1 cells were stimulated with TFAM, IFN- γ or TFAM plus IFN- γ for 24 h, following which the released MPs were isolated by differential centrifugation. Both unstimulated and stimulated THP-1 cells released MPs (Table 2). This was to be expected, as resting cells show a constitutive release of MPs^{174, 175}. Additionally, being seeded into a plastic plate can be considered a stressful environment for the cells; stressful conditions, such as shearing stress or hypoxia have been shown to induce the release of MPs^{91, 176}. TFAM was the only stimulant to trigger a significant release of MPs above the levels released by the unstimulated control cells. The other stimulants still enhanced the release of MPs; albeit not significantly (Table 2).

To determine whether the isolated MPs possessed cytotoxic properties, supernatant transfer experiments were conducted using MPs to stimulate THP-1 cells. MPs (10 μ g of protein/ml) were isolated from THP-1 cells that had been stimulated with TFAM, IFN- γ or TFAM plus IFN- γ for 24 h. The MPs derived from donor THP-1 cells stimulated with TFAM

plus IFN- γ induced toxicity of THP-1 cells towards the SH-SY5Y cells, resulting in a decreased viability of the neuronal cells. However, when the MPs were investigated for their ability to induce the release of pro-inflammatory cytokines by THP-1 cells, only the MPs isolated from IFN- γ plus LPS-stimulated donor THP-1 cells induced the release of MCP-1 above the levels of the unstimulated control cells. MPs were also tested for their ability to prime the respiratory burst activity in HL-60 cells, but no significant results were obtained (data not shown).

These results are contrary to the data obtained by Bardelli et al.¹³². MPs isolated from human monocytes stimulated with the calcium ionophore A23187 were able to induce O₂^{•-}, as well as IL-6 and TNF- α release from human monocytes¹³². Moreover, MPs induced NF- κ B activation, which would explain the observed increase in pro-inflammatory cytokine secretion¹³². The difference in results obtained may be due to several reasons, including: (1) the cell types used from which the MPs were isolated, as different cell types shed different numbers of MPs^{97, 98, 132, 177, 178}, (2) the stimulating agents used, as different stimulants induce distinct MP populations¹⁷⁷, and (3) the incubation times with the stimulants, as incubation time has been shown to have an effect on the numbers of MPs released⁹⁷ and on the MP structure⁹⁷. All of these factors can affect the physiological function of the MPs generated, leading to a different response elicited in the target cells. In addition, the high diversity in the results obtained in different laboratories is mainly due to the absence of a standardized method for isolating MPs. Due to the increasing evidence supporting the involvement of MPs in the pathogenesis of a variety of diseases, it is important that standardized methods are developed to decrease the differences in isolating protocols between different research laboratories. Therefore, it may still be possible that TFAM induces the release of MPs that have the ability to induce pro-inflammatory cytokine secretion; however, this hypothesis will require further investigations.

Chapter 5. Conclusions and future work

5.1. Limitations of research

One of the main limitations of this research is the use of cell lines, which are derived from tumors from different cells types (e.g. U-118 MG astrocytoma cells as a model for astrocytes), and may, therefore, differ with respect to gene or protein expression from their primary cell counterparts. This may lead to altered physiological responses compared to the primary cells. To overcome this limitation, key experiments showing positive results were confirmed using primary human astrocytes.

Another potential limitation of this study is the use of supernatant transfer experiments to identify the effect of TFAM on glial cell-mediated neurotoxicity. Glial cells and neuronal cells were cultured separately, which is not an accurate representation of their interactions in the brain *in vivo*. By culturing the cells separately and transferring the cultured supernatants, only a unidirectional flow of effects can be investigated. As a result of culturing cells individually, other key interactions and bidirectional effects between glial cells and neurons may be missed or under-investigated. Trans-well or co-culture experiments that allow for the glial cells and the neuronal cells to be seeded into the same well may provide additional insights into the glial-neuronal cell interactions that occur *in vivo*. Although the supernatant transfer experiments may oversimplify the interactions between glial cells and neurons, they allow us to tease out the effects of a single variable, providing us with a stepping stone towards more complex research experiments.

5.2. Future work

This thesis work provides substantial evidence that TFAM is a novel DAMP in the CNS. Although stimulation of the pro-inflammatory cytokine release from glial cells (THP-1 cell and primary human astrocytes) and the decrease in neuronal viability provided direct evidence of the activation of glial cells by extracellular TFAM, these results need to be confirmed using primary microglia and, more importantly, they need to be confirmed *in vivo*. In this regard, injecting TFAM into the brain of healthy mice or rats may confirm the role of TFAM as a novel CNS DAMP, and demonstrate the ability of TFAM to activate glial cells and induce the secretion of pro-inflammatory cytokines, chemokines and ROS, potentially leading to neuronal damage in healthy animals.

Moreover, additional studies need to focus on further describing and identifying the detailed signaling pathways that mediate the pro-inflammatory activity of TFAM. This thesis demonstrated the involvement of RAGE and Mac-1 in the activity of TFAM; however, additional receptors need to be explored in order to fully elucidate the mode of action of TFAM. Studies on HMGB1 have identified several TLR receptors involved in mediating its activity, and due to the homology between HMGB1 and TFAM, the TLR receptors may represent potential candidates targeted by TFAM, as well. A natural extension of this study would be to focus on assessing whether blockade of the involved receptors and pathways could inhibit the pro-inflammatory responses and attenuate neuronal damage *in vivo*.

5.3. Significance of Findings

In conclusion, this thesis confirms the role of TFAM as a potential glial cell activator that has the ability to induce cytotoxic responses from the glial cells, including the release of pro-

inflammatory cytokines, chemokines and ROS. In addition, TFAM was shown to induce the release of MPs, novel intercellular signaling agents that can contribute to the onset and progression of some neurodegenerative and neuroinflammatory diseases.

Moreover, based on published studies describing the mode of action of HMGB1 in the CNS and TFAM in peripheral tissues, this thesis identified RAGE and Mac-1 as the key glial receptors engaged by TFAM. This has the potential to provide targets for ameliorating and altering the CNS inflammatory processes. RAGE, in particular, appears to be a good candidate for inhibiting TFAM activity, as RAGE expression levels are elevated during pathological conditions, including Alzheimer's disease^{179, 180}. Under physiological conditions RAGE is expressed at low levels in all adult tissues, with exception of the lung where RAGE is expressed at high levels¹⁸¹. Therefore, developing specific inhibitors of RAGE to prevent TFAM binding may prove to be a promising strategy for ameliorating glial cell activation and inflammation in neurodegenerative diseases. Accordingly, the novel *in vitro* properties of TFAM discovered within this thesis work warrant further testing of TFAM in animal models to assess its neurotoxic potential *in vivo*.

This thesis contributes to expanding the fundamental knowledge of CNS functioning by providing new information about the role of endogenous intercellular signaling molecules in communication between different CNS cell types. My research provides additional insight into the physiological glial activation, which has been implicated as a contributing factor to the onset and progression of a variety of neurodegenerative diseases, including AD. The prevalence of AD worldwide is continuously increasing and currently there are no effective therapies. Results of this research highlight novel molecular and therapeutic targets for a variety of pathologies that involve sterile neuroinflammatory processes such as AD.

References

- 1.Lobo, A., Launer, L.J., Fratiglioni, L., Andersen, K., Di Carlo, A., Breteler, M.M., Copeland, J.R., Dartigues, J.F., Jagger, C., Martinez-Lage, J., Soininen, H. & Hofman, A. (2000) Prevalence of dementia and major subtypes in Europe: A collaborative study of population-based cohorts. Neurologic Diseases in the Elderly Research Group. *Neurology*, **54**, S4-9.
- 2.Cummings, J.L., Morstorf, T. & Zhong, K. (2014) Alzheimer's disease drug-development pipeline: few candidates, frequent failures. *Alzheimers Res Ther*, **6**, 37.
- 3.Cummings, J.L. & Cole, G. (2002) Alzheimer disease. *JAMA*, **287**, 2335-2338.
- 4.Alzheimer, A., Stelzmann, R.A., Schnitzlein, H.N. & Murtagh, F.R. (1995) An English translation of Alzheimer's 1907 paper, "Über eine eigenartige Erkrankung der Hirnrinde". *Clin Anat*, **8**, 429-31.
- 5.Bamberger, M.E. & Landreth, G.E. (2002) Inflammation, apoptosis, and Alzheimer's disease. *Neuroscientist*, **8**, 276-283.
- 6.Hardy, J.A. & Higgins, G.A. (1992) Alzheimer's disease: the amyloid cascade hypothesis. *Science*, **256**, 184-185.
- 7.Hardy, J. & Selkoe, D.J. (2002) The amyloid hypothesis of Alzheimer's disease: progress and problems on the road to therapeutics. *Science*, **297**, 353-356.
- 8.von Bernhardi, R. (2007) Glial cell dysregulation: a new perspective on Alzheimer disease. *Neurotox Res*, **12**, 215-232.
- 9.Halliday, G., Robinson, S.R., Shepherd, C. & Kril, J. (2000) Alzheimer's disease and inflammation: A review of cellular and therapeutic mechanisms. *Clin Exp Pharmacol Physiol*, **27**, 1-8.
- 10.Cornejo, F. & von Bernhardi, R. (2013) Role of scavenger receptors in glia-mediated neuroinflammatory response associated with Alzheimer's disease. *Mediators Inflamm*, **2013**, 895651.
- 11.Akiyama, H. (2000) Inflammation in Alzheimer's disease. *Brain Pathology*, **10**, 707-708.
- 12.Combs, C.K. (2009) Inflammation and Microglia Actions in Alzheimer's Disease. *J Neuroimmune Pharm* **4**, 380-388.
- 13.Gao, H.M., Jiang, J., Wilson, B., Zhang, W., Hong, J.S. & Liu, B. (2002) Microglial activation-mediated delayed and progressive degeneration of rat nigral dopaminergic neurons: relevance to Parkinson's disease. *J Neurochem*, **81**, 1285-1297.

14. Rezaie, P. & Male, D. (2002) Mesoglia & microglia--a historical review of the concept of mononuclear phagocytes within the central nervous system. *J Hist Neurosci* **11**, 325-374.
15. Lawson, L.J., Perry, V.H., Dri, P. & Gordon, S. (1990) Heterogeneity in the distribution and morphology of microglia in the normal adult mouse brain. *Neuroscience*, **39**, 151-170.
16. Schwab, C. & McGeer, P.L. (2008) Inflammatory aspects of Alzheimer disease and other neurodegenerative disorders. *J Alzheimers Dis* **13**, 359-369.
17. Nimmerjahn, A., Kirchhoff, F. & Helmchen, F. (2005) Resting microglial cells are highly dynamic surveillants of brain parenchyma in vivo. *Science*, **308**, 1314-1318.
18. Block, M.L., Zecca, L. & Hong, J.S. (2007) Microglia-mediated neurotoxicity: uncovering the molecular mechanisms. *Nat Rev Neurosci*, **8**, 57-69.
19. Kettenmann, H., Hanisch, U.K., Noda, M. & Verkhratsky, A. (2011) Physiology of microglia. *Physiol Rev* **91**, 461-553.
20. Akiyama, H., Mori, H., Saito, T., Kondo, H., Ikeda, K. & McGeer, P.L. (1999) Occurrence of the diffuse amyloid beta-protein (Abeta) deposits with numerous Abeta-containing glial cells in the cerebral cortex of patients with Alzheimer's disease. *Glia*, **25**, 324-331.
21. Tuppo, E.E. & Arias, H.R. (2005) The role of inflammation in Alzheimer's disease. *Int J Biochem Cell B*, **37**, 289-305.
22. Klegeris, A., Bissonnette, C.J. & McGeer, P.L. (2005) Modulation of human microglia and THP-1 cell toxicity by cytokines endogenous to the nervous system. *Neurobiol Aging*, **26**, 673-682.
23. Pawate, S., Shen, Q., Fan, F. & Bhat, N.R. (2004) Redox regulation of glial inflammatory response to lipopolysaccharide and interferon gamma. *J Neurosci Res* **77**, 540-551.
24. Gao, H.M., Zhou, H. & Hong, J.S. (2012) NADPH oxidases: novel therapeutic targets for neurodegenerative diseases. *Trends Pharmacol Sci* **33**, 295-303.
25. Choi, S.H., Aid, S., Kim, H.W., Jackson, S.H. & Bosetti, F. (2012) Inhibition of NADPH oxidase promotes alternative and anti-inflammatory microglial activation during neuroinflammation. *J Neurochem* **120**, 292-301.
26. Combs, C.K., Karlo, J.C., Kao, S.C. & Landreth, G.E. (2001) beta-Amyloid stimulation of microglia and monocytes results in TNFalpha-dependent expression of inducible nitric oxide synthase and neuronal apoptosis. *J Neurosci* **21**, 1179-1188.
27. Schindler, S.M., Spielman, L.J., E., B., Slattery, W.T., Harris, D.B. & Klegeris, A. (2015) The Diversity of Microglial Activators and Their Elicited Responses: Implications for

Central Nervous System Functions. in *Microglia: Physiology, Regulation and Health Implications*, E.R. Giffards. Nova Science Publishers.

28. Yoshiyama, Y., Higuchi, M., Zhang, B., Huang, S.M., Iwata, N., Saido, T.C., Maeda, J., Suhara, T., Trojanowski, J.Q. & Lee, V.M. (2007) Synapse loss and microglial activation precede tangles in a P301S tauopathy mouse model. *Neuron*, **53**, 337-351.
29. Klegeris, A., Pelech, S., Giasson, B.I., Maguire, J., Zhang, H., McGeer, E.G. & McGeer, P.L. (2008) alpha-Synuclein activates stress signaling protein kinases in THP-1 cells and microglia. *Neurobiol Aging* **29**, 739-752.
30. Mandrekar-Colucci, S. & Landreth, G.E. (2010) Microglia and Inflammation in Alzheimer's Disease. *CNS Neurol Disord Drug Targets*, **9**, 156-167.
31. Okun, E., Griffioen, K.J., Lathia, J.D., Tang, S.-C., Mattson, M.P. & Arumugam, T.V. (2009) Toll-like receptors in neurodegeneration. *Brain Res Rev*, **59**, 278-292.
32. Chuah, Y.K., Basir, R., Talib, H., Tie, T.H. & Nordin, N. (2013) Receptor for Advanced Glycation End Products and Its Involvement in Inflammatory Diseases. *Int J Inflamm*, **2013**, 403460.
33. Bianchi, M.E. (2009) HMGB1 loves company. *J Leukoc Biol*, **86**, 573-576.
34. Bianchi, M.E. (2007) DAMPs, PAMPs and alarmins: all we need to know about danger. *J Leukoc Biol*, **81**, 1-5.
35. Chen, G.Y. & Nunez, G. (2010) Sterile inflammation: sensing and reacting to damage. *Nat Rev Immunol*, **10**, 826-837.
36. Zhang, Q., Raouf, M., Chen, Y., Sumi, Y., Sursal, T., Junger, W., Brohi, K., Itagaki, K. & Hauser, C.J. (2010) Circulating mitochondrial DAMPs cause inflammatory responses to injury. *Nature*, **464**, 104-115.
37. Krysko, D.V., Agostinis, P., Krysko, O., Garg, A.D., Bachert, C., Lambrecht, B.N. & Vandenabeele, P. Emerging role of damage-associated molecular patterns derived from mitochondria in inflammation. *Trends Immunol*, **32**, 157-164.
38. Mathew, A., Lindsley, T.A., Sheridan, A., Bhoiwala, D.L., Hushmendy, S.F., Yager, E.J., Ruggiero, E.A. & Crawford, D.R. (2012) Degraded mitochondrial DNA is a newly identified subtype of the damage associated molecular pattern (DAMP) family and possible trigger of neurodegeneration. *J Alzheimers Dis*, **30**, 617-627.
39. Di Filippo, M., Chiasserini, D., Tozzi, A., Picconi, B. & Calabresi, P. (2010) Mitochondria and the link between neuroinflammation and neurodegeneration. *J Alzheimers Dis*, **20 Suppl 2**, S369-379.

40. Uchiyama, T. & Kang, D.C. (2012) The role of TFAM-associated proteins in mitochondrial RNA metabolism. *Biochim Biophys Acta*, **1820**, 565-570.
41. Lezza, A.S. (2012) Mitochondrial transcription factor A (TFAM): one actor for different roles. *Front Biol*, **7**, 30-39.
42. Rubio-Cosials, A. & Sola, M. (2013) U-turn DNA bending by human mitochondrial transcription factor A. *Curr Opin Struct Biol*, **23**, 116-124.
43. Hallberg, B.M. & Larsson, N.G. (2011) TFAM forces mtDNA to make a U-turn. *Nat Struct Mol Biol*, **18**, 1179-1181.
44. Campbell, C.T., Kolesar, J.E. & Kaufman, B.A. (2012) Mitochondrial transcription factor A regulates mitochondrial transcription initiation, DNA packaging, and genome copy number. *Biochim Biophys Acta*, **1819**, 921-929.
45. Bogenhagen, D.F., Rousseau, D. & Burke, S. (2008) The layered structure of human mitochondrial DNA nucleoids. *J Biol Chem*, **283**, 3665-3675.
46. Kaufman, B.A., Durisic, N., Mativetsky, J.M., Costantino, S., Hancock, M.A., Grutter, P. & Shoubridge, E.A. (2007) The mitochondrial transcription factor TFAM coordinates the assembly of multiple DNA molecules into nucleoid-like structures. *Mol Biol Cell*, **18**, 3225-3236.
47. Gangelhoff, T.A., Mungalachetty, P.S., Nix, J.C. & Churchill, M.E.A. (2009) Structural analysis and DNA binding of the HMG domains of the human mitochondrial transcription factor A. *Nucleic Acids Res*, **37**, 3153-3164.
48. Crouser, E.D., Shao, G., Julian, M.W., Macre, J.E., Shadel, G.S., Tridandapani, S., Huang, Q. & Wewers, M.D. (2009) Monocyte activation by necrotic cells is promoted by mitochondrial proteins and formyl peptide receptors. *Crit Care Med* **37**, 2000-2009.
49. Julian, M.W., Shao, G., Bao, S., Knoell, D.L., Papenfuss, T.L., VanGundy, Z.C. & Crouser, E.D. (2012) Mitochondrial transcription factor A serves as a danger signal by augmenting plasmacytoid dendritic cell responses to DNA. *J Immunol* **189**, 433-443.
50. Chaung, W.W., Wu, R., Ji, Y., Dong, W. & Wang, P. (2012) Mitochondrial transcription factor A is a proinflammatory mediator in hemorrhagic shock. *Int J Mol Med*, **30**, 199-203.
51. Julian, M.W., Shao, G., Vangundy, Z.C., Papenfuss, T.L. & Crouser, E.D. (2013) Mitochondrial transcription factor A, an endogenous danger signal, promotes TNF α release via RAGE- and TLR9-responsive plasmacytoid dendritic cells. *Plos One*, **8**, e72354.

52. Yang, H., Antoine, D.J., Andersson, U. & Tracey, K.J. (2013) The many faces of HMGB1: molecular structure-functional activity in inflammation, apoptosis, and chemotaxis. *J Leukoc Biol*, **93**, 865-873.
53. Fang, P., Schachner, M. & Shen, Y.Q. (2012) HMGB1 in development and diseases of the central nervous system. *Mol Neurobiol* **45**, 499-506.
54. Hreggvidsdottir, H.S., Ostberg, T., Wahamaa, H., Schierbeck, H., Aveberger, A.C., Klevenvall, L., Palmblad, K., Ottosson, L., Andersson, U. & Harris, H.E. (2009) The alarmin HMGB1 acts in synergy with endogenous and exogenous danger signals to promote inflammation. *J Leukoc Biol*, **86**, 655-662.
55. Li, J.H., Kokkola, R., Tabibzadeh, S., Yang, R.K., Ochani, M., Qiang, X.L., Harris, H.E., Czura, C.J., Wang, H.C., Ulloa, L., Wang, H., Warren, H.S., Moldawer, L.L., Fink, M.P., Andersson, U., Tracey, K.J. & Yang, H. (2003) Structural basis for the proinflammatory cytokine activity of high mobility group box 1. *Mol Med*, **9**, 37-45.
56. Rouhiainen, A., Tumova, S., Valmu, L., Kalkkinen, N. & Rauvala, H. (2007) Analysis of proinflammatory activity of highly purified eukaryotic recombinant HMGB1 (amphoterin). *J Leukoc Biol*, **81**, 49-58.
57. Dumitriu, I.E., Baruah, P., Valentinis, B., Voll, R.E., Herrmann, M., Nawroth, P.P., Arnold, B., Bianchi, M.E., Manfredi, A.A. & Rovere-Querini, P. (2005) Release of high mobility group box 1 by dendritic cells controls T cell activation via the receptor for advanced glycation end products. *J Immunol*, **174**, 7506-7515.
58. Li, G., Liang, X. & Lotze, M.T. (2013) HMGB1: The Central Cytokine for All Lymphoid Cells. *Front Immunol*, **4**, 68.
59. Gardella, S., Andrei, C., Ferrera, D., Lotti, L.V., Torrisi, M.R., Bianchi, M.E. & Rubartelli, A. (2002) The nuclear protein HMGB1 is secreted by monocytes via a non-classical, vesicle-mediated secretory pathway. *EMBO Rep*, **3**, 995-1001.
60. Enokido, Y., Yoshitake, A., Ito, H. & Okazawa, H. (2008) Age-dependent change of HMGB1 and DNA double-strand break accumulation in mouse brain. *Biochem Biophys Res Commun*, **376**, 128-133.
61. Faraco, G., Fossati, S., Bianchi, M.E., Patrone, M., Pedrazzi, M., Sparatore, B., Moroni, F. & Chiarugi, A. (2007) High mobility group box 1 protein is released by neural cells upon different stresses and worsens ischemic neurodegeneration in vitro and in vivo. *J Neurochem*, **103**, 590-603.
62. Gao, H.M., Zhou, H., Zhang, F., Wilson, B.C., Kam, W. & Hong, J.S. (2011) HMGB1 acts on microglia Mac1 to mediate chronic neuroinflammation that drives progressive neurodegeneration. *J Neurosci* **31**, 1081-1092.

63. Fossati, S. & Chiarugi, A. (2007) Relevance of high-mobility group protein box 1 to neurodegeneration. *Int Rev Neurobiol*, **82**, 137-148.
64. Kim, J.B., Sig Choi, J., Yu, Y.M., Nam, K., Piao, C.S., Kim, S.W., Lee, M.H., Han, P.L., Park, J.S. & Lee, J.K. (2006) HMGB1, a novel cytokine-like mediator linking acute neuronal death and delayed neuroinflammation in the postischemic brain. *J Neurosci* **26**, 6413-6421.
65. Orlova, V.V., Choi, E.Y., Xie, C., Chavakis, E., Bierhaus, A., Ihanus, E., Ballantyne, C.M., Gahmberg, C.G., Bianchi, M.E., Nawroth, P.P. & Chavakis, T. (2007) A novel pathway of HMGB1-mediated inflammatory cell recruitment that requires Mac-1-integrin. *EMBO J*, **26**, 1129-1139.
66. Pedrazzi, M., Patrone, M., Passalacqua, M., Ranzato, E., Colamassaro, D., Sparatore, B., Pontremoli, S. & Melloni, E. (2007) Selective proinflammatory activation of astrocytes by high-mobility group box 1 protein signaling. *J Immunol*, **179**, 8525-8532.
67. Mazarati, A.y., Maroso, M., Iori, V., Vezzani, A. & Carli, M. (2011) High-mobility group box-1 impairs memory in mice through both toll-like receptor 4 and Receptor for Advanced Glycation End Products. *Experimental Neurology*, **232**, 143-148.
68. Ross, G.D. & Vetvicka, V. (1993) CR3 (CD11b, CD18): a phagocyte and NK cell membrane receptor with multiple ligand specificities and functions. *Clin Exp Immunol*, **92**, 181-184.
69. Akiyama, H. & McGeer, P.L. (1990) Brain microglia constitutively express beta-2 integrins. *J Neuroimmunol*, **30**, 81-93.
70. Plow, E.F. & Zhang, L. (1997) A MAC-1 attack: integrin functions directly challenged in knockout mice. *J Clin Invest*, **99**, 1145-1146.
71. Gahmberg, C.G. (1997) Leukocyte adhesion: CD11/CD18 integrins and intercellular adhesion molecules. *Curr Opin Cell Biol*, **9**, 643-650.
72. Zhang, D., Hu, X., Qian, L., Chen, S.H., Zhou, H., Wilson, B., Miller, D.S. & Hong, J.S. (2011) Microglial MAC1 receptor and PI3K are essential in mediating beta-amyloid peptide-induced microglial activation and subsequent neurotoxicity. *J Neuroinflammation*, **8**, 3.
73. Pei, Z., Pang, H., Qian, L., Yang, S., Wang, T., Zhang, W., Wu, X., Dallas, S., Wilson, B., Reece, J.M., Miller, D.S., Hong, J.S. & Block, M.L. (2007) MAC1 mediates LPS-induced production of superoxide by microglia: the role of pattern recognition receptors in dopaminergic neurotoxicity. *Glia*, **55**, 1362-1373.
74. Hu, X., Zhang, D., Pang, H., Caudle, W.M., Li, Y., Gao, H., Liu, Y., Qian, L., Wilson, B., Di Monte, D.A., Ali, S.F., Zhang, J., Block, M.L. & Hong, J.S. (2008) Macrophage antigen complex-1 mediates reactive microgliosis and progressive dopaminergic

- neurodegeneration in the MPTP model of Parkinson's disease. *J Immunol*, **181**, 7194-7204.
75. Block, M.L. (2008) NADPH oxidase as a therapeutic target in Alzheimer's disease. *BMC Neurosci*, **9 Suppl 2**, S8.
76. Shimohama, S., Tanino, H., Kawakami, N., Okamura, N., Kodama, H., Yamaguchi, T., Hayakawa, T., Nunomura, A., Chiba, S., Perry, G., Smith, M.A. & Fujimoto, S. (2000) Activation of NADPH oxidase in Alzheimer's disease brains. *Biochem Biophys Res Commun*, **273**, 5-9.
77. Wu, D.C., Teismann, P., Tieu, K., Vila, M., Jackson-Lewis, V., Ischiropoulos, H. & Przedborski, S. (2003) NADPH oxidase mediates oxidative stress in the 1-methyl-4-phenyl-1,2,3,6-tetrahydropyridine model of Parkinson's disease. *Proc Natl Acad Sci U S A*, **100**, 6145-6150.
78. Bucciarelli, L.G., Wendt, T., Rong, L., Lalla, E., Hofmann, M.A., Goova, M.T., Taguchi, A., Yan, S.F., Yan, S.D., Stern, D.M. & Schmidt, A.M. (2002) RAGE is a multiligand receptor of the immunoglobulin superfamily: implications for homeostasis and chronic disease. *Cell Mol Life Sci*, **59**, 1117-1128.
79. Kleinert, H., Schwarz, P.M. & Forstermann, U. (2003) Regulation of the expression of inducible nitric oxide synthase. *Biol Chem*, **384**, 1343-1364.
80. Muhammad, S., Waleed, B., Murikinati, S., Stoyanov, S., Yang, H., Tracey, K.J., Bendszus, M., Nawroth, P.P., Bierhaus, A., Rossetti, G. & Schwaninger, M. (2008) The HMGB1 receptor RAGE mediates ischemic brain damage. *J Neurosci* **28**, 12023-12031.
81. Steenvoorden, M.M., Toes, R.E., Ronday, H.K., Huizinga, T.W. & Degroot, J. (2007) RAGE activation induces invasiveness of RA fibroblast-like synoviocytes in vitro. *Clin Exp Rheumatol*, **25**, 740-2.
82. Takuma, K., Fang, F., Zhang, W., Yan, S., Fukuzaki, E., Du, H., Sosunov, A., McKhann, G., Funatsu, Y., Nakamichi, N., Nagai, T., Mizoguchi, H., Ibi, D., Hori, O., Ogawa, S., Stern, D.M., Yamada, K. & Yan, S.S. (2009) RAGE-mediated signaling contributes to intraneuronal transport of amyloid-beta and neuronal dysfunction. *Proc Natl Acad Sci U S A*, **106**, 20021-20026.
83. Yan, S.F., Yan, S.D., Ramasamy, R. & Schmidt, A.M. (2009) Tempering the wrath of RAGE: an emerging therapeutic strategy against diabetic complications, neurodegeneration, and inflammation. *Ann Med*, **41**, 408-422.
84. Xu, D., Young, J., Song, D. & Esko, J.D. (2011) Heparan sulfate is essential for high mobility group protein 1 (HMGB1) signaling by the receptor for advanced glycation end products (RAGE). *J Biol Chem*, **286**, 41736-44.

- 85.Ling, Y., Yang, Z.Y., Yin, T., Li, L., Yuan, W.W., Wu, H.S. & Wang, C.Y. (2011) Heparin changes the conformation of high-mobility group protein 1 and decreases its affinity toward receptor for advanced glycation endproducts in vitro. *Int Immunopharmacol*, **11**, 187-193.
- 86.Ardoin, S.P. & Pisetsky, D.S. (2008) The role of cell death in the pathogenesis of autoimmune disease: HMGB1 and microparticles as intercellular mediators of inflammation. *Mod Rheumatol*, **18**, 319-326.
- 87.Pisetsky, D.S., Gauley, J. & Ullal, A.J. (2011) HMGB1 and microparticles as mediators of the immune response to cell death. *Antioxid Redox Signal*, **15**, 2209-2219.
- 88.Bianco, F., Pravettoni, E., Colombo, A., Schenk, U., Moller, T., Matteoli, M. & Verderio, C. (2005) Astrocyte-derived ATP induces vesicle shedding and IL-1 beta release from microglia. *J Immunol*, **174**, 7268-77.
- 89.Colombo, E., Borgiani, B., Verderio, C. & Furlan, R. (2012) Microvesicles: novel biomarkers for neurological disorders. *Front Physiol*, **3**, 63.
- 90.Wolf, P. (1967) The nature and significance of platelet products in human plasma. *Br J Haematol*, **13**, 269-88.
- 91.Barteneva, N.S., Fasler-Kan, E., Bernimoulin, M., Stern, J.N., Ponomarev, E.D., Duckett, L. & Vorobjev, I.A. (2013) Circulating microparticles: square the circle. *BMC Cell Biol*, **14**, 23.
- 92.Horstman, L.L., Jy, W., Minagar, A., Bidot, C.J., Jimenez, J.J., Alexander, J.S. & Ahn, Y.S. (2007) Cell-derived microparticles and exosomes in neuroinflammatory disorders. *Int Rev Neurobiol*, **79**, 227-268.
- 93.Minagar, A., Jy, W., Jimenez, J.J., Sheremata, W.A., Mauro, L.M., Mao, W.W., Horstman, L.L. & Ahn, Y.S. (2001) Elevated plasma endothelial microparticles in multiple sclerosis. *Neurology*, **56**, 1319-24.
- 94.Combes, V., Coltel, N., Alibert, M., van Eck, M., Raymond, C., Juhan-Vague, I., Grau, G.E. & Chimini, G. (2005) ABCA1 gene deletion protects against cerebral malaria: potential pathogenic role of microparticles in neuropathology. *Am J Pathol*, **166**, 295-302.
- 95.Eyre, J., Burton, J.O., Saleem, M.A., Mathieson, P.W., Topham, P.S. & Brunskill, N.J. (2011) Monocyte- and Endothelial-Derived Microparticles Induce an Inflammatory Phenotype in Human Podocytes. *Nephron Exp Nephrol*, **119**, e58-e66.
- 96.Ben-Hadj-Khalifa-Kechiche, S., Hezard, N., Poitevin, S., Remy, M.G., Florent, B., Mahjoub, T. & Nguyen, P. (2010) Differential inhibitory effect of fondaparinux on the procoagulant potential of intact monocytes and monocyte-derived microparticles. *J Thromb Thrombolysis*, **30**, 412-8.

97. Gauley, J. & Pisetsky, D.S. (2010) The release of microparticles by RAW 264.7 macrophage cells stimulated with TLR ligands. *J Leukoc Biol*, **87**, 1115-1123.
98. Cerri, C., Chimenti, D., Conti, I., Neri, T., Paggiaro, P. & Celi, A. (2006) Monocyte/macrophage-derived microparticles up-regulate inflammatory mediator synthesis by human airway epithelial cells. *J Immunol*, **177**, 1975-1980.
99. Spencer, D.M., Mobarrez, F., Wallen, H. & Pisetsky, D.S. (2014) The expression of HMGB1 on microparticles from Jurkat and HL-60 cells undergoing apoptosis in vitro. *Scand J Immunol*, **80**, 101-110.
100. Pisetsky, D.S. (2014) The Expression of HMGB1 on microparticles released during cell activation and cell death in vitro and in vivo. *Mol Med*, **20**, 158-163.
101. Carson, M.J., Crane, J. & Xie, A.X. (2008) Modeling CNS microglia: the quest to identify predictive models. *Drug Discov Today Dis Models*, **5**, 19-25.
102. Tsuchiya, S., Yamabe, M., Yamaguchi, Y., Kobayashi, Y., Konno, T. & Tada, K. (1980) Establishment and characterization of a human acute monocytic leukemia cell line (THP-1). *Int J Cancer*, **26**, 171-6.
103. Crehan, H., Hardy, J. & Pocock, J. (2013) Blockage of CR1 prevents activation of rodent microglia. *Neurobiol Dis*, **54**, 139-149.
104. Hickstein, D.D., Baker, D.M., Gollahon, K.A. & Back, A.L. (1992) Identification of the promoter of the myelomonocytic leukocyte integrin CD11b. *Proc Natl Acad Sci U S A*, **89**, 2105-2109.
105. Restrepo, A., Smith, C.A., Agnihotri, S., Shekarforoush, M., Kongkham, P.N., Seol, H.J., Northcott, P. & Rutka, J.T. (2011) Epigenetic regulation of glial fibrillary acidic protein by DNA methylation in human malignant gliomas. *Neuro Oncol*, **13**, 42-50.
106. Sultana, S., Zhou, R., Sadagopan, M.S. & Skalli, O. (1998) Effects of growth factors and basement membrane proteins on the phenotype of U-373 MG glioblastoma cells as determined by the expression of intermediate filament proteins. *Am J Pathol*, **153**, 1157-1168.
107. Almeida, A.C., Rehder, J., Severino, S.D., Martins-Filho, J., Newburger, P.E. & Condino-Neto, A. (2005) The effect of IFN-gamma and TNF-alpha on the NADPH oxidase system of human colostrum macrophages, blood monocytes, and THP-1 cells. *J Interferon Cytokine Res*, **25**, 540-546.
108. Dong, J.M., Zhao, S.G., Huang, G.Y. & Liu, Q. (2004) NADPH oxidase-mediated generation of reactive oxygen species is critically required for survival of undifferentiated human promyelocytic leukemia cell line HL-60. *Free Radic Res*, **38**, 629-637.

109. Muranaka, S., Fujita, H., Fujiwara, T., Ogino, T., Sato, E.F., Akiyama, J., Imada, I., Inoue, M. & Utsumi, K. (2005) Mechanism and characteristics of stimuli-dependent ROS generation in undifferentiated HL-60 cells. *Antioxid Redox Signal*, **7**, 1367-1376.
110. Ross, R.A., Biedler, J.L., Spengler, B.A. & Reis, D.J. (1981) Neurotransmitter-synthesizing enzymes in 14 human neuroblastoma cell lines. *Cell Mol Neurobiol*, **1**, 301-311.
111. Klegeris, A. & McGeer, P.L. (2003) Toxicity of human monocytic THP-1 cells and microglia toward SH-SY5Y neuroblastoma cells is reduced by inhibitors of 5-lipoxygenase and its activating protein FLAP. *J Leukoc Biol*, **73**, 369-378.
112. Klegeris, A. & McGeer, P.L. (2001) Inflammatory cytokine levels are influenced by interactions between THP-1 monocytic, U-373 MG astrocytic, and SH-SY5Y neuronal cell lines of human origin. *Neurosci Lett*, **313**, 41-44.
113. Hashioka, S., Klegeris, A., Schwab, C. & McGeer, P.L. (2009) Interferon-gamma-dependent cytotoxic activation of human astrocytes and astrocytoma cells. *Neurobiol Aging*, **30**, 1924-35.
114. Klegeris, A. & McGeer, P.L. (2000) Interaction of various intracellular signaling mechanisms involved in mononuclear phagocyte toxicity toward neuronal cells. *J Leukoc Biol* **67**, 127-133.
115. Klegeris, A., Walker, D.G. & McGeer, P.L. (1999) Toxicity of human THP-1 monocytic cells towards neuron-like cells is reduced by non-steroidal anti-inflammatory drugs (NSAIDs). *Neuropharmacology*, **38**, 1017-1025.
116. Szczepanik, A.M., Funes, S., Petko, W. & Ringheim, G.E. (2001) IL-4, IL-10 and IL-13 modulate A beta(1-42)-induced cytokine and chemokine production in primary murine microglia and a human monocyte cell line. *J Neuroimmunol*, **113**, 49-62.
117. McGeer, P.L., Itagaki, S., Boyes, B.E. & McGeer, E.G. (1988) Reactive microglia are positive for HLA-DR in the substantia nigra of Parkinson's and Alzheimer's disease brains. *Neurology*, **38**, 1285-1291.
118. Schapansky, J., Nardozi, J.D. & LaVoie, M.J. (2014) The complex relationships between microglia, alpha-synuclein, and LRRK2 in Parkinson's disease. *Neuroscience*,
119. Harris, H.E., Andersson, U. & Pisetsky, D.S. (2012) HMGB1: a multifunctional alarmin driving autoimmune and inflammatory disease. *Nat Rev Rheumatol*, **8**, 195-202.
120. Little, J.P., Simtchouk, S., Schindler, S.M., Villanueva, E.B., Gill, N.E., Walker, D.G., Wolthers, K.R. & Klegeris, A. (2014) Mitochondrial transcription factor A (Tfam) is a pro-inflammatory extracellular signaling molecule recognized by brain microglia. *Mol Cell Neurosci*, **60C**, 88-96.

- 121.Koh, J.Y. & Choi, D.W. (1987) Quantitative determination of glutamate mediated cortical neuronal injury in cell culture by lactate dehydrogenase efflux assay. *J Neurosci Methods*, **20**, 83-90.
- 122.Slater, T.F., Sawyer, B. & Straeuli, U. (1963) Studies on Succinate-Tetrazolium Reductase Systems. Iii. Points of Coupling of Four Different Tetrazolium Salts. *Biochim Biophys Acta*, **77**, 383-393.
- 123.Villanueva, E.B., Little, J.P., Lambeau, G. & Klegeris, A. (2012) Secreted phospholipase A(2) group IIA is a neurotoxin released by stimulated human glial cells. *Mol Cell Neurosci*, **49**, 430-438.
- 124.Loo, D.T. & Rillema, J.R. (1998) Measurement of cell death. *Methods Cell Biol*, **57**, 251-264.
- 125.Orden, S., De Pablo, C., Rios-Navarro, C., Martinez-Cuesta, M.A., Peris, J.E., Barrachina, M.D., Esplugues, J.V. & Alvarez, A. (2014) Efavirenz induces interactions between leucocytes and endothelium through the activation of Mac-1 and gp150,95. *J Antimicrob Chemother*, **69**, 995-1004.
- 126.Patel, S., Djerdjouri, B., Raoul-Des-Essarts, Y., Dang, P.M., El-Benna, J. & Perianin, A. (2010) Protein kinase B (AKT) mediates phospholipase D activation via ERK1/2 and promotes respiratory burst parameters in formylpeptide-stimulated neutrophil-like HL-60 cells. *J Biol Chem*, **285**, 32055-32063.
- 127.Mo, M., Peng, F., Wang, L., Peng, L., Lan, G. & Yu, S. (2013) Roles of mitochondrial transcription factor A and microRNA-590-3p in the development of bladder cancer. *Oncol Lett*, **6**, 617-623.
- 128.Bustin, S.A., Benes, V., Garson, J.A., Hellemans, J., Huggett, J., Kubista, M., Mueller, R., Nolan, T., Pfaffl, M.W., Shipley, G.L., Vandesompele, J. & Wittwer, C.T. (2009) The MIQE guidelines: minimum information for publication of quantitative real-time PCR experiments. *Clin Chem*, **55**, 611-622.
- 129.Hellemans, J. & Vandesompele, J. (2011) Quantitative PCR data analysis – unlocking the secret to successful results. in *PCR Troubleshooting and Optimization: The Essential Guide*, S. Kennedy & N. Oswalds. Caister Academic Press. 235.
- 130.Antonucci, F., Turola, E., Riganti, L., Caleo, M., Gabrielli, M., Perrotta, C., Novellino, L., Clementi, E., Giussani, P., Viani, P., Matteoli, M. & Verderio, C. (2012) Microvesicles released from microglia stimulate synaptic activity via enhanced sphingolipid metabolism. *EMBO J*, **31**, 1231-40.
- 131.Bianco, F., Perrotta, C., Novellino, L., Francolini, M., Riganti, L., Menna, E., Saglietti, L., Schuchman, E.H., Furlan, R., Clementi, E., Matteoli, M. & Verderio, C. (2009) Acid

- sphingomyelinase activity triggers microparticle release from glial cells. *EMBO J*, **28**, 1043-1054.
132. Bardelli, C., Amoruso, A., Federici Canova, D., Fresu, L., Balbo, P., Neri, T., Celi, A. & Brunelleschi, S. (2012) Autocrine activation of human monocyte/macrophages by monocyte-derived microparticles and modulation by PPARgamma ligands. *Br J Pharmacol*, **165**, 716-28.
133. Hughes, J.E., Stewart, J., Barclay, G.R. & Govan, J.R. (1997) Priming of neutrophil respiratory burst activity by lipopolysaccharide from *Burkholderia cepacia*. *Infect Immun*, **65**, 4281-4287.
134. McLeish, K.R., Klein, J.B., Lederer, E.D., Head, K.Z. & Ward, R.A. (1996) Azotemia, TNF alpha, and LPS prime the human neutrophil oxidative burst by distinct mechanisms. *Kidney Int*, **50**, 407-416.
135. Berton, G., Zeni, L., Cassatella, M.A. & Rossi, F. (1986) Gamma interferon is able to enhance the oxidative metabolism of human neutrophils. *Biochem Biophys Res Commun*, **138**, 1276-1282.
136. Ellis, T.N. & Beaman, B.L. (2004) Interferon-gamma activation of polymorphonuclear neutrophil function. *Immunology*, **112**, 2-12.
137. Dheen, S.T., Kaur, C. & Ling, E.A. (2007) Microglial activation and its implications in the brain diseases. *Curr Med Chem*, **14**, 1189-1197.
138. Lee, M., Suk, K., Kang, Y., McGeer, E. & McGeer, P.L. (2011) Neurotoxic factors released by stimulated human monocytes and THP-1 cells. *Brain Res*, **1400**, 99-111.
139. Kigerl, K.A., de Rivero Vaccari, J.P., Dietrich, W.D., Popovich, P.G. & Keane, R.W. (2014) Pattern recognition receptors and central nervous system repair. *Exp Neurol*, **258**, 5-16.
140. Andersson, U., Wang, H., Palmblad, K., Aveberger, A.C., Bloom, O., Erlandsson-Harris, H., Janson, A., Kokkola, R., Zhang, M., Yang, H. & Tracey, K.J. (2000) High mobility group 1 protein (HMG-1) stimulates proinflammatory cytokine synthesis in human monocytes. *J Exp Med*, **192**, 565-570.
141. Sha, Y., Zmijewski, J., Xu, Z. & Abraham, E. (2008) HMGB1 develops enhanced proinflammatory activity by binding to cytokines. *J Immunol*, **180**, 2531-2537.
142. Plataniias, L.C. & Fish, E.N. (1999) Signaling pathways activated by interferons. *Exp Hematol*, **27**, 1583-1592.
143. Rawlings, J.S., Rosler, K.M. & Harrison, D.A. (2004) The JAK/STAT signaling pathway. *J Cell Sci*, **117**, 1281-1283.

144. Morrison, D.K. (2012) MAP kinase pathways. *Cold Spring Harb Perspect Biol*, **4**, 1-5.
145. Kaminska, B., Gozdz, A., Zawadzka, M., Ellert-Miklaszewska, A. & Lipko, M. (2009) MAPK signal transduction underlying brain inflammation and gliosis as therapeutic target. *Anat Rec (Hoboken)*, **292**, 1902-1913.
146. Heinrich, P.C., Behrmann, I., Haan, S., Hermanns, H.M., Muller-Newen, G. & Schaper, F. (2003) Principles of interleukin (IL)-6-type cytokine signalling and its regulation. *Biochem J*, **374**, 1-20.
147. Yang, H., Ochani, M., Li, J., Qiang, X., Tanovic, M., Harris, H.E., Susarla, S.M., Ulloa, L., Wang, H., DiRaimo, R., Czura, C.J., Roth, J., Warren, H.S., Fink, M.P., Fenton, M.J., Andersson, U. & Tracey, K.J. (2004) Reversing established sepsis with antagonists of endogenous high-mobility group box 1. *Proc Natl Acad Sci U S A*, **101**, 296-301.
148. Wong, T.S., Rajagopalan, S., Freund, S.M., Rutherford, T.J., Andreeva, A., Townsley, F.M., Petrovich, M. & Fersht, A.R. (2009) Biophysical characterizations of human mitochondrial transcription factor A and its binding to tumor suppressor p53. *Nucleic Acids Res*, **37**, 6765-6783.
149. Rabenstein, D.L. (2002) Heparin and heparan sulfate: structure and function. *Nat Prod Rep*, **19**, 312-331.
150. Lever, R., Smailbegovic, A. & Page, C. (2001) Role of glycosaminoglycans in inflammation. *InflammoPharmacology*, **9**, 165-169.
151. Hinojosa, A.E., Garcia-Bueno, B., Leza, J.C. & Madrigal, J.L. (2011) CCL2/MCP-1 modulation of microglial activation and proliferation. *J Neuroinflammation*, **8**, 77.
152. Yang, G., Meng, Y., Li, W., Yong, Y., Fan, Z., Ding, H., Wei, Y., Luo, J. & Ke, Z.J. (2011) Neuronal MCP-1 mediates microglia recruitment and neurodegeneration induced by the mild impairment of oxidative metabolism. *Brain Pathol*, **21**, 279-297.
153. Ramesh, G., MacLean, A.G. & Philipp, M.T. (2013) Cytokines and chemokines at the crossroads of neuroinflammation, neurodegeneration, and neuropathic pain. *Mediators Inflamm*, **2013**, 480739.
154. Viola, A. & Luster, A.D. (2008) Chemokines and their receptors: drug targets in immunity and inflammation. *Annu Rev Pharmacol Toxicol*, **48**, 171-197.
155. Nagai, A., Nakagawa, E., Hatori, K., Choi, H.B., McLarnon, J.G., Lee, M.A. & Kim, S.U. (2001) Generation and characterization of immortalized human microglial cell lines: expression of cytokines and chemokines. *Neurobiol Dis*, **8**, 1057-1068.

156. Madeira, J.M., Renschler, C.J., Mueller, B., Hashioka, S., Gibson, D.L. & Klegeris, A. (2013) Novel protective properties of auranofin: inhibition of human astrocyte cytotoxic secretions and direct neuroprotection. *Life Sci*, **92**, 1072-1080.
157. Benveniste, E.N. (1998) Cytokine actions in the central nervous system. *Cytokine Growth Factor Rev*, **9**, 259-275.
158. Dahlgren, C. & Karlsson, A. (1999) Respiratory burst in human neutrophils. *J Immunol Methods*, **232**, 3-14.
159. Qin, L., Liu, Y., Cooper, C., Liu, B., Wilson, B. & Hong, J.S. (2002) Microglia enhance beta-amyloid peptide-induced toxicity in cortical and mesencephalic neurons by producing reactive oxygen species. *Journal of Neurochemistry*, **83**, 973-83.
160. Qin, L., Liu, Y., Wang, T., Wei, S.J., Block, M.L., Wilson, B., Liu, B. & Hong, J.S. (2004) NADPH oxidase mediates lipopolysaccharide-induced neurotoxicity and proinflammatory gene expression in activated microglia. *J Biol Chem*, **279**, 1415-1421.
161. Park, J.S., Gamboni-Robertson, F., He, Q., Svetkauskaite, D., Kim, J.Y., Strassheim, D., Sohn, J.W., Yamada, S., Maruyama, I., Banerjee, A., Ishizaka, A. & Abraham, E. (2006) High mobility group box 1 protein interacts with multiple Toll-like receptors. *Am J Physiol Cell Physiol*, **290**, C917-924.
162. Tian, J., Avalos, A.M., Mao, S.-Y., Chen, B., Senthil, K., Wu, H., Parroche, P., Drabic, S., Golenbock, D., Sirois, C., Hua, J., An, L.L., Audoly, L., La Rosa, G., Bierhaus, A., Naworth, P., Marshak-Rothstein, A., Crow, M.K., Fitzgerald, K.A., Latz, E., Kiener, P.A. & Coyle, A.J. (2007) Toll-like receptor 9-dependent activation by DNA-containing immune complexes is mediated by HMGB1 and RAGE. *Nat Immunol*, **8**, 487-496.
163. Zhou, H., Liao, J., Aloor, J., Nie, H., Wilson, B.C., Fessler, M.B., Gao, H.M. & Hong, J.S. (2013) CD11b/CD18 (Mac-1) is a novel surface receptor for extracellular double-stranded RNA to mediate cellular inflammatory responses. *J Immunol*, **190**, 115-125.
164. Deng, Y.Y., Lu, J., Ling, E.A. & Kaur, C. (2009) Monocyte chemoattractant protein-1 (MCP-1) produced via NF- κ B signaling pathway mediates migration of amoeboid microglia in the periventricular white matter in hypoxic neonatal rats. *Glia*, **57**, 604-621.
165. Chavakis, T., Bierhaus, A., Al-Fakhri, N., Schneider, D., Witte, S., Linn, T., Nagashima, M., Morser, J., Arnold, B., Preissner, K.T. & Nawroth, P.P. (2003) The pattern recognition receptor (RAGE) is a counterreceptor for leukocyte integrins: a novel pathway for inflammatory cell recruitment. *J Exp Med*, **198**, 1507-1515.
166. Hallett, M.B. & Lloyds, D. (1995) Neutrophil priming: the cellular signals that say 'amber' but not 'green'. *Immunol Today*, **16**, 264-268.

167. Iles, K.E. & Forman, H.J. (2002) Macrophage signaling and respiratory burst. *Immunol Res*, **26**, 95-105.
168. Kaul, N. & Forman, H.J. (1996) Activation of NF kappa B by the respiratory burst of macrophages. *Free Radic Biol Med*, **21**, 401-405.
169. Torres, M. & Forman, H.J. (1999) Activation of several MAP kinases upon stimulation of rat alveolar macrophages: role of the NADPH oxidase. *Arch Biochem Biophys*, **366**, 231-9.
170. Whelan, S.P. & Zuckerbraun, B.S. (2013) Mitochondrial signaling: forwards, backwards, and in between. *Oxid Med Cell Longev*, **2013**, 351613.
171. Lezza, A.M.S., Pesce, V., Cormio, A., Fracasso, F., Vecchiet, J., Felzani, G., Cantatore, P. & Gadaleta, M.N. (2001) Increased expression of mitochondrial transcription factor A and nuclear respiratory factor-1 in skeletal muscle from aged human subjects. *FEBS Letters*, **501**, 74-78.
172. Doeuvre, L., Plawinski, L., Toti, F. & Angles-Cano, E. (2009) Cell-derived microparticles: a new challenge in neuroscience. *J Neurochem*, **110**, 457-68.
173. Verderio, C., Muzio, L., Turola, E., Bergami, A., Novellino, L., Ruffini, F., Riganti, L., Corradini, I., Francolini, M., Garzetti, L., Maiorino, C., Servida, F., Vercelli, A., Rocca, M., Dalla Libera, D., Martinelli, V., Comi, G., Martino, G., Matteoli, M. & Furlan, R. (2012) Myeloid microvesicles are a marker and therapeutic target for neuroinflammation. *Ann Neurol*, **72**, 610-24.
174. Distler, J.H.W., Pisetsky, D.S., Huber, L.C., Kalden, J.R., Gay, S. & Distler, O. (2005) Microparticles as regulators of inflammation: novel players of cellular crosstalk in the rheumatic diseases. *Arthritis Rheum.*, **52**, 3337-3348.
175. Cocucci, E., Racchetti, G. & Meldolesi, J. (2009) Shedding microvesicles: artefacts no more. *Trends Cell Biol*, **19**, 43-51.
176. Ratajczak, J., Wysoczynski, M., Hayek, F., Janowska-Wieczorek, A. & Ratajczak, M.Z. (2006) Membrane-derived microvesicles: important and underappreciated mediators of cell-to-cell communication. *Leukemia*, **20**, 1487-95.
177. Bernimoulin, M., Waters, E.K., Foy, M., Steele, B.M., Sullivan, M., Falet, H., Walsh, M.T., Barteneva, N., Geng, J.G., Hartwig, J.H., Maguire, P.B. & Wagner, D.D. (2009) Differential stimulation of monocytic cells results in distinct populations of microparticles. *J Thromb Haemost*, **7**, 1019-28.
178. Li, M., Yu, D., Williams, K.J. & Liu, M.L. (2010) Tobacco smoke induces the generation of procoagulant microvesicles from human monocytes/macrophages. *Arterioscler Thromb Vasc Biol*, **30**, 1818-24.

179. Arancio, O., Zhang, H.P., Chen, X., Lin, C., Trinchese, F., Puzzo, D., Liu, S., Hegde, A., Yan, S.F., Stern, A., Luddy, J.S., Lue, L.F., Walker, D.G., Roher, A., Buttini, M., Mucke, L., Li, W., Schmidt, A.M., Kindy, M., Hyslop, P.A., Stern, D.M. & Du Yan, S.S. (2004) RAGE potentiates Abeta-induced perturbation of neuronal function in transgenic mice. *EMBO J*, **23**, 4096-4105.
180. Chen, X., Walker, D.G., Schmidt, A.M., Arancio, O., Lue, L.-F. & Yan, S.D. (2007) RAGE: a potential target for Abeta-mediated cellular perturbation in Alzheimer's disease. *Curr Mol Med*, **7**, 735-742.
181. Kierdorf, K. & Fritz, G. (2013) RAGE regulation and signaling in inflammation and beyond. *J Leukoc Biol*, **94**, 55-68.

Appendices

Appendix A: Enzyme-linked immunosorbent assay (ELISA) reagents

A. **Phosphate stock solution (200mM):** 3.7 g of monobasic sodium phosphate, and 40.3 g of dibasic sodium phosphate were dissolved in 500 ml milli-Q water. The solution was stored at room temperature in an airtight bottle.

B. **PBS-Tween:** 9 g of NaCl were dissolved in 950 mL mili-Q water (9 g NaCl in 1 l=0.09%). 50 mL of phosphate stock and 500 μ L of Tween 20 were added. The solution was stored at room temperature in an airtight bottle.

C. **Blocking solution:** 1% w/v skim milk powder and 1% w/v bovine serum albumin (BSA) were dissolved in PBS, covered with Parafilm and stored at 4°C for up to one week.

D. **Coating buffer** (0.1 M sodium bicarbonate (NaHCO_3) buffer): Dissolved 0.159 g of Na_2HCO_3 and 0.293 g of NaHCO_3 in 100 ml mili-Q water. pH was adjusted to 9.6. The buffer was stored at room temperature in an airtight bottle.

E. **Substrate buffer:** 101 mg of $\text{MgCl}_2 \cdot 5\text{H}_2\text{O}$ (50 mM) were dissolved in 800 ml mili-Q water. Added 97 ml diethanolamine and mixed thoroughly. pH was adjusted to 9.8 with concentrated HCl. Milli-Q water was added to make up a final volume of 1 l. The solution was stored in the dark at 4°C.

Appendix B: This research paper was published in Molecular and Cellular Neuroscience

Mitochondrial transcription factor A (Tfam) is a pro-inflammatory extracellular signaling molecule recognized by brain microglia

Jonathan P. Little ^{a,b}, Svetlana Simtchouk ^{b,c}, Stephanie M. Schindler ^a, Erika B. Villanueva ^a, Nichole E. Gill ^a, Douglas G. Walker ^d, Kirsten R. Wolthers ^c, Andis Klegeris ^{a,*}

^a Department of Biology, University of British Columbia Okanagan Campus, Kelowna, BC, Canada;

^b School of Health and Exercise Sciences, University of British Columbia Okanagan Campus, Kelowna, BC, Canada;

^c Department of Chemistry, University of British Columbia Okanagan Campus, Kelowna, BC, Canada;

^d Banner Sun Health Research Institute, Sun City, AZ, USA.

* Corresponding author: Department of Biology, University of British Columbia Okanagan Campus, Kelowna, BC, V1V 1V7, Canada. E-mail: andis.klegeris@ubc.ca

Abstract

Microglia represent mononuclear phagocytes in the brain and perform immune surveillance, recognizing a number of signaling molecules released from surrounding cells in both healthy and pathological situations. Microglia interact with several damage-associated molecular pattern molecules (DAMPs) and recent data indicate that mitochondrial transcription factor A (Tfam) could act as a specific DAMP in peripheral tissues. This study tested the hypothesis that extracellular Tfam induces pro-inflammatory and cytotoxic responses of microglia. Three different types of human mononuclear phagocytes were used to model human microglia: human peripheral blood monocytes from healthy donors, human THP-1 monocytic cells, and human primary microglia obtained from autopsy samples. When combined with interferon (IFN)- γ , recombinant human Tfam (rhTfam) induced secretions that were toxic to human SH-SY5Y neuroblastoma cells in all three models. Similar cytotoxic responses were observed when THP-1 cells and human microglia were exposed to human mitochondrial proteins in the presence of IFN- γ . rhTfam alone induced expression of pro-inflammatory cytokines interleukin (IL)-6 and IL-8 by THP-1 cells. This induction was further enhanced in the presence of IFN- γ . Upregulated secretion of IL-6 in response to rhTfam plus IFN- γ was confirmed in primary human microglia. Use of specific inhibitors showed that the rhTfam-induced cytotoxicity of human THP-1 cells depended partially on activation of c-Jun N-terminal kinase (JNK), but not p38 mitogen-activated protein kinase (MAPK). Overall, our data support the hypothesis that, in human brain, Tfam could act as an intercellular signaling molecule that is recognized by microglia to cause pro-inflammatory and cytotoxic responses.

Keywords: DAMPs; glial cells; mitochondrial proteins; mononuclear phagocytes; neuroinflammation; neurotoxicity

Abbreviations:

ANOVA, analysis of variance;

DAMPs, damage-associated molecular pattern molecules;

DMEM-F12, Dulbecco's modified Eagle's medium-nutrient mixture F12 Ham;

DTT, dithiothreitol;

EDTA, ethylene diamine tetraacetic acid;

ELISA, enzyme-linked immunosorbent assay;

FBS, fetal bovine serum;

GST, glutathione S-transferase;

HMGB1, high-mobility group box 1;

HSD, honestly significant difference;

IFN, interferon;

IL, interleukin;

JNK, c-Jun N-terminal kinase;

LDH, lactate dehydrogenase;

MAPK, mitogen-activated protein kinase;

MMACHC, methylmalonic aciduria cblC type with homocystinuria;

MTT, 3-(4,5-dimethylthiazol-2-yl)-2,5-diphenyl tetrazolium bromide;

NF- κ B, nuclear factor κ B;

PBMCs, peripheral blood mononuclear cells;

PBS, phosphate-buffered saline;

qPCR, quantitative polymerase chain reaction;

RAGE, receptor for advanced glycation end products;

rhTfam, recombinant human mitochondrial transcription factor A;

Tfam, mitochondrial transcription factor A;

TLR, toll-like receptor;

TNF, tumor necrosis factor.

Introduction

Microglia are non-neuronal cells of the central nervous system that belong to the mononuclear phagocyte system. As brain macrophages, microglia orchestrate innate immune responses, detecting and destroying foreign pathogens and responding to tissue injury (Akiyama et al., 2000; Kettenmann et al., 2011). Although this function is critical for protecting neurons and other cells in the brain, it is believed that uncontrolled or chronic microglial activation can lead to release of toxins that cause collateral neuronal damage (Colton, 2009; Graeber, 2010; Hoarau et al., 2011). Such pathological activation of microglia is hypothesized to contribute to neuronal damage in neurodegenerative disorders including Alzheimer's and Parkinson's disease, ischemic stroke, trauma and aging-related cognitive decline (Block et al., 2007; Eikelenboom et al., 2012; Jin et al., 2010; Zhang et al., 2013). As such, identifying molecules and pathways contributing to chronic microglial activation has potential for developing novel neuroprotective strategies.

It is well established that proteins associated with pathological states of the brain could be recognized by microglia and induce their activation; these include amyloid-beta protein and alpha-synuclein that are deposited in Alzheimer's and Parkinson's disease respectively, as well as combinations of endogenous pro-inflammatory cytokines (Eikelenboom et al., 2012; Kettenmann et al., 2011; Klegeris et al., 2005, 2008b). Recent evidence indicates that endogenous intracellular proteins released from damaged or dying cells, termed damage-associated molecular pattern molecules (DAMPs), can activate microglia through a select group of specific receptors (Kettenmann et al., 2011). The most studied of these is the high-mobility group box 1 (HMGB1), a non-histone DNA-binding protein expressed by glia and neurons of the central nervous system. HMGB1 is normally located within the nucleus where it acts as a DNA chaperone (Stros, 2010). Upon its release into extracellular space HMGB1 can interact with

several different cell types causing diverse cellular effects, including potent activation of inflammatory responses (Qiu et al., 2008; Yang et al., 2013). Extracellular HMGB1 has been shown to interact with receptor for advanced glycation end products (RAGE) and complement receptor 3 (CR3) on glial cells, followed by activation of the mitogen-activated protein kinase (MAPK) intracellular signaling cascade and nuclear factor κ B (NF- κ B) (Gao et al., 2011; Muhammad et al., 2008; Pedrazzi et al., 2007). Brain microinjection of the recombinant HMGB1 induces expression of pro-inflammatory cytokines (Faraco et al., 2007).

Based on their endosymbiotic origin from bacterial predecessors, mitochondria are hypothesized to display DAMP features as they contain specific molecular signatures (e.g., N-formyl peptides, circular DNA) that may trigger innate immune responses (Zhang et al., 2010). Recent data have implicated mitochondrial transcription factor A (Tfam), which is a structural and functional homolog of HMGB1, as a possible DAMP that can be recognized by immune cells in periphery (Crouser et al., 2009; Julian et al., 2012). The main physiological function of Tfam is initiating mitochondrial gene transcription through binding to mitochondrial DNA via two tandem DNA binding HMG-box domains (Gangelhoff et al., 2009; Ngo et al., 2011; Rubio-Cosials et al., 2011; Wong et al., 2009). However, Tfam can also be released from damaged cells and may - similar to HMGB1 - initiate immunological responses (Chaung et al., 2012). Tfam has been shown to stimulate peripheral blood monocytes (Crouser et al., 2009) and plasmacytoid dendritic cells (Julian et al., 2012) in the presence of additional stimuli (N-formyl peptides and CpG-enriched DNA respectively). RAGE and intracellular signaling pathways similar to those engaged by HMGB1 were also implicated in the cellular actions of Tfam (Julian et al., 2012). Even though expression of this protein in the central nervous system has been demonstrated (Hokari et al., 2010; Yin et al., 2008), to the best of our knowledge the effects of extracellular

Tfam on glial or neuronal cells are unknown. Here we demonstrate that both human mitochondrial proteins and recombinant human Tfam (rhTfam) are recognized by three different types of human mononuclear phagocytes, including primary microglia. We also show that rhTfam in combination with interferon (IFN)- γ induces secretion of pro-inflammatory cytokines and cytotoxins by monocytic cells and that this effect is partially dependent on activation of c-Jun N-terminal kinases (JNK).

Material and methods

Reagents

The following substances were used in various assays and were obtained from Sigma-Aldrich (Oakville, ON, Canada): diaphorase (EC 1.8.1.4, from *Clostridium kluyveri*, 5.8 U/mg solid), dimethyl sulfoxide (DMSO), Triton X-100, p-iodonitrotetrazolium violet, NAD⁺, MTT (3-(4,5-dimethylthiazol-2-yl)-2,5-diphenyl tetrazolium bromide), a highly selective cell permeable inhibitor of p38 mitogen-activated protein kinases (p38 MAPK, SB202190), and a selective inhibitor of JNK (SP600125). Recombinant human IFN- γ and interleukin (IL)-6 enzyme-linked immunosorbent assay (ELISA) development kits were obtained from PeproTech (Rocky Hill, NJ). Goat polyclonal anti-human Tfam antibody was obtained from Santa Cruz Biotechnology (K-18, Santa Cruz, CA). All other reagents were obtained from Thermo Fisher Scientific (Nepean, ON, Canada) unless stated otherwise.

Cells and cell lines

The human THP-1 promonocytic cell line was obtained from the American Type Culture Collection (ATCC, Manassas, VA, USA). Human SH-SY5Y dopaminergic neuroblastoma cells

were donated by Dr. R. Ross, Department of Biological Sciences, Fordham University, Bronx, NY, USA. Primary human monocytes were isolated from venous blood samples obtained from healthy human volunteers as described by Elkord et al. (2005). Peripheral blood mononuclear cells (PBMCs) were separated first by gradient centrifugation on Histopaque-1077; enriched monocyte cultures were obtained by allowing cells to adhere to plastic for 2 h followed by removal of non-adherent cells. Preparation and use of human monocyte cultures were authorized by the University of British Columbia Clinical Research Ethics Board.

Primary human microglia cells were obtained from post-mortem brain tissues according to established protocols (Walker et al., 2009). Tissues were donated to the Banner Sun Health Research Institute (Sun City, AZ, USA) through their Brain and Body Donation Program with informed consent and the approval of the Banner Research Institutional Review Board (IRB).

Preparation of recombinant human Tfam (rhTfam)

The plasmid for expression of the full-length rhTfam was a gift from Dr. M.E. Churchill, University of Colorado, Denver, CO, USA (Gangelhoff et al., 2009). The Tfam plasmid incorporates a cleavable glutathione S-transferase (GST) tag onto the N-terminus of the protein, enabling purification of the protein by glutathione affinity chromatography. The plasmid was transformed into Rosetta2 (DE3) pLysS strain of *Escherichia coli*, (EMD Biosciences, Gibbstown, NJ, USA) and a single transformed colony was used to inoculate 100 ml of Luria Broth medium containing 100 µg/ml ampicillin and 35 µg/ml of chloramphenicol. Following growth for 16 h at 37 °C, 10 ml of the starter culture was used to inoculate Terrific Broth (0.5 l) containing ampicillin (100 µg/ml) and chloramphenicol (35 µg/ml). The culture was grown at 37 °C at 220 rpm until it reached an optical density of 0.8 at 600 nm, at which time isopropyl β-D-1-

thiogalactopyranoside was added to a final concentration of 0.1 mM. The temperature of the incubator was reduced to 25 °C, and the culture was allowed to grow for a further 16 h. Cells were harvested by centrifugation (4,000 × g, 15 min, 4 °C), and the cell pellet was stored at -80 °C until purification.

All protein purification steps were performed at 4 °C or on ice. The harvested cell pellet (45 g) was resuspended in 150 ml of 50 mM GST-binding buffer (4.3 mM Na₂HPO₄, 1.5 mM KH₂PO₄, 137 mM NaCl, 2.7 mM KCl, pH 7.3 with 1 mM ethylene diamine tetraacetic acid [EDTA], 1 mM dithiothreitol [DTT]), with 0.4 mM benzamidine and 1 mM phenylmethylsulfonyl fluoride. The cells were lysed by sonication and then centrifuged at 25,000 × g for 50 min to remove particulates. The supernatant was applied at 1 ml/min to a 100 ml Glutathione Sepharose 4B (GE Healthcare) column equilibrated with GST-binding buffer. The resin was washed with 500 ml of GST-binding buffer and the GST-tagged protein was eluted with 50 mM Tris-HCl pH 8.0, containing 10 mM glutathione, 1 mM EDTA and 10 mM DTT. The eluted protein was concentrated to 10 ml by ultrafiltration and incubated with PreScission protease (GE Healthcare) while undergoing a 16 h dialysis against GST-binding buffer. The dialysate was applied to a 10 ml Glutathione Sepharose column equilibrated with GST-binding buffer to remove uncleaved protein and the GST-tag. The column was washed with GST-binding buffer and the cleaved protein was collected in the flow through and concentrated by ultrafiltration. The protein was then further purified by cation exchange chromatography (Resource S, GE Healthcare) followed by anion-exchange chromatography (Resource Q, GE Healthcare). The concentration of protein was determined by a Lowry assay (BioRad, Mississauga, ON, Canada) using bovine serum albumin as a standard. The purity and molecular size of the protein was checked by polyacrylamide gel electrophoresis and western blotting using

anti-human Tfam antibody as described previously (Klegeris and McGeer, 2003; Wolthers et al., 2003). In addition, we routinely treated rhTfam samples in High Capacity Endotoxin Removal Spin Columns and monitored endotoxin levels by the Limulus Amebocyte Lysate (LAL) Chromogenic Endotoxin Quantitation Kit (both from Pierce/Thermo Fisher Scientific). Several independently prepared batches of rhTfam with endotoxin levels of less than 2 pg/ μ g protein were shown to be biologically active in our assay systems.

Preparation of mitochondrial proteins from cultured cells

Samples of mitochondrial proteins were prepared from ~100 million THP-1 cells grown in 175 cm² flasks using a modified procedure adapted from Safdar et al. (2011). Briefly, cells were collected by centrifugation at 250 x g, washed with phosphate-buffered saline (PBS) containing 100 μ M EDTA and then gently homogenized in a glass homogenizer using a Teflon pestle in ice-cold isolation buffer A (10 mM sucrose, 10 mM Tris/HCl, 50 mM KCl, and 1 mM EDTA, pH 7.4) supplemented with Halt protease inhibitor cocktail from Pierce/Thermo Fisher Scientific. Resulting homogenates were centrifuged at 1,000 x g. The supernatants containing mitochondria were centrifuged at 12,000 x g to obtain a mitochondrial pellet, which was washed twice in ice-cold buffer B (10 mM sucrose, 0.1 mM ethylene glycol tetraacetic acid (EGTA)/Tris, and 10 mM Tris/HCl, pH 7.4, supplemented with Halt protease inhibitor cocktail). All centrifugation steps were carried out at 4 °C. Isolated mitochondrial pellets were resuspended in 80 μ l Dulbecco's modified Eagle's medium-nutrient mixture F12 Ham (DMEM-F12) and subjected to three freeze-thaw cycles using liquid nitrogen to release mitochondrial proteins. Concentration of mitochondrial proteins (diluted 1:10 in PBS) was determined by Bradford assay (Sigma-Aldrich) prior to use in experiments. Purity and enrichment of mitochondrial protein fractions was

confirmed as described previously (Safdar et al., 2011) by a lack of lactate dehydrogenase (LDH) activity and abundance of succinate dehydrogenase activity assessed by colorimetric assay, as well as presence of mitochondrial proteins Tfam and ATP synthase β detected by western blotting (data not shown).

Cell culture

Cells were cultured in DMEM-F12 supplemented with 10% fetal bovine serum (FBS), penicillin (100 U/ml) and streptomycin (100 μ g/ml). Cell cultures were incubated in a CO₂ incubator at 37°C with 5% CO₂ and 100% humidity. For the quantitative polymerase chain reaction (qPCR) experiments, THP-1 cells were seeded in 6-well plates at a concentration of 1 million/ml in DMEM-F12 with 5% FBS. For the cytotoxicity and ELISA experiments, THP-1 cells, primary human monocytes and microglia were seeded in 24-well plates at 0.5 million/ml.

Induction of monocytic cell cytotoxicity by rhTfam and mitochondrial proteins

Experiments to test the cytotoxicity of monocytes, THP-1 cells and microglia were performed as described previously (Klegeris et al., 2005). Cells were treated with different concentrations of rhTfam or mitochondrial proteins in the presence or absence of IFN- γ (150 U/ml). In order to eliminate the possibility that the stimulatory effects of rhTfam observed in our study were due to endotoxin contamination of recombinant protein samples, the following additional control experiments were performed: testing of rhTfam that had been heated for 10 min at 95°C prior to adding to cells (see Fig. 3) showing loss of activity; treatment of rhTfam with polymixin B (1 h at 10 μ g/ml) before adding to THP-1 cells showing no reduction of activity, pretreatment of THP-1 cells with anti-toll-like receptor (TLR)-4 antibody (1 h at 20 μ g/ml, clone HTA125 from

eBioscience, San Diego, CA, USA) showing no reduction of cytotoxic activity or cytokine secretion (Supplemental Figure 1); treatment of cells with the combination of IFN- γ and a control protein, recombinant methylmalonic aciduria cblC type with homocystinuria (MMACHC; expressed and isolated from *E. coli* by a similar method to that of rhTfam), showing no activity.

Supernatants from microglia and THP-1 cells incubated in the presence or absence (unstimulated) of mitochondrial proteins and IFN- γ for 24–48 h were collected and added to SH-SY5Y neuronal cells that had been seeded 24 h earlier onto 24-well plates at 0.2 million/ml in DMEM-F12 plus 5% FBS, 0.4 ml/well. Following 72 h, viability of SH-SY5Y cells was measured by the MTT assay, which detects live cells, and LDH release, which estimates percent of dead cells, as described previously (Villanueva et al., 2012). Percentages of cell viability were assessed relative to untreated control wells containing SH-SY5Y cells incubated in fresh medium. Percentages of cell death were assessed relative to control wells where SH-SY5Y cells were lysed with 5% Triton X-100. In addition, the effects of various treatments on THP-1 cell and microglia viability were assessed using the MTT cell viability assay.

ELISA

IL-6 concentrations in supernatants collected from monocytes or microglia stimulated for 48 h with rhTfam and IFN- γ were measured by Peprotech ELISA development kits following the manufacturer's instructions and using a BMG Fluostar Omega plate reader (BMG Labtech, Offenburg, Germany).

RNA extraction and qPCR

A previously published procedure was employed (Madeira et al., 2012). Total RNA from THP-1 cells was isolated using the Aurum™ Total RNA mini kit with on-column DNase I digestion (BioRad). RNA concentration was measured using a spectrophotometer with the 260/280 ratios of all samples being >1.9. One µg total RNA was converted to cDNA using the iScript™ (BioRad) kit as specified by the manufacturer's protocol. qPCR was performed using SsoFast™ Evagreen® supermix (BioRad) on a BioRad CFX-96 real-time PCR detection system. The final reaction volume was 15 µl, which contained 1.5 ng cDNA (in 1.5 µl), 2.5 µl each of 5 µM forward and reverse primers, 5 µl master mix, and 3.5 µl nuclease-free water. Primers with previously published sequences for IL-1 β , IL-6, IL-8 and β -actin (Hayashi et al., 2003; Vogel et al., 2005) were obtained from Integrated DNA Technologies (Vancouver, BC, Canada). β -actin, levels of which did not change with any of the treatments (cycle threshold [Ct] difference of <0.5), was used as a housekeeping gene and relative quantification of RNA was calculated using the $\Delta\Delta$ Ct method with unstimulated THP-1 cells serving as the control. The efficiency of each primer set was determined by plotting template dilutions against threshold cycle (Ct) values; the results obtained were within standard accepted values of 90-110% (Bustin et al., 2009). Duplicate experimental samples were analyzed simultaneously with negative control that contained no cDNA. Melting point dissociation curves generated by the instrument were used to confirm specificity of the amplified product.

Statistical analysis

SPSS software (version 16.0; IBM SPSS, Chicago, IL, USA) was used to conduct statistical analyses. Randomized block design analysis of variance (ANOVA), which controls for

variability between experimental days by assigning data from each day as a block, was used to analyze all data. Significant differences were further evaluated by the Dunnett's or Tukey's Honestly Significant Difference (HSD) post hoc tests for multiple comparisons. Data are presented as means \pm standard deviation (SD) with $p < 0.05$ considered statistically significant.

Results

Tfam induces human monocytic cell toxicity towards neuronal cells.

Primary human microglia, human peripheral blood monocytes, and human THP-1 monocytic cells were used to study interactions between Tfam and mononuclear phagocytes. Initial experiments revealed that 48 h incubation of 5 μ g/ml of rhTfam alone with human peripheral blood monocytes did not induce their toxicity towards human SH-SY5Y neuronal cells (Figure 1). However, when 5 μ g/ml rhTfam was combined with IFN- γ (150 U/ml) and added to monocyte cultures for 48h, such conditioned media became toxic towards human SH-SY5Y neuronal cells. Figure 1 shows that the toxic action of rhTfam plus IFN- γ stimulated cell supernatants can be detected as reduced viability of SH-SY5Y cells by the MTT assay (Fig. 1A) and reciprocal increase in SH-SY5Y cell lysis measured by the LDH assay (Fig. 1B) after 72 h incubation. A similar reciprocal relationship was found between data obtained by the MTT and LDH assays for toxicity experiments with other monocytic cell types described below; however, for clarity of data presentation only results from the MTT assay are presented (see Supplemental data for LDH assay results). Supernatants from untreated peripheral blood monocyte supernatants (Unstimulated) or monocytes treated with IFN- γ (150 U/ml) alone had no effect on toxicity towards SH-SY5Y cells (Figure 1). In addition to the above two biochemical assays, the toxic action of supernatants from rhTfam plus IFN- γ -stimulated monocytes could be observed

visually under phase contrast microscope. Figure 1C illustrates that exposure to conditioned medium resulted in lowered density and altered morphology of SH-SY5Y cells.

Next, the concentration-dependent effect of rhTfam was studied using THP-1 monocytic cells that are commonly used as surrogates of human peripheral blood monocytes as well as brain microglia. Figure 2A illustrates that rhTfam, only when combined with IFN- γ , induced THP-1 cell toxicity towards SH-SY5Y cells in a concentration-dependent manner. This effect was statistically significant for concentrations of rhTfam ≥ 0.36 $\mu\text{g/ml}$. The same concentrations of rhTfam (except 5 $\mu\text{g/ml}$) combined with IFN- γ were slightly toxic to THP-1 cells (Fig. 2B); a similar decrease in THP-1 cell viability can be observed with other stimuli that induce THP-1 cell toxic secretions (Madeira et al., 2012). The control non-mitochondrial recombinant human protein MMACHC (Kim et al., 2008), which was produced and purified in the same manner as rhTFAM, even when combined with IFN- γ , had no direct effect on viability of THP-1 cells (Fig. 2B) and also did not influence SH-SY5Y cells exposed to supernatants from THP-1 cells incubated with this combination of stimulants (Fig. 2A). MMACHC has approximately the same molecular weight as Tfam (~26 kDa); both these proteins were produced by using the same equipment in an identical manner.

Heat treatment reduces the monocytic cell-stimulating potential of rhTfam.

Heating rhTfam for 10 min at 95°C prior to its addition, in combination with IFN- γ , to THP-1 cells resulted in a significant reduction in monocytic cell supernatant toxicity towards SH-SY5Y cells compared to untreated rhTfam (treatment x concentration interaction, $P < 0.05$; Fig. 3). Post-hoc analyses by Tukey's HSD test revealed that heat-treated rhTfam when combined with IFN- γ induced less THP-1 cell-mediated toxicity at the three highest concentrations used (1.25, 2.5, and

5.0 µg/ml). Both heated and unheated rhTfam on their own failed to induce THP-1 cell toxicity towards SH-SY5Y cells at all concentrations tested (Supplemental Figure 3).

Tfam induces inflammatory cytokine mRNA expression

To determine whether rhTfam elicited a pro-inflammatory response in monocytic cells, THP-1 cells were treated with 5 µg/ml rhTfam, in the presence and absence of IFN- γ (150 U/ml), for 24 h and IL-1 β , IL-6 and IL-8 mRNA expression were measured using qPCR. Figure 4 shows that rhTfam on its own produced a robust increase in IL-1 β (749-fold), IL-6 (~25-fold) and IL-8 mRNA (~900-fold) over unstimulated cells. The magnitude of induction was even greater when rhTfam was combined with IFN- γ (~9000-fold increase for IL-1 β , ~3000-fold increase for IL-6, and ~4500-fold increase for IL-8).

JNK activation is partially involved in THP-1 monocytic cell activation by Tfam

To elucidate the potential intracellular signaling pathways involved, THP-1 cells were treated with inhibitors of key inflammatory signaling pathways, which have been previously shown to mediate the cytotoxic response of THP-1 cells to other stimuli (Klegeris et al., 2008b). Adding JNK inhibitor SP600125 (20 µM) prior to stimulation of THP-1 cells with rhTfam (5 µg/ml) plus IFN- γ (150 U/ml) significantly reduced their toxic secretions ($P < 0.05$ vs. DMSO control) whereas inhibition of p38 MAPK using SB202190 (20 µM) had no significant effects (Fig. 5). Adding these concentrations of inhibitors to unstimulated THP-1 cells did not alter SH-SY5Y cell viability after transfer of the THP-1 cell supernatants (data not shown).

Mitochondrial proteins induce THP-1 cell toxicity towards SH-SY5Y cells

Similar to the effects seen with rhTfam, mitochondrial proteins (50 and 100 µg/ml), when combined with IFN- γ (150 U/ml), induced significant toxicity of THP-1 cells towards SH-SY5Y neuronal cells (Fig. 6A). Treatment of THP-1 cells with isolated mitochondrial proteins, with or without IFN- γ , had no effect on their viability (Fig. 6B). Importantly, when the same concentrations and combinations of mitochondrial proteins with IFN- γ were applied directly to SH-SY5Y cells, their viability after 72 h incubation was unaffected (>90% viability via MTT assay, <15% lysis by LDH release; data not shown).

rhTfam and mitochondrial proteins induce primary human microglial neurotoxicity

To determine whether rhTfam and/or mitochondrial proteins could elicit similar cytotoxic responses in microglia, which also belong to the mononuclear phagocyte system, similar experiments using primary adult human microglia isolated from post-mortem brains were performed. When combined with IFN- γ (150 U/ml), rhTfam (5 µg/ml) and mitochondrial proteins (100 µg/ml) both induced microglia supernatant-mediated toxicity towards SH-SY5Y neuronal cells (Fig. 7). This was accompanied by a significant increase in IL-6 secretion from primary human microglia (Fig. 8). Similar induction of IL-6 secretion by combinations of IFN- γ (150 U/ml) with rhTfam (5 µg/ml) were also measured using human peripheral blood monocytes (data not shown).

Discussion

To test the hypothesis that extracellular Tfam can induce pro-inflammatory and cytotoxic responses of microglia, full-length rhTFAM was prepared and added alone or in combination

with IFN- γ to three different types of cultured human mononuclear phagocytes, including microglia obtained from human surgical samples. We and others have previously shown that unstimulated monocytic cells do not secrete substances toxic to human neuronal cells, but that supernatants from cells exposed to select stimuli exhibit cytotoxicity (Combs et al., 2000; Dzenko et al., 1997; Klegeris et al., 2005, 2008a; Little et al., 2012; Taylor et al., 2003). In this study we used an analogous human cell culture system which involved the initial exposure of monocytic cells to rhTfam and other stimuli for 48 h, followed by transfer of cell-free supernatants to cultured human SH-SY5Y cells. Our data indicate that rhTfam alone lacks the ability to induce monocytic cell cytotoxicity and that additional stimulation of cells with IFN- γ is required for induction of the cytotoxic response. We have previously observed that similar co-stimulation with IFN- γ is required to reveal the cytotoxicity-inducing activity of α -synuclein and tumor necrosis factor (TNF)- α , which on their own do not cause monocytic cell cytotoxicity. It is also important to note that IFN- γ alone is not capable of inducing significant monocytic cell cytotoxicity (Klegeris et al., 2005, 2008b) (Fig. 2, 6, 7).

Even though two consecutive chromatographic steps (cation-exchange and anion-exchange) were used to purify rhTfam, endotoxin contamination of recombinant protein samples is always a concern (Chaung et al., 2012). We adopted several strategies used by others in studies with recombinant proteins to demonstrate that Tfam, and not any contaminating endotoxin, is responsible for the effects observed (Chaung et al., 2012; Crouser et al., 2009; Li et al., 2003; Pedrazzi et al., 2007). The cytotoxicity-inducing ability of rhTfam was heat-sensitive and was not inhibited by polymyxin B. In addition, a non-mitochondrial human control protein MMACHC prepared under the same conditions as Tfam did not induce cellular responses. Furthermore, mitochondrial proteins extracted from human cells induced THP-1 cell and human

microglia toxicity when combined with IFN- γ . Additional control experiments were performed demonstrating that at the concentrations used, neither rhTfam nor mitochondrial proteins alone or in combination with IFN- γ were toxic when applied to SH-SY5Y cells directly, therefore the cytotoxic activity of Tfam towards the neuronal cells was indirect and could not be explained by the possible transfer of some rhTfam to SH-SY5Y cells along with the monocytic cell supernatants.

Although induction of THP-1 cytotoxicity required their exposure to a combination of rhTFAM or mitochondrial proteins with IFN- γ , induction of mRNA expression three pro-inflammatory cytokines (IL-1 β , IL-6 and IL-8) could be achieved by their exposure to rhTfam in the absence of any co-stimuli. All these cytokines have been implicated in microglia-mediated inflammatory reactions associated with neurodegenerative diseases (Kettenmann et al., 2011). IFN- γ alone did not induce cytokine mRNA, but it significantly enhanced the effects of rhTfam; therefore, Tfam and IFN- γ acted synergistically to induce both cytotoxicity and cytokine secretion of monocytic cells studied.

To the best of our knowledge this study is the first to demonstrate interaction between microglia and Tfam leading to potentially pro-inflammatory response of this brain glial cell type. Only very limited information is available about the physiological consequences of interaction of extracellular Tfam with cells. Thus far it has been demonstrated that secretion of IL-8 by human monocytes (Crouser et al., 2009), TNF- α by murine macrophages (Chaung et al., 2012), and IFN- α by human plasmacytoid dendritic cells (Julian et al., 2012) is induced by Tfam alone or in combination with co-stimulatory molecules such as CpG-containing oligonucleotides and the bacterial formyl peptide N-formylmethionine-leucine-phenylalanine (fMLP). The receptor for

advanced glycation endproducts (RAGE) and formyl peptide receptors (FPR) have been shown to mediate some of the cellular effects of Tfam (Crouser et al., 2009; Julian et al., 2012).

Identification of receptor(s) responsible for interaction between Tfam and microglia will require further studies, but FPRs appear not to be predominantly responsible for the effect of Tfam observed in our study since exposure of THP-1 cells to rhTfam plus IFN- γ in the presence of FPR inhibitor cyclosporin H (CsH) (Crouser et al., 2009) did not inhibit the cellular responses; combining Tfam with fMLP also did not induce monocytic cell activation (data not shown).

The potential receptor targets for Tfam are not limited to RAGE and FPR; since Tfam is a structural and functional homolog of HMGB1, it could potentially interact with any or all of the HMGB1 receptors, which include RAGE, toll-like receptor TLR-2, -4, -9, complement receptor CR3, and others (Gao et al., 2011; Julian et al., 2012; Lotze and Tracey, 2005; Maroso et al., 2010; Muhammad et al., 2008; Pedrazzi et al., 2007; Qiu et al., 2008; Yang et al., 2013). The key intracellular signaling pathways and molecules that have been shown to mediate the cellular effects of Tfam and HMGB1 include NF- κ B, IL-1-receptor-associated kinase (IRAK), phosphatidylinositol 3-kinase (PI3K) and several MAPKs (Julian et al., 2012; Lotze and Tracey, 2005). We studied the effects of two different MAPK inhibitors and demonstrated that rhTfam plus IFN- γ induced cytotoxicity of THP-1 cells was partially dependent on JNK, but not p38 MAPK activation. JNK has already been shown to partially mediate the cellular effects of HMGB1 in human monocytic U937 cells (Kuniyasu et al., 2005), mouse liver dendritic cells (Zeng et al., 2009), and Kupffer cells (Luo et al., 2010). Although inhibition of JNK using SP600125 reduced cytotoxicity of supernatants from THP-1 monocytes treated with the combination of rhTfam with IFN- γ , future work is needed to confirm conclusively JNK activation and its role in Tfam-mediated monocyte inflammation. Further studies directed at

establishing receptors and intracellular signaling pathways mediating Tfam-human microglia interactions are currently under way in our laboratory. Our preliminary data show that the stimulatory effects of Tfam on monocytic cells are not mediated by TLR-4 (see Supplementary Figure 1).

Taken together, these data indicate that Tfam, similar to HMGB1 (Qiu et al., 2008), could serve as an endogenous intercellular signaling molecule in the brain. Since Tfam can be released by damaged cells (Crouser et al., 2009) and is recognized by microglia, Tfam could potentially contribute to sterile neuroimmune responses that are observed in a number of human pathologies including neurodegenerative disorders, stroke, and neurotrauma. Microglial responses resulting from interaction with Tfam appear to be pro-inflammatory and potentially harmful to surrounding neuronal cells. Further elucidation of the receptors and signaling pathways responsible for the observed microglial activation by Tfam is warranted as it may lead to identification of novel therapeutic targets for a range of pathologies that involve sterile neuroinflammatory responses.

Acknowledgments

This work was supported by grants from the Natural Sciences and Engineering Research Council of Canada (NSERC) and the Jack Brown and Family Alzheimer's Disease Research Foundation. JPL was the recipient of an NSERC postdoctoral fellowship.

Fig. 1. Tfam induces human peripheral blood monocyte toxicity towards human SH-SY5Y neuronal cells. **A)** Cell viability assessed by the MTT assay; and **B)** Cell lysis assessed by lactate dehydrogenase (LDH) release from SH-SY5Y neuronal cells that were exposed for 72 h to conditioned media from monocytes that had been left unstimulated or were stimulated for 48 h with 5 µg/ml rhTfam combined with 150 U/ml IFN-γ. Data from 3 independent experiments are presented. Percent viability is expressed relative to untreated SH-SY5Y control cell cultures. Percent lysed is expressed relative to SH-SY5Y cultures lysed with 5% Triton X-100. *P<0.05 vs. unstimulated cells, Dunnett's post-hoc test. **C)** Representative phase contrast microscopy images of SH-SY5Y cells following 72 h treatment with conditioned media from unstimulated and stimulated (48 h with rhTfam + IFN-γ) monocytes. Magnification bars = 200 µm.

Fig. 2. Tfam induces human THP-1 monocytic cell toxicity towards SH-SY5Y neuronal cells in a concentration-dependent manner. **A)** The MTT assay was used to assess viability of SH-SY5Y cells exposed for 72 h to conditioned media from unstimulated THP-1 cells and cells that had been stimulated for 48 h with a combination of IFN-γ (150 U/ml) and different concentrations of rhTfam. Percent viability is expressed relative to untreated SH-SY5Y control cell cultures. The non-mitochondrial protein MMACHC (Kim et al., 2008) was tested in combination with IFN-γ at the highest concentration of rhTfam used (5 µg/ml). **B)** Viability of THP-1 cells was assessed by the MTT assay at the end of the 48 h incubation period with the various stimuli. Data from 5 independent experiments are presented. *P<0.05 vs. unstimulated cells, Dunnett's post-hoc test.

Fig. 3. Heating Tfam reduces its ability to induce THP-1 cell toxicity towards SH-SY5Y cells. rhTfam was left untreated or was heated for 10 min at 95°C (heat-treated Tfam). Combinations

of IFN- γ (150 U/ml) and different concentrations of rhTfam were added to THP-1 cells for 48 h. Subsequently, conditioned media was transferred to SH-SY5Y cells and neuronal cell viability assessed by the MTT assay at the end of 72 h incubation period. Percent viability is expressed relative to untreated SH-SY5Y control cell cultures. Data from 5 independent experiments are presented. *P<0.05 vs. untreated Tfam at the same concentration, Tukey's post-hoc test.

Fig. 4. Tfam induces inflammatory cytokine mRNA expression in THP-1 monocytic cells. **A)** IL-1 β , **B)** IL-6 and **C)** IL-8 mRNA expression was measured by qPCR in THP-1 cells after 24 h exposure to IFN- γ (150 U/ml), rhTfam (5 μ g/ml) or combination of the two stimuli. Data from 3-5 independent experiments are presented. *P<0.05 vs. unstimulated, Dunnett's post-hoc test.

Fig. 5. Toxicity of THP-1 cell towards SH-SY5Y cells induced by a combination of Tfam and IFN- γ is partially dependent on c-Jun N-terminal kinase (JNK). THP-1 cells were stimulated for 48 h with rhTfam (5 μ g/ml) combined with IFN- γ (150 U/ml) in the presence or absence of SP600125 (20 μ M, JNK inhibitor) and SB202190 (20 μ M, p38 MAPK inhibitor) and conditioned media was transferred to human SH-SY5Y neuronal cells. After a 72 h incubation period, neuronal cell viability was assessed by the MTT assay. Percent viability is expressed relative to untreated SH-SY5Y control cell cultures. Data from 5 independent experiments are presented. ^a, P<0.05 vs unstimulated; ^b, P<0.05 vs. DMSO solvent (Tukey's post-hoc test).

Fig. 6. Isolated human mitochondrial proteins that are non-toxic to THP-1 cells induce secretion of toxins when applied to THP-1 cells in combination with IFN- γ . **A)** The MTT assay was used to assess viability of SH-SY5Y cells exposed for 72 h to conditioned media from unstimulated

THP-1 cells and cells that had been stimulated for 48 h with different concentrations of mitochondrial proteins in the presence or absence of IFN- γ (150 U/ml). Percent viability is expressed relative to untreated SH-SY5Y control cell cultures. **B)** Viability of THP-1 monocytic cells was assessed by the MTT assay at the end of the 48 h incubation period with the various stimuli. Data from 5 independent experiments are presented. *P<0.05 vs. unstimulated, Dunnett's post-hoc test.

Fig. 7. Tfam and isolated mitochondrial proteins induce primary human microglial cell toxicity towards SH-SY5Y neuronal cells. **A)** The MTT assay was used to assess viability of SH-SY5Y cells exposed for 72 h to conditioned media from unstimulated human microglia and cells that had been stimulated for 48 h with IFN- γ (150 U/ml) alone and IFN- γ combined with rhTfam (5 μ g/ml) or mitochondrial proteins (100 μ g/ml). Percent viability is expressed relative to untreated SH-SY5Y control cell cultures. **B)** Primary human microglial cell viability was measured by the MTT assay at the end of the 48 h incubation period with the various stimuli. Human microglia were prepared from two independent autopsy samples (n=4) *P<0.05 vs. unstimulated, Dunnett's post-hoc test. **C)** Representative phase contrast microscopy images of SH-SY5Y cells following 72 h treatment with conditioned media from unstimulated and stimulated (48 h with rhTfam + IFN- γ) primary human microglia. Magnification bars = 100 μ m.

Fig. 8. Tfam and isolated mitochondrial proteins induce IL-6 secretion from primary human microglia. Cells were treated with rhTfam or isolated mitochondrial proteins as indicated and ELISA used to measure IL-6 in cell-free supernatants after 48 h incubation with the stimuli.

Human microglia were prepared from two independent autopsy samples (n=4). *P<0.05 vs. unstimulated, Dunnett's post-hoc test.

Fig. 1

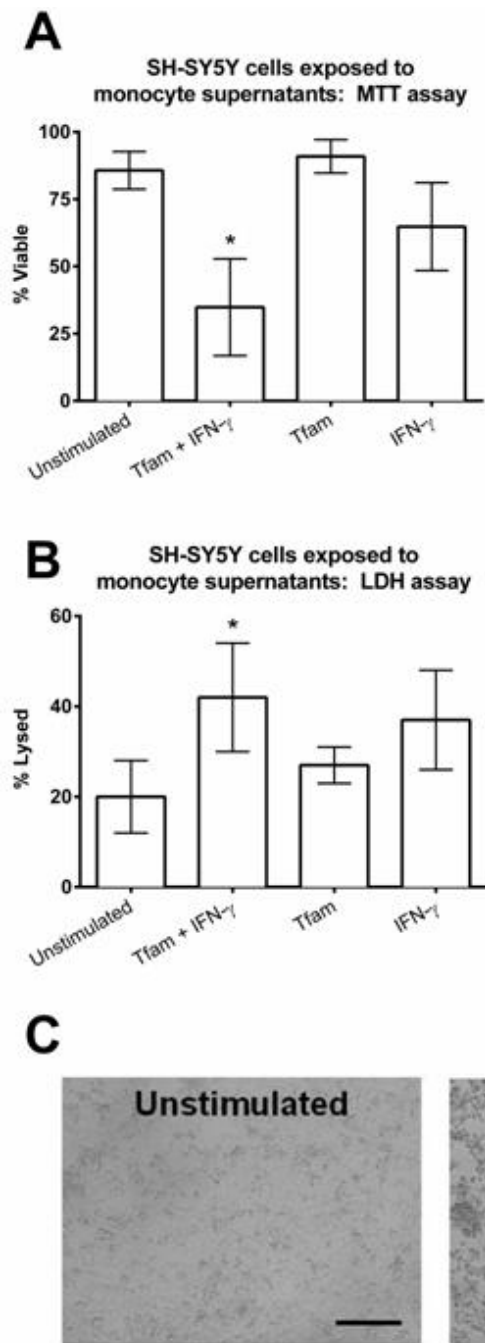


Fig. 2

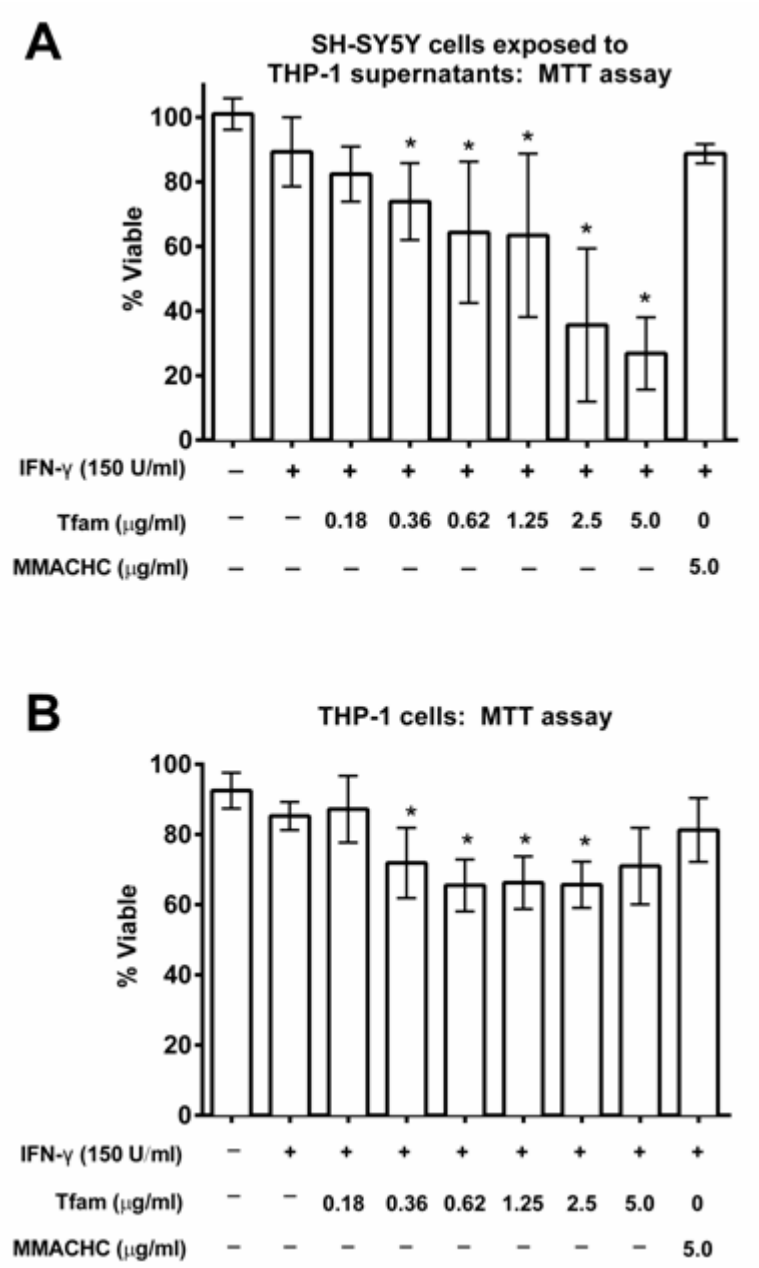


Fig. 3

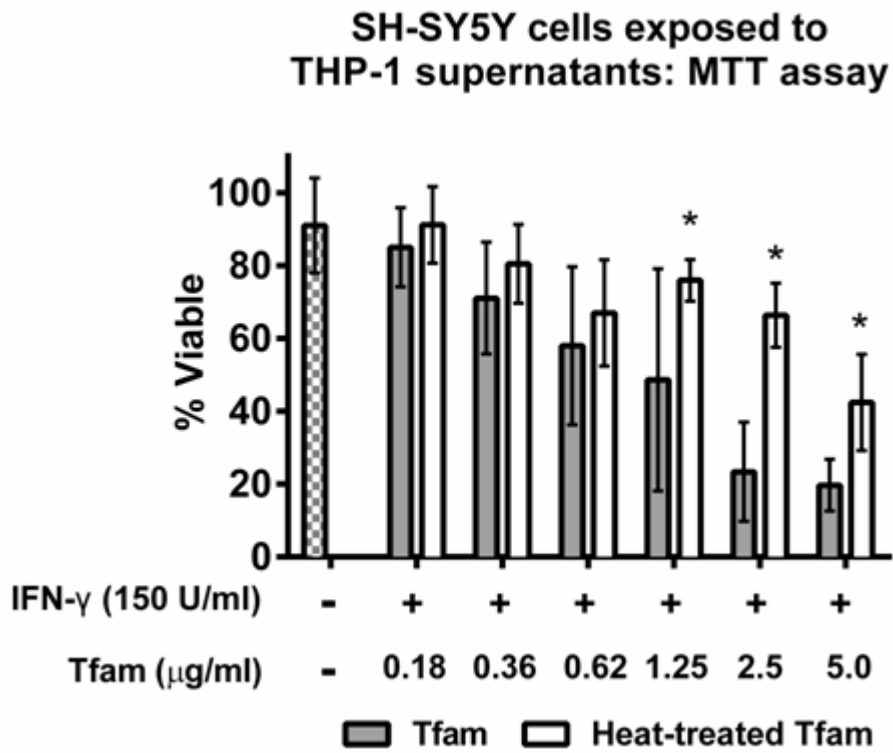


Fig. 4

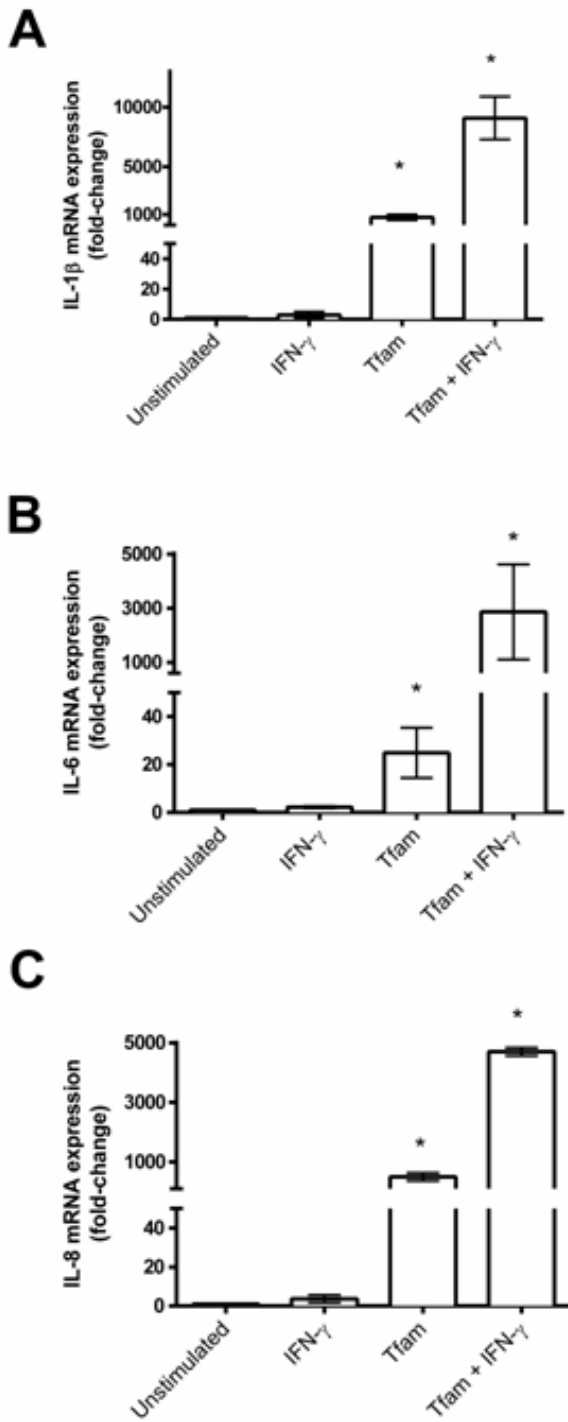


Fig. 5

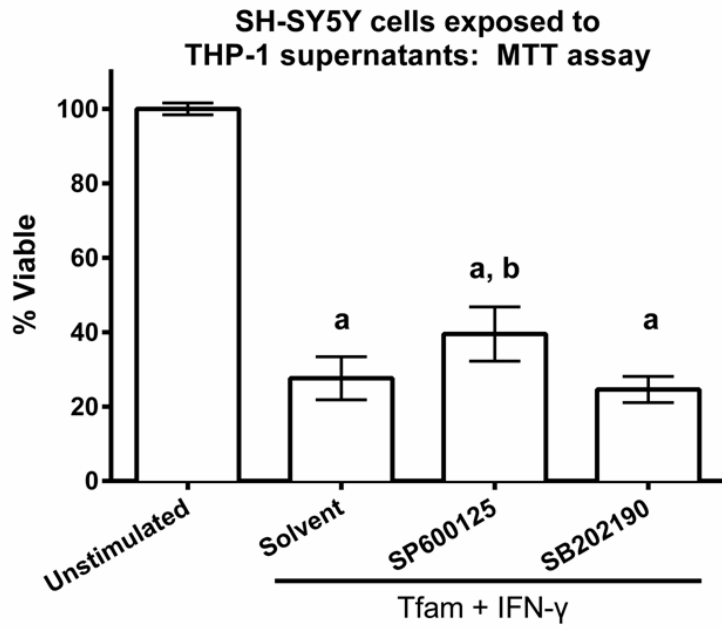


Fig. 6

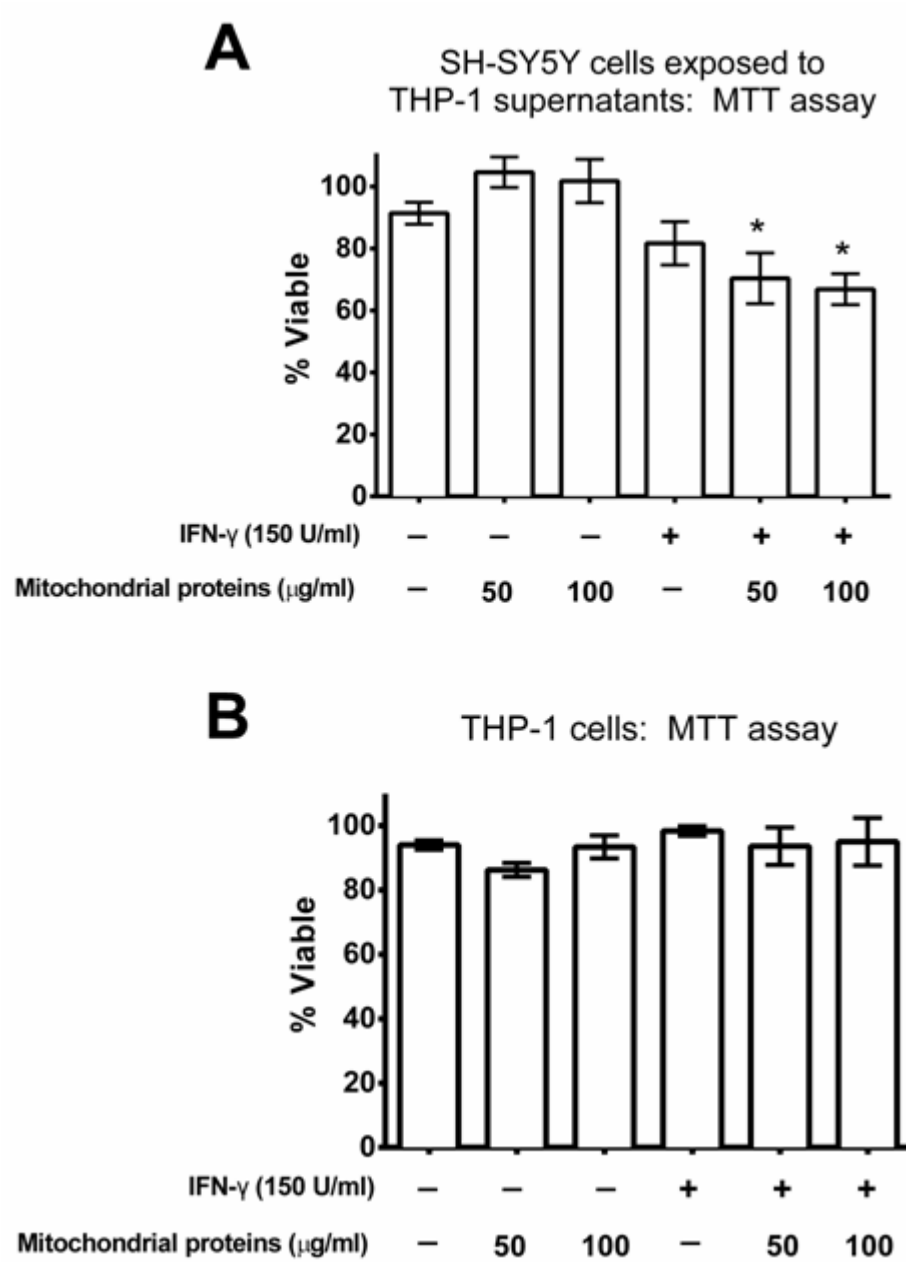


Fig. 7

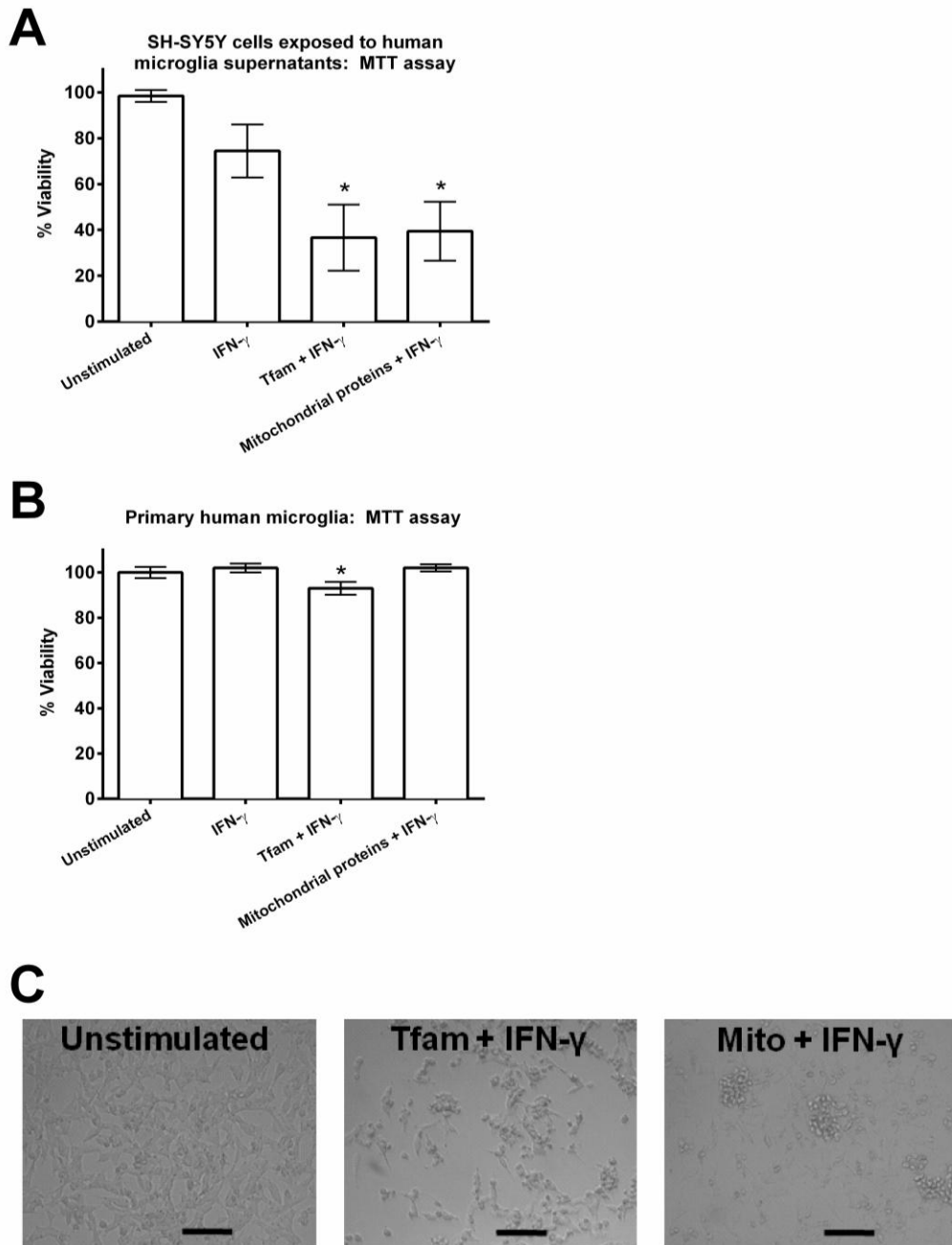
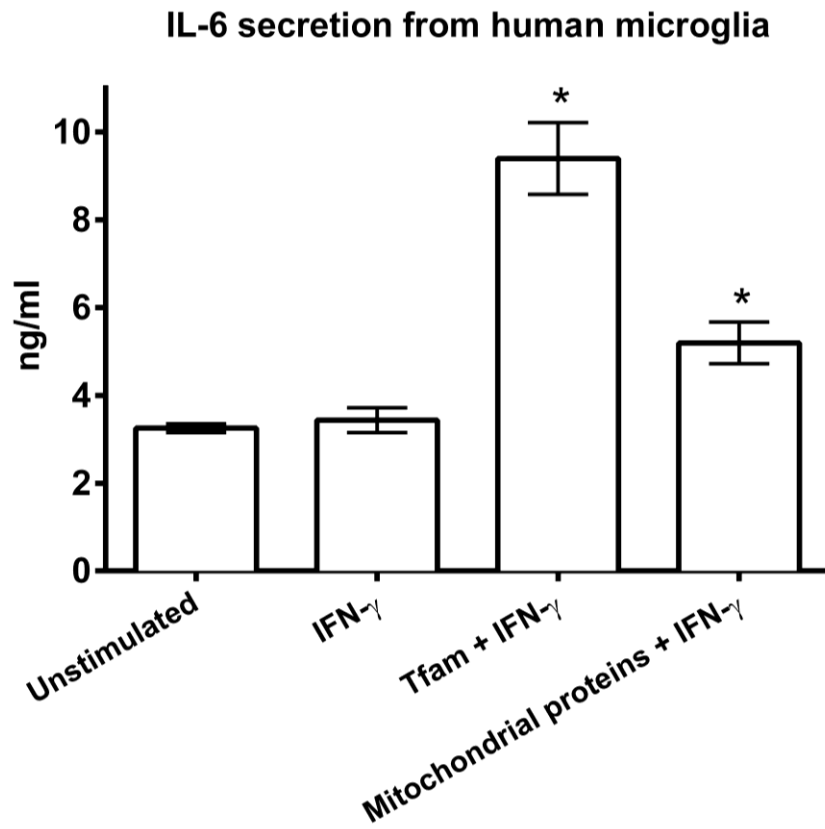


Fig. 8



References

- Akiyama, H., Barger, S., Barnum, S., Bradt, B., Bauer, J., Cole, G.M., Cooper, N.R., Eikelenboom, P., Emmerling, M., Fiebich, B.L., Finch, C.E., Frautschy, S., Griffin, W.S., Hampel, H., Hull, M., Landreth, G., Lue, L., Mrak, R., Mackenzie, I.R., McGeer, P.L., O'Banion, M.K., Pachter, J., Pasinetti, G., Plata-Salaman, C., Rogers, J., Rydel, R., Shen, Y., Streit, W., Strohmeyer, R., Tooyoma, I., Van Muiswinkel, F.L., Veerhuis, R., Walker, D., Webster, S., Wegrzyniak, B., Wenk, G., Wyss-Coray, T., 2000. Inflammation and Alzheimer's disease. *Neurobiol. Aging* 21, 383-421.
- Block, M.L., Zecca, L., Hong, J.S., 2007. Microglia-mediated neurotoxicity: uncovering the molecular mechanisms. *Nat. Rev. Neurosci.* 8, 57-69.
- Bustin, S.A., Benes, V., Garson, J.A., Hellemans, J., Huggett, J., Kubista, M., Mueller, R., Nolan, T., Pfaffl, M.W., Shipley, G.L., Vandesompele, J., Wittwer, C.T., 2009. The MIQE guidelines: minimum information for publication of quantitative real-time PCR experiments. *Clin. Chem.* 55, 611-622.
- Chang, W.W., Wu, R., Ji, Y., Dong, W., Wang, P., 2012. Mitochondrial transcription factor A is a proinflammatory mediator in hemorrhagic shock. *Int. J. Mol. Med.* 30, 199-203.
- Colton, C.A., 2009. Heterogeneity of microglial activation in the innate immune response in the brain. *J. Neuroim. Pharmacol.* 4, 399-418.
- Combs, C.K., Johnson, D.E., Karlo, J.C., Cannady, S.B., Landreth, G.E., 2000. Inflammatory mechanisms in Alzheimer's disease: inhibition of beta-amyloid-stimulated proinflammatory responses and neurotoxicity by PPARgamma agonists. *J. Neurosci.* 20, 558-567.

- Crouser, E.D., Shao, G., Julian, M.W., Macre, J.E., Shadel, G.S., Tridandapani, S., Huang, Q., Wewers, M.D., 2009. Monocyte activation by necrotic cells is promoted by mitochondrial proteins and formyl peptide receptors. *Crit. Care Med.* 37, 2000-2009.
- Dzenko, K.A., Weltzien, R.B., Pachter, J.S., 1997. Suppression of A beta-induced monocyte neurotoxicity by antiinflammatory compounds. *J. Neuroimmunol.* 80, 6-12.
- Eikelenboom, P., Hoozemans, J.J., Veerhuis, R., van Exel, E., Rozemuller, A.J., van Gool, W.A., 2012. Whether, when and how chronic inflammation increases the risk of developing late-onset Alzheimer's disease. *Alzheimers Res. Ther.* 4, 15.
- Elkord, E., Williams, P.E., Kynaston, H., Rowbottom, A.W., 2005. Human monocyte isolation methods influence cytokine production from in vitro generated dendritic cells. *Immunology* 114, 204-212.
- Faraco, G., Fossati, S., Bianchi, M.E., Patrone, M., Pedrazzi, M., Sparatore, B., Moroni, F., Chiarugi, A., 2007. High mobility group box 1 protein is released by neural cells upon different stresses and worsens ischemic neurodegeneration in vitro and in vivo. *J. Neurochem.* 103, 590-603.
- Gangelhoff, T.A., Mungalachetty, P.S., Nix, J.C., Churchill, M.E., 2009. Structural analysis and DNA binding of the HMG domains of the human mitochondrial transcription factor A. *Nucleic Acids Res.* 37, 3153-3164.
- Gao, H.M., Zhou, H., Zhang, F., Wilson, B.C., Kam, W., Hong, J.S., 2011. HMGB1 acts on microglia Mac1 to mediate chronic neuroinflammation that drives progressive neurodegeneration. *J. Neurosci.* 31, 1081-1092.
- Graeber, M.B., 2010. Changing face of microglia. *Science* 330, 783-788.

- Hayashi, F., Means, T.K., Luster, A.D., 2003. Toll-like receptors stimulate human neutrophil function. *Blood* 102, 2660-2669.
- Hoarau, J.J., Krejbich-Trotot, P., Jaffar-Bandjee, M.C., Das, T., Thon-Hon, G.V., Kumar, S., Neal, J.W., Gasque, P., 2011. Activation and control of CNS innate immune responses in health and diseases: a balancing act finely tuned by neuroimmune regulators (NIReg). *CNS Neurol. Disord. Drug Targets* 10, 25-43.
- Hokari, M., Kuroda, S., Kinugawa, S., Ide, T., Tsutsui, H., Iwasaki, Y., 2010. Overexpression of mitochondrial transcription factor A (TFAM) ameliorates delayed neuronal death due to transient forebrain ischemia in mice. *Neuropathology* 30, 401-407.
- Jin, R., Yang, G., Li, G., 2010. Inflammatory mechanisms in ischemic stroke: role of inflammatory cells. *J. Leukoc. Biol.* 87, 779-789.
- Julian, M.W., Shao, G., Bao, S., Knoell, D.L., Papenfuss, T.L., VanGundy, Z.C., Crouser, E.D., 2012. Mitochondrial transcription factor A serves as a danger signal by augmenting plasmacytoid dendritic cell responses to DNA. *J. Immunol.* 189, 433-443.
- Kettenmann, H., Hanisch, U.K., Noda, M., Verkhratsky, A., 2011. Physiology of microglia. *Physiol. Rev.* 91, 461-553.
- Kim, J., Gherasim, C., Banerjee, R., 2008. Decyanation of vitamin B12 by a trafficking chaperone. *Proc. Natl. Acad. Sci. USA* 105, 14551-14554.
- Klegeris, A., Bissonnette, C.J., McGeer, P.L., 2005. Modulation of human microglia and THP-1 cell toxicity by cytokines endogenous to the nervous system. *Neurobiol. Aging* 26, 673-682.
- Klegeris, A., Li, J., Bammler, T.K., Jin, J., Zhu, D., Kashima, D.T., Pan, S., Hashioka, S., Maguire, J., McGeer, P.L., Zhang, J., 2008a. Prolyl endopeptidase is revealed following

- SILAC analysis to be a novel mediator of human microglial and THP-1 cell neurotoxicity. *Glia* 56, 675-685.
- Klegeris, A., McGeer, P.L., 2003. Toxicity of human monocytic THP-1 cells and microglia toward SH-SY5Y neuroblastoma cells is reduced by inhibitors of 5-lipoxygenase and its activating protein FLAP. *J. Leukoc. Biol.* 73, 369-378.
- Klegeris, A., Pelech, S., Giasson, B.I., Maguire, J., Zhang, H., McGeer, E.G., McGeer, P.L., 2008b. Alpha-synuclein activates stress signaling protein kinases in THP-1 cells and microglia. *Neurobiol. Aging* 29, 739-752.
- Kuniyasu, H., Yano, S., Sasaki, T., Sasahira, T., Sone, S., Ohmori, H., 2005. Colon cancer cell-derived high mobility group 1/amphoterin induces growth inhibition and apoptosis in macrophages. *Am. J. Pathol.* 166, 751-760.
- Li, J., Kokkola, R., Tabibzadeh, S., Yang, R., Ochani, M., Qiang, X., Harris, H.E., Czura, C.J., Wang, H., Ulloa, L., Warren, H.S., Moldawer, L.L., Fink, M.P., Andersson, U., Tracey, K.J., Yang, H., 2003. Structural basis for the proinflammatory cytokine activity of high mobility group box 1. *Mol. Med.* 9, 37-45.
- Little, J.P., Madeira, J.M., Klegeris, A., 2012. The saturated fatty acid palmitate induces human monocytic cell toxicity toward neuronal cells: exploring a possible link between obesity-related metabolic impairments and neuroinflammation. *J. Alzheimers Dis.* 30 Suppl 2, S179-183.
- Lotze, M.T., Tracey, K.J., 2005. High-mobility group box 1 protein (HMGB1): nuclear weapon in the immune arsenal. *Nat. Rev. Immunol.* 5, 331-342.

- Luo, Y., Ohmori, H., Fujii, K., Moriwaka, Y., Sasahira, T., Kurihara, M., Tatsumoto, N., Sasaki, T., Yamashita, Y., Kuniyasu, H., 2010. HMGB1 attenuates anti-metastatic defence of the liver in colorectal cancer. *Eur. J. Cancer* 46, 791-799.
- Madeira, J.M., Beloukhina, N., Boudreau, K., Boettcher, T.A., Gurley, L., Walker, D.G., McNeil, W.S., Klegeris, A., 2012. Cobalt(II) beta-ketoamino complexes as novel inhibitors of neuroinflammation. *Eur. J. Pharmacol.* 676, 81-88.
- Maroso, M., Balosso, S., Ravizza, T., Liu, J., Aronica, E., Iyer, A.M., Rossetti, C., Molteni, M., Casalgrandi, M., Manfredi, A.A., Bianchi, M.E., Vezzani, A., 2010. Toll-like receptor 4 and high-mobility group box-1 are involved in ictogenesis and can be targeted to reduce seizures. *Nat. Med.* 16, 413-419.
- Muhammad, S., Barakat, W., Stoyanov, S., Murikinati, S., Yang, H., Tracey, K.J., Bendszus, M., Rossetti, G., Nawroth, P.P., Bierhaus, A., Schwaninger, M., 2008. The HMGB1 receptor RAGE mediates ischemic brain damage. *J. Neurosci.* 28, 12023-12031.
- Ngo, H.B., Kaiser, J.T., Chan, D.C., 2011. The mitochondrial transcription and packaging factor Tfam imposes a U-turn on mitochondrial DNA. *Nat. Struct. Mol. Biol.* 18, 1290-1296.
- Pedrazzi, M., Patrone, M., Passalacqua, M., Ranzato, E., Colamassaro, D., Sparatore, B., Pontremoli, S., Melloni, E., 2007. Selective proinflammatory activation of astrocytes by high-mobility group box 1 protein signaling. *J. Immunol.* 179, 8525-8532.
- Qiu, J., Nishimura, M., Wang, Y., Sims, J.R., Qiu, S., Savitz, S.I., Salomone, S., Moskowitz, M.A., 2008. Early release of HMGB-1 from neurons after the onset of brain ischemia. *J. Cereb. Blood. Flow. Metab.* 28, 927-938.
- Rubio-Cosials, A., Sidow, J.F., Jimenez-Menendez, N., Fernandez-Millan, P., Montoya, J., Jacobs, H.T., Coll, M., Bernado, P., Sola, M., 2011. Human mitochondrial transcription

- factor A induces a U-turn structure in the light strand promoter. *Nat. Struct. Mol. Biol.* 18, 1281-1289.
- Safdar, A., Little, J.P., Stokl, A.J., Hettinga, B.P., Akhtar, M., Tarnopolsky, M.A., 2011. Exercise increases mitochondrial PGC-1 α content and promotes nuclear-mitochondrial cross-talk to coordinate mitochondrial biogenesis. *J. Biol. Chem.* 286, 10605-10617.
- Stros, M., 2010. HMGB proteins: interactions with DNA and chromatin. *Biochim. Biophys. Acta.* 1799, 101-113.
- Taylor, D.L., Diemel, L.T., Pocock, J.M., 2003. Activation of microglial group III metabotropic glutamate receptors protects neurons against microglial neurotoxicity. *J. Neurosci.* 23, 2150-2160.
- Villanueva, E.B., Little, J.P., Lambeau, G., Klegeris, A., 2012. Secreted phospholipase A(2) group IIA is a neurotoxin released by stimulated human glial cells. *Mol. Cell. Neurosci.* 49, 430-438.
- Vogel, C.F., Sciuillo, E., Wong, P., Kuzmicky, P., Kado, N., Matsumura, F., 2005. Induction of proinflammatory cytokines and C-reactive protein in human macrophage cell line U937 exposed to air pollution particulates. *Environ. Health Perspect.* 113, 1536-1541.
- Walker, D.G., Dalsing-Hernandez, J.E., Campbell, N.A., Lue, L.F., 2009. Decreased expression of CD200 and CD200 receptor in Alzheimer's disease: a potential mechanism leading to chronic inflammation. *Exp. Neurol.* 215, 5-19.
- Wolthers, K.R., Basran, J., Munro, A.W., Scrutton, N.S., 2003. Molecular dissection of human methionine synthase reductase: determination of the flavin redox potentials in full-length enzyme and isolated flavin-binding domains. *Biochemistry* 42, 3911-3920.

- Wong, T.S., Rajagopalan, S., Freund, S.M., Rutherford, T.J., Andreeva, A., Townsley, F.M., Petrovich, M., Fersht, A.R., 2009. Biophysical characterizations of human mitochondrial transcription factor A and its binding to tumor suppressor p53. *Nucleic Acids Res.* 37, 6765-6783.
- Yang, H., Antoine, D.J., Andersson, U., Tracey, K.J., 2013. The many faces of HMGB1: molecular structure-functional activity in inflammation, apoptosis, and chemotaxis. *J. Leukoc. Biol.* 93, 865-873.
- Yin, W., Signore, A.P., Iwai, M., Cao, G., Gao, Y., Chen, J., 2008. Rapidly increased neuronal mitochondrial biogenesis after hypoxic-ischemic brain injury. *Stroke* 39, 3057-3063.
- Zeng, S., Dun, H., Ippagunta, N., Rosario, R., Zhang, Q.Y., Lefkowitz, J., Yan, S.F., Schmidt, A.M., Emond, J.C., 2009. Receptor for advanced glycation end product (RAGE)-dependent modulation of early growth response-1 in hepatic ischemia/reperfusion injury. *J. Hepatol.* 50, 929-936.
- Zhang, G., Li, J., Purkayastha, S., Tang, Y., Zhang, H., Yin, Y., Li, B., Liu, G., Cai, D., 2013. Hypothalamic programming of systemic ageing involving IKK-beta, NF-kappaB and GnRH. *Nature* 497, 211-216.
- Zhang, Q., Raouf, M., Chen, Y., Sumi, Y., Sursal, T., Junger, W., Brohi, K., Itagaki, K., Hauser, C.J., 2010. Circulating mitochondrial DAMPs cause inflammatory responses to injury. *Nature* 464, 104-107.